Available online at www.sciencedirect.com

ScienceDirect

Advances in Space Research xxx (xxxx) xxx

ADVANCES IN SPACE RESEARCH (a COSPAR publication)

www.elsevier.com/locate/asr

Review

Prediction of solar energetic events impacting space weather conditions

Manolis K. Georgoulis [ae,a,*], Stephanie L. Yardley [b,c,d], Jordan A. Guerra [e,f], Sophie A. Murray [g], Azim Ahmadzadeh [ap], Anastasios Anastasiadis [i], Rafal Angryk [h], Berkay Aydin [h], Dipankar Banerjee [j], Graham Barnes [k], Alessandro Bemporad [l], Federico Benvenuto [m], D. Shaun Bloomfield [b], Monica Bobra [n], Cristina Campi [m], Enrico Camporeale [e,aq,ar], Craig E. DeForest [o], A. Gordon Emslie [p], David Falconer [q,r], Li Feng [s,u], Weiqun Gan [s,u], Lucie M. Green [t], Sabrina Guastavino [m], Mike Hapgood [v], Dustin Kempton [h], Irina Kitiashvili [w], Ioannis Kontogiannis [x], Marianna B. Korsos [y,z,aa], K.D. Leka [k], Paolo Massa [p], Anna Maria Massone [m], Dibyendu Nandy [ab], Alexander Nindos [ac], Athanasios Papaioannou [i], Sung-Hong Park [ad], Spiros Patsourakos [ac], Michele Piana [m,l], Nour E. Rawafi [ae], Viacheslav M. Sadykov [af], Shin Toriumi [ag], Angelos Vourlidas [ae], Haimin Wang [aj], Jason T. L. Wang [aj], Kathryn Whitman [ah,ai], Yihua Yan [ak,al,am], Andrei N. Zhukov [an,ao]

[a] *Research Center for Astronomy and Applied Mathematics of the Academy of Athens, 11527 Athens, Greece*
[b] *Department of Mathematics, Physics and Electrical Engineering, Northumbria University, Newcastle upon Tyne NE1 8ST, UK*
[c] *Department of Meteorology, University of Reading, Reading RG6 6ET, UK*
[d] *Donostia International Physics Center (DIPC), Paseo Manuel de Lardizabal 4, 20018 San Sebastián, Spain*
[e] *CIRES, University of Colorado, Boulder, CO 80309, USA*
[f] *NOAA Space Weather Prediction Center, Boulder, CO 80305, USA*
[g] *School of Cosmic Physics, Dublin Institute for Advanced Studies, Dunsink Observatory, Dublin D15 XR2R, Ireland*
[h] *Computer Science Department, Georgia State University, Atlanta, GA 30303, USA*
[i] *Institute for Astronomy, Astrophysics, Space Applications and Remote Sensing (IAASARS), National Observatory of Athens, 15236 Penteli, Greece*
[j] *Aryabhatta Research Institute for Observational Sciences (ARIES), Nainital 263001, Uttarakhand, India*
[k] *NorthWest Research Associates, Boulder, CO 80301, USA*
[l] *INAF, Turin Astrophysical Observatory, via Osservatorio 20, 10025 Pino Torinese, Torino, Italy*
[m] *MIDA, Dipartimento di Matematica, Università di Genova, via Dodecaneso 35 16146 Genova Italy*
[n] *State of California, Office of Data and Innovation, 401 I Street, Ste 200, Sacramento, CA 95814, USA*
[o] *Southwest Research Institute, Boulder, CO 80302, USA*
[p] *Department of Physics & Astronomy, Western Kentucky University, Bowling Green, KY 42101, USA*
[q] *Center for Space Plasma and Aeronomic Research, University of Alabama in Huntsville, Huntsville, AL 35899, USA*
[r] *NASA/Marshall Space Flight Center, Huntsville, AL 35812, USA*
[s] *Key Laboratory of Dark Matter and Space Astronomy, Purple Mountain Observatory, Chinese Academy of Sciences, Nanjing 210023, China*

* Corresponding author at: Research Center for Astronomy and Applied Mathematics of the Academy of Athens, 11527 Athens, Greece.
E-mail addresses: manolis.georgoulis@jhuapl.edu (M.K. Georgoulis), steph.yardley@northumbria.ac.uk (S.L. Yardley), jordan.guerra@noaa.gov (J. A. Guerra), sophie.murray@dias.ie (S.A. Murray), azim.ahmadzadeh@gmail.com (A. Ahmadzadeh), anastasi@noa.gr (A. Anastasiadis), baydin2@gsu.edu (B. Aydin), dipu@aries.res.in (D. Banerjee), graham@nwra.com (G. Barnes), alessandro.bemporad@inaf.it (A. Bemporad), benvenuto@dima.unige.it (F. Benvenuto), shaun.bloomfield@northumbria.ac.uk (D.S. Bloomfield), monica.bobra@innovation.ca.gov (M. Bobra), cristina.campi@unige.it (C. Campi), enrico.camporeale@colorado.edu (E. Camporeale), deforest@boulder.swri.edu (C.E. DeForest), gordon.emslie@wku.edu (A.G. Emslie), lfeng@pmo.ac.cn (L. Feng), wqgan@pmo.ac.cn (W. Gan), lucie.green@ucl.ac.uk (L.M. Green), guastavino@dima.unige.it (S. Guastavino), mike.hapgood@stfc.ac.uk (M. Hapgood), irina.n.kitiashvili@nasa.gov (I. Kitiashvili), ikontogiannis@aip.de (I. Kontogiannis), m.korsos@sheffield.ac.uk (M. B. Korsos), leka@nwra.com (K.D. Leka), paolo.massa@wku.edu (P. Massa), massone@dima.unige.it (A.M. Massone), dnandi@iiserkol.ac.in (D. Nandy), anindos@uoi.gr (A. Nindos), atpapaio@noa.gr (A. Papaioannou), shpark@kasi.re.kr (S.-H. Park), spatsour@uoi.gr (S. Patsourakos), piana@dima.unige.it (M. Piana), nour.raouafi@jhuapl.edu (N.E. Rawafi), vsadykov@gsu.edu (V.M. Sadykov), toriumi.shin@jaxa.jp (S. Toriumi), angelos.vourlidas@jhuapl.edu (A. Vourlidas), haimin.wang@njit.edu (H. Wang), wangj@njit.edu (J.T. L. Wang), kathryn.whitman@nasa.gov (K. Whitman), yanyihua@nssc.ac.cn (Y. Yan), Andrei.Zhukov@sidc.be (A.N. Zhukov), .

https://doi.org/10.1016/j.asr.2024.02.030
0273-1177/

Please cite this article as: M. K. Georgoulis, S. L. Yardley, J. A. Guerra et al., Prediction of solar energetic events impacting space weather conditions, Advances in Space Research, https://doi.org/10.1016/j.asr.2024.02.030

[t] Mullard Space Science Laboratory, University College London, Holmbury St. Mary RH5 6NT, UK
[u] University of Chinese Academy of Sciences, Nanjing 211135, China
[v] Visiting Scientist, RAL Space, STFC Rutherford Appleton Laboratory, Didcot, Oxfordshire OX11 0QX, UK
[w] NASA Ames Research Center, Moffett Field, CA 94035, USA
[x] Leibniz-Institut für Astrophysik Potsdam (AIP), An der Sternwarte 16, 14482 Potsdam, Germany
[y] Dipartimento di Fisica e Astronomia "Ettore Majorana", Università di Catania, Via S. Sofia 78, I 95123 Catania, Italy
[z] Department of Astronomy, Eötvös Loránd University, Pázmány Péter sétány, 1/A, H-1112 Budapest, Hungary
[aa] School of Mathematics and Statistics, University of Sheffield, Hounsfield Road, Sheffield S3 7RH, UK
[ab] Indian Institute of Science Education and Research (IISER) Kolkata, Mohanpur, Nadia - 741 246, West Bengal, India
[ac] Physics Department, University of Ioannina, Ioannina 45110, Greece
[ad] Korea Astronomy & Space Science Institute, 776 Daedeok-daero, Yuseong-gu, Daejeon 34055, Republic of Korea
[ae] Johns Hopkins University Applied Physics Laboratory Laurel, MD 20375, USA
[af] Physics & Astronomy Department, Georgia State University, Atlanta, GA 30303, USA
[ag] Institute of Space and Astronautical Science, Japan Aerospace Exploration Agency, 3-1-1 Yoshinodai, Chuo-ku, Sagamihara, Kanagawa 252-5210, Japan
[ah] KBR, 2400 E NASA Pkwy, Houston, TX 77058, USA
[ai] Space Radiation Analysis Group, NASA Johnson Space Center, 2101 E NASA Pkwy, Houston, TX 77058, USA
[aj] Institute for Space Weather Sciences, New Jersey Institute of Technology, Newark, NJ 07102, USA
[ak] National Space Science Center, Chinese Academy of Science, Beijing 100190, China
[al] National Astronomical Observatories, Chinese Academy of Science, Beijing 100101, China
[am] School of Astronomy and Space Science, University of Chinese Academy of Science, Beijing 100049, China
[an] Solar-Terrestrial Centre of Excellence – SIDC, Royal Observatory of Belgium, Ringlaan -3- Av. Circulaire, 1180 Brussels, Belgium
[ao] Skobeltsyn Institute of Nuclear Physics, Moscow State University, 119992 Moscow, Russia
[ap] Department of Computer Science, University of Missouri-St.Louis, St. Louis, MO 63103, USA
[aq] Space Weather Technology, Research and Education (SWx TREC), University of Colorado, Boulder, CO 80309, USA
[ar] School of Physical and Chemical Sciences, Queen Mary University of London, E1 4NS, London, UK

Received 6 February 2023; received in revised form 9 February 2024; accepted 17 February 2024

Abstract

Aiming to assess the progress and current challenges on the formidable problem of the prediction of solar energetic events since the COSPAR/ International Living With a Star (ILWS) Roadmap paper of Schrijver et al. (2015), we attempt an overview of the current status of global research efforts. By solar energetic events we refer to flares, coronal mass ejections (CMEs), and solar energetic particle (SEP) events. The emphasis, therefore, is on the prediction methods of solar flares and eruptions, as well as their associated SEP manifestations. This work complements the COSPAR International Space Weather Action Teams (ISWAT) review paper on the understanding of solar eruptions by Linton et al. (2023) (hereafter, ISWAT review papers are conventionally referred to as 'Cluster' papers, given the ISWAT structure). Understanding solar flares and eruptions as instabilities occurring above the nominal background of solar activity is a core solar physics problem. We show that effectively predicting them stands on two pillars: physics and statistics. With statistical methods appearing at an increasing pace over the last 40 years, the last two decades have brought the critical realization that data science needs to be involved, as well, as volumes of diverse ground- and space-based data give rise to a Big Data landscape that cannot be handled, let alone processed, with conventional statistics. Dimensionality reduction in immense parameter spaces with the dual aim of both interpreting and forecasting solar energetic events has brought artificial intelligence (AI) methodologies, in variants of machine and deep learning, developed particularly for tackling Big Data problems. With interdisciplinarity firmly present, we outline an envisioned framework on which statistical and AI methodologies should be verified in terms of performance and validated against each other. We emphasize that a homogenized and streamlined method validation is another open challenge. The performance of the plethora of methods is typically far from perfect, with physical reasons to blame, besides practical shortcomings: imperfect data, data gaps and a lack of multiple, and meaningful, vantage points of solar observations. We briefly discuss these issues, too, that shape our desired short- and long-term objectives for an efficient future predictive capability. A central aim of this article is to trigger meaningful, targeted discussions that will compel the community to adopt standards for performance verification and validation, which could be maintained and enriched by institutions such as NASA's Community Coordinated Modeling Center (CCMC) and the community-driven COSPAR/ISWAT initiative.

Keywords: International space weather action teams; Forecasting; Solar flares and eruptions; Methods – statistical; Methods – machine learning; Future missions

Contents

1. Introduction

For millennia, human curiosity has been captured by the natural world and its phenomena, and this has led to a quest to understand them, as far as our eyes, or our instruments much later, could reach. As human society clustered in communities living and acting jointly, it became clear that several natural phenomena below and above ground impact everyday life in such a way that humans had to adapt and, to the extent possible, predict them to mitigate their most adverse effects. Real-world problems with significant consequences to human life and well-being included terrestrial weather, earthquakes, volcanic activity and oceanic behavior. Each of them was witnessed to have its extremes, from tornadoes and hurricanes to devastating quakes, globe-affecting volcanic eruptions and tsunamis occurring with or without a locally observed cause. With physics and mathematics evolving, such phenomena were attributed to complexity (see, e.g., Sharma et al., 2012, and references therein), that came to be synonymous to

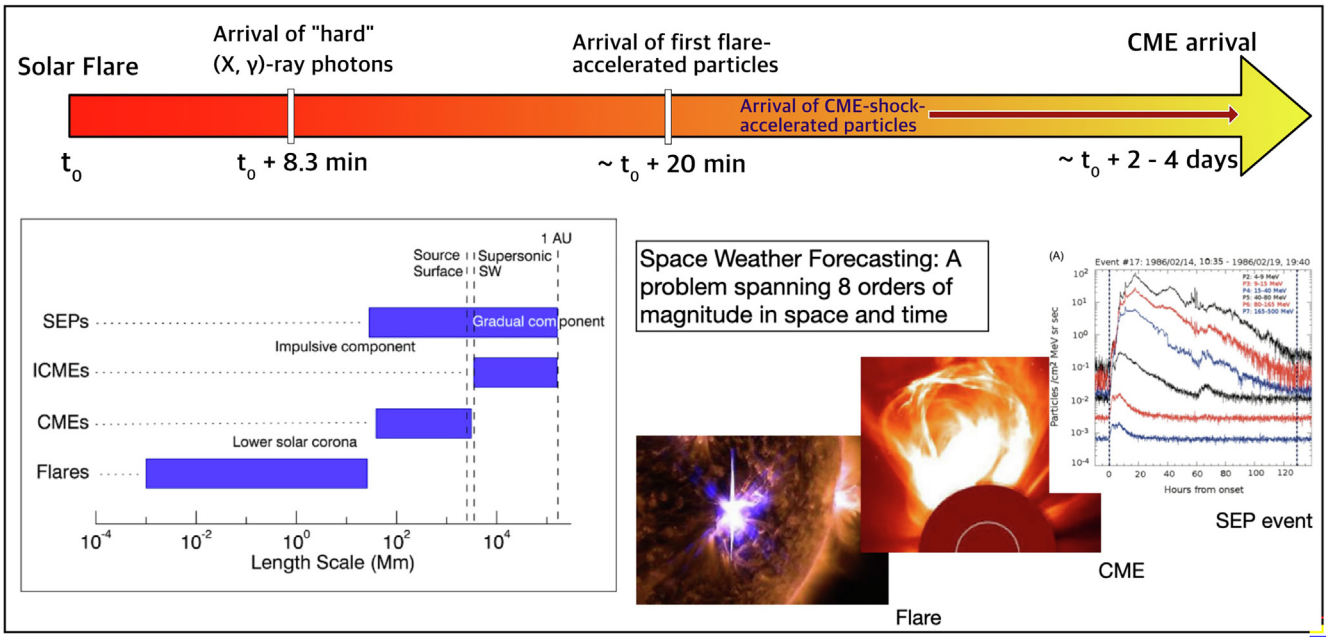

Fig. 1. Spatial and temporal span of the solar flare and eruption problem and their repercussions: in time, from the second timescales involved in magnetic reconnection events that give rise to flares, to the week-long ($\sim 6 \times 10^5$ s) recovery time for Earth's magnetosphere due to the passing of a fast, geoffective CME, to the 11-year solar cycle modulation ($\sim 3.5 \times 10^8$ s). In space, from the km-size magnetic reconnection area to eruption transients propagating to 1 astronomical unit and beyond($\sim 1.5 \times 10^8$ km).

lack of predictability (Meyers, 2010), stochasticity and/or chaotic behavior, from 'black swans' to 'dragon kings' (Taleb, 2007; Sornette, 2009, and references therein). In recent decades, with our choice of robotic and human exploration of space, space weather has been added to this list of natural hazards (Hapgood et al., 2021).

The Sun's influence sphere, known as heliosphere, can be seen as a 'system of systems', where Sun's continuously variable magnetic forcing generates conditions amounting to what is known as space weather (Schwenn, 2006; Zhang et al., 2021; Temmer, 2021, and references therein). Cosmic radiation from the galaxy also shapes space weather conditions (Lockwood, 1971), acting antagonistically to solar activity (e.g., Cane, 2000, and references therein). Hazardous space weather is caused by extreme solar events (Cliver et al., 2022, and references therein) that correspond to the higher end of the size distribution of solar flares, coronal mass ejections (CMEs), and solar energetic particle (SEP) events. For an overview of the physics of these events and our present understanding, see Section 2 and the Cluster review by Linton et al. (2023). Flares are operationally quantified mainly by means of their peak photon flux in soft X-rays, with the most commonly used scale being the Geostationary Operational Environmental Satellites (GOES) flare scale, implemented by the National Oceanic and Atmospheric Administration (NOAA). This is logarithmic and coded by A, B, C, M, and X for peak fluxes of $n \times 10^{-8} W/m^2$ in $1-8$Å soft X-rays, with $n \equiv \{1, 10, 10^2, 10^3, and\ 10^4\}$, respectively. Each of these flare classes has subdivisions from 1.0 to 9.9, with the exception of the X-class that can exceed 10.0. CMEs are quantified by their speed, mass, angular width, while SEP (typically, proton) events by their peak flux, duration and fluence. To effectively predict these phenomena, we need to predict, in a timely manner, (i) time of arrival for CMEs and SEP events in geospace, on top of the event characteristics, and (ii) CME geoeffectiveness, i.e., their ability to trigger geomagnetic storms. We note here that another Cluster paper on the geomagnetic environment is in preparation, along the lines of Opgenoorth et al. (2019). For CMEs, other heliospheric ejecta and SEP event forecasting, see Cluster reviews by Temmer et al. (2023) and Whitman et al. (2022), respectively.

For flares, with electromagnetic radiation signatures moving at the speed of light, there is no early warning, so flares must be forecast hours, ideally, before their occurrence on the Sun (e.g., Sawyer et al., 1986; Leka et al., 2018; Georgoulis et al., 2021, and references therein). Recent trends also place CME and SEP event forecasting in this framework, namely, before events actually occur. For a recent overview of SEP event forecast methods, see also Malandraki and Crosby (2018), the Cluster review by Whitman et al. (2022) and Section 3.3 below.

Predicting all of these energetic manifestations is a daunting task, spanning ~ 8 orders of magnitude in space and time (Fig. 1). At present, we are far from claiming or even considering any success in dealing with all these problems simultaneously.

Solar eruptions of space weather significance primarily occur from solar active regions, namely, accumulations of intense magnetic flux in the solar atmosphere (e.g., Martres and Bruzek, 1977; Harvey and Zwaan, 1993; van

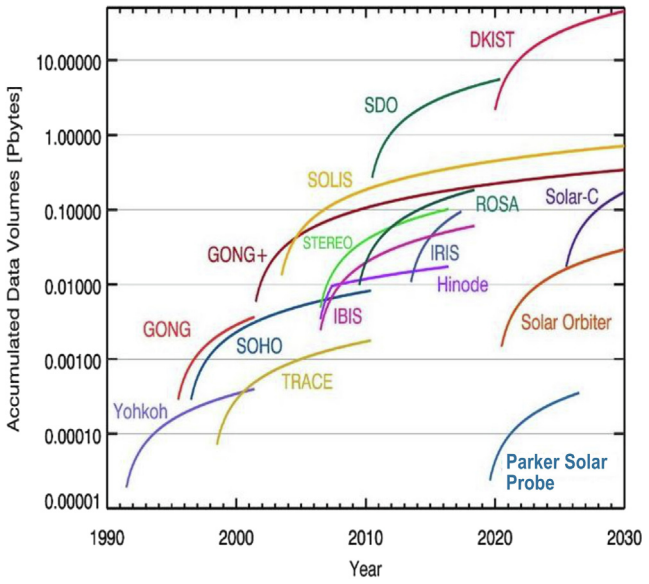

Fig. 2. Actual and projected science-grade data accumulation from multiple ground- and space-based observatories devoted to heliophysics (i.e., solar and inner heliosphere) over this and the previous three decades. Credit: National Solar Observatory (NSO)/ K. Reardon.

Driel-Gesztelyi and Green, 2015). Only a minority of active regions give major (i.e., in excess of GOES M1.0) flares and only a fraction of flares are eruptive, namely, associated with a CME. A sub-class of flaring active regions, therefore, is called eruptive regions, if at least one of their flares is eruptive. There is an increasing association between flares and fast/wide CMEs (namely, those of relevance to space weather), starting from approximately 1 : 3 (1 CME for 3 flares) for low C–class events and progressing to a nearly one-to-one association for flares >X2.0 (Yashiro, 2005; Anastasiadis et al., 2017). A flare may be eruptive or not (confined), but a CME originating from an active region will be associated with a flare: potential exceptions of this rule may refer to high-altitude CMEs above active regions, at significant fractions of the solar radius (O'Kane et al., 2019), or weak CMEs originating from low altitudes at the periphery of active regions, potentially as eruptions sympathetic to activity happening within the regions (Yardley et al., 2021b). The study of flare – CME association began in the 1970s with CME observations made by Skylab (Munro et al., 1979) and is still ongoing, with substantial literature on the topic (see, e.g. Harrison, 1995; Zhang et al., 2001; Zhang and Dere, 2006). Investigation focuses mostly on the repercussions of the so-called standard flare model, otherwise known as Carmichael-Sturrock-Hirayama-Kopp-Pneumann (CSHKP) model. For reviews, see Forbes et al. (2006) and the Cluster review by Linton et al. (2023).

Flares higher than GOES C–class occur exclusively in active regions, as the quiet-Sun does not possess sufficient magnetic energy density to produce them. CMEs may also originate from remnant active regions that no longer display strong-field photospheric sunspots, and are typically associated with unstable filaments and eruptive prominences visible in the chromosphere (Munro et al., 1979). In some cases, however, low-atmospheric pre-CME signatures are lacking, in which case these CMEs are called 'stealth' CMEs (e.g., Robbrecht et al., 2009; Howard and Harrison, 2013; Nitta et al., 2021, for a review). CMEs originating from weak-field solar regions, far from active regions, be them stealth or otherwise (i.e., associated with large-scale, quiet-Sun filament eruptions), have generally less space weather interest, because of their relatively low magnetic energy and speed (Gopalswamy et al., 2009). Sheeley et al. (1999) found that CMEs with speeds higher than 750 km/s correspond primarily to active regions. **These** CMEs, with speeds higher than that of the fast solar wind (i.e., $\sim$ 800 km/s), are more capable of producing shocks that give rise to SEP events in the heliosphere. Therefore, we will not be focusing on quiet-Sun eruptions in this review.

The first step towards predicting solar energetic events (in a research – not necessarily operational – sense), is to physically distinguish between two active region populations: flaring vs. non-flaring or eruptive vs. non-eruptive ones. On this problem there is also substantial literature (e.g., Hagyard et al., 1984a; Zirin and Liggett, 1987; Sawyer et al., 1986; McIntosh, 1990; Leka and Barnes, 2003b; Abramenko, 2005; Chintzoglou and Zhang, 2013; Pagano et al., 2019), with reviews by Green et al. (2018), Toriumi and Wang (2019), Georgoulis et al. (2019), Patsourakos et al. (2020) and references therein. The practical challenge is to achieve a clear separation between the two populations in some meaningful one-dimensional or multi-dimensional parameter space. A clear, non-overlapping separation would allow a binary [YES/NO] classification of sub-volumes of the parameter space that would characterize the local population as flaring/eruptive or non-flaring. In case of overlap, partial or full, a probability would be assigned as per the local densities of the different active-region populations.

The definition of the different parameters comprising the parameter space is, therefore, critical to our ability to predict solar energetic phenomena. Virtually all of these parameters are either directly physical or intuitively/semi-empirically linked to some fundamental physical parameter. Each parameter is either a scalar or a vector characterizing the state of a certain active region at a certain time. There have been hundreds of parameters proposed over the last 20 years (Falconer et al., 2002; Leka and Barnes, 2003a; Abramenko, 2005; McAteer et al., 2005; Georgoulis and Rust, 2007; Conlon et al., 2010; McAteer et al., 2010; Mason and Hoeksema, 2010; Reinard et al., 2010; Bobra et al., 2014; Korsós et al., 2015; Kontogiannis et al., 2017; Guennou et al., 2017; Murray et al., 2018; Park et al., 293(8),; Guerra et al., 2018; Kontogiannis et al., 2019; Kusano et al., 2020; Georgoulis et al., 2021; Leka et al., 2023, and others). Parameters or properties with a potential predictive capability and their rationale are discussed in Section 2.3. In the next Sections, we will be discussing potentially flare

predictive and eruptivity parameters, too, with an emphasis on the methods utilizing them; not necessarily on the parameters themselves.

Scores of metadata parameters and immense parametric spaces fulfill the requirements of a 'Big Data' ecosystem (e.g., Chen et al., 2014; De Mauro et al., 2015) that clearly brings interdisciplinarity into the solar eruption prediction problem. Besides metadata, Big Data is also due to the exponentially increasing volumes of ground- and space-based data of Level 1.0 and above (for a description of data levels, see NASA/EOSDIS Data Processing Levels online), as can be seen in Fig. 2: from the tens of Gigabytes in the 1990s to the tens of Petabytes in the 2020s, 6+ orders of magnitude apart. Subjecting these data to scientific processing and assimilation calls for specialized data science techniques and, naturally, for artificial intelligence (AI) methodologies such as machine learning (ML; Mitchell, 1997; Jordan and Mitchell, 2015) and deep learning (DL; LeCun et al., 2015; Goodfellow et al., 2016). As put together eloquently by Mitchell (2006), ML aims to address the question *"How can we build computer systems that automatically improve with experience, and what are the fundamental laws that govern all learning processes?*". This can be achieved in three different ways: (i) a *supervised* approach, in which an unknown input–output mapping is approximated by means of learning (training) on known (i.e., labeled) input–output samples. For space weather applications, an example is flare prediction using active region data as a testing sample, after training on a sample that includes similar data of the past for which we know the outcome. (ii) An *unsupervised* approach, in which data structures are inferred from the data themselves typically via a clustering process and by training on unlabeled data. Finally, (iii) a *hybrid* approach, in which supervised and unsupervised methodologies are combined between training and testing. For a discussion on these methodologies for flare prediction, in particular, see Massone and Piana (2018).

Deep learning (DL), on the other hand, as a subset of ML, aims to imitate the human brain on the basis of the rudimentary understanding we have about it. It represents a given problem as a nested hierarchy of concepts, each of which is described by a collection of simpler concepts, in a neural network fashion. A comprehensive overview of DL applications in solar astronomy was presented in Xu et al. (2022). The concept and details of network design, experimental results, and comparison with the state-of-the-art were reported as a guide in that work. DL does not rely on a priori extracted descriptors (even though it works on labeled samples) and produces results by focusing on automatically computed, generally unspecified, features of the training sample. If performance is quantified, then DL methodologies show a higher performance than plain ML ones, under the major caveat of the availability of sufficient training data. Goodfellow et al. (2016) mentions, in particular, that as a rule of thumb, *"a supervised deep learning algorithm will generally achieve acceptable performance with around 5,000 labeled examples per category and will match or exceed human performance when trained with a dataset containing at least 10 million labeled examples*". This immediately triggers the question whether DL is applicable for space weather forecasting applications, as we are orders of magnitude below the millions of events purportedly needed: we have been observing flares, CMEs and SEPs events for a few decades and each typical 11-year solar cycle includes a few tens of thousands of CMEs, several hundred flares of GOES class M and above, and a couple of hundred SEP events, at best. This further implies severely class-imbalanced training and testing samples with the overwhelming majority belonging to the negative class (i.e., no event) leading to the "black swan" or "dragon king" (for extreme but understood and entirely not understood, respectively) concepts already discussed.

As will be explained in Sections 3 and 4, the current performance of even the most elaborate methodologies for predicting solar energetic events is far from optimal. This includes ML and DL methodologies, applied in spite of the above looming assessment by Goodfellow et al. (2016). Challenges notwithstanding, many of which are discussed in Camporeale (2019), space weather forecasting is a central task of, and lack thereof can be a showstopper to, future space exploration, particularly crewed expeditions (e.g., Mertens and Slaba, 2019; Zaman et al., 2022). On the surface of Earth, the economic and societal impacts can be staggering (see, for example MacAlester and Murtagh, 2014; Eastwood et al., 2017; Oughton et al., 2018), prompting key space-faring nations to issue governmental guidelines and emergency operation plans (EOP, 2016; EOP, 2019). This pressing need was the driving force behind the Schrijver et al. (2015) review and roadmap paper. Previously, a compelling case was made by the 2008 National Research Council's *Severe Space Weather Events: Understanding Societal and Economic Impacts Workshop Report* (NRC, 2008). In the report's Fig. 3.1, economy and the societal structure with its various sectors are presented as a series of domino blocks interconnected in an inherently nonlinear manner, i.e., lacking a central prior coordination. If any one block is disabled due to space weather, either temporarily, or in a sustained timescale, consequences and repercussions can be unpredictable. Impacts worsen in case where more than one blocks are disabled. The severity and temporal length of each disruption drive the societal and economic cost upward.

The paper is structured as follows: in Section 2 we present a brief discussion of the pre-eruption state in solar active regions, pointing the reader to the dedicated Cluster review of Linton et al. (2023). In Section 3 we review the different methodologies applied so far for the prediction of major solar eruptions, connecting also to the dedicated Cluster reviews of Temmer et al. (2023) and Whitman et al. (2022) on CME and SEP event prediction, respectively. In Section 4 we outline the key principles of a possible eruption prediction framework that could be used to

homogenize results from various methodologies, in this way enabling a standard and streamlined comparison between methods focused on a particular problem. Standardized performance verification and validation are at the core of this discussion. In Section 5 we discuss the immediate difficulties that need to be addressed in order to facilitate effective space weather forecasting, while in Section 6 we discuss what future needs and actions are required to effectively address some of these challenges and afford us access to information that is entirely inaccessible at present. Section 6 is complemented by Appendix A. Section 7 summarizes the report by listing some of the top-level conclusions, expectations and recommendations for the future. Finally, Appendix B provides an auxiliary list of the acronyms and abbreviations used in the article.

2. The preflare/ pre-eruption state

As mentioned already. 1 there is no early warning that a flare is about to occur and, once initiated, it takes less that 8.5 minutes until its effects are felt at Earth. However, flare forecasts are issued for the coming few days and rely upon predictions made using the morphological features of active regions or magnetic parameters defined from white-light and photospheric magnetic field observations, as well as Hα images of the chromosphere, historically (Section 3).

Regarding CMEs, the Sun is constantly monitored for their occurrence using mostly space-based coronagraphs. Once a CME is detected, prediction tools that model CME propagation post-eruption (e.g. WSA-ENLIL/EUHFORIA), based on input parameters from coronagraph observations, are used to provide an estimated CME arrival time at Earth. This leads to an advanced warning of 1–3 days before the CME reaches geospace (Mays et al., 2015). The problem is discussed in the Cluster review of Temmer et al. (2023). Besides applicable uncertainties, sometimes substantial, this lead time is often insufficient to help mitigate potential effects for our ground- and space-based technological infrastructure. For example, UK power grids require up to a 5-day warning of CME arrival to protect their transmission systems (European Commission, 2016). Therefore, accurate predictions prior to eruption onset is a valuable asset to decisively improve the capabilities of both forecasting of geoeffectiveness and lead times. To predict the occurrence of solar eruptive phenomena in advance, a sufficient understanding of the pre-eruption state is required along with the determination of the onset mechanism(s). Understanding this state in active regions is the topic of the Cluster review of Linton et al. (2023), but we briefly discuss some key concepts here.

2.1. Genesis and evolution of flare-productive solar active regions

To better comprehend space weather and achieve efficient and accurate forecasting, it is critically important to understand and quantify the magnetic circumstances of

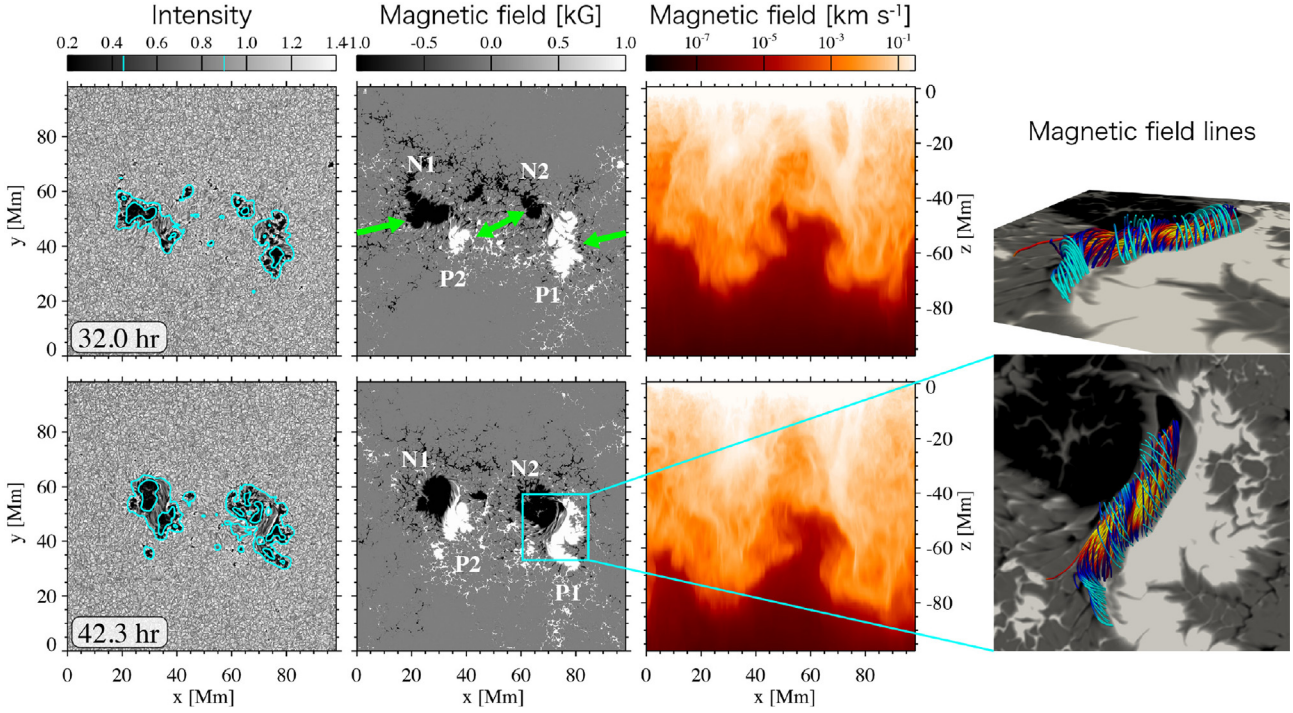

Fig. 3. Convective flux emergence simulation for modeling an eruptive active region. From left to right, each column shows the emergent intensity (turquoise contours outline the penumbra), the vertical magnetic field strength (B_z) in the photosphere (green arrows highlight the flux emergence), and total field strength in the vertical slice of the simulation domain, normalized by the local background plasma density $(4\pi\rho)^{1/2}$ and thus having dimensions of speed, at the two selected times. The fourth column shows the magnetic field lines above the δ-sunspot N2-P1, which exhibits a flux rope structure. Figure reproduced from Toriumi and Hotta (2019) by permission of the AAS.

solar eruptive phenomena in time and space, namely the process by which magnetic flux emerges from the solar interior to form sunspots and active regions (van Driel-Gesztelyi and Green, 2015; Toriumi and Wang, 2019).

Observations have shown that large flares tend to occur in those sunspot groups that have complex shapes. The most magnetically-complex sunspot configurations include a "δ-sunspot", in which umbrae of opposite polarities are enveloped within a common penumbra (Künzel, 1960; McIntosh, 1990). δ-sunspots are known to be the source of some of the largest flares (Krall et al., 1982; Patty and Hagyard, 1986; Zirin and Liggett, 1987; McIntosh, 1990; Sammis et al., 2000). Flare-productive active regions are formed via the emergence of twisted, current-carrying magnetic flux tubes and thus exhibit shearing and rotational motions in the photosphere, which leads to the development of sheared and twisted magnetic fields along magnetic polarity inversion lines (PILs; Hagyard et al., 1984b; Zirin and Liggett, 1987; Leka et al., 1996; López Fuentes et al., 2000; Brown et al., 2003; Toriumi et al., 2017). This means that as active regions evolve, non-potential (i.e., free, caused by plasma-spawned electric currents) magnetic energy is injected into the corona. Complementary to free magnetic energy is magnetic helicity, namely a measure of twist, writhe and linkage. Flares and eruptions, in general, occur when free magnetic energy and helicity exist in sufficient budgets (Leka and Barnes, 2003a; LaBonte et al., 2007; LaBonte et al., 2007; Park et al., 2010; Tziotziou et al., 2012; Liokati et al., 2022). Recent numerical simulations (Toriumi et al., 2023) suggest that turbulent convection in sub-photospheric layers also injects magnetic helicity into the active region corona, albeit not necessarily of the same sign (or of any consistent sign) to the one that is dominant in the active region.

It is not possible to investigate the solar interior with direct observations, so studies based on theory and numerical simulations are also paramount in order to understand the formation of active regions that become flare productive. A prime scenario proposed to explain the formation of δ-spots is the emergence of a strongly twisted flux tube due to the kink instability (Tanaka, 1991; Linton et al., 1996). Simulations of kink-unstable flux emergence successfully reproduced the δ-shaped sunspots with sheared PILs and complex morphology (Fan et al., 1999; Takasao et al., 2015; Knizhnik et al., 2018; Toriumi and Takasao, 2017). Other scenarios for δ-spot formation include multiple flux tubes emerging simultaneously and in close proximity (Murray and Hood, 2007; Jaeggli and Norton, 2016) as well as multiple portions of a single flux tube emerging and spots of opposite polarity colliding in the photosphere (Toriumi et al., 2014; Fang and Fan, 2015; Syntelis et al., 2019). While it is challenging to completely understand the physical mechanisms responsible for forming δ-spots by only using photospheric observations, a study by Norton et al. (2022) has recently used observed photospheric quantities in order to distinguish between the different proposed scenarios.

In recent years, flux emergence simulations that take into account the turbulent solar convection below the photosphere have enabled a more realistic modeling of eruptive regions. Among others, Cheung et al. (2019) used the MPS/University of Chicago Radiative MHD (MURaM) code to model the emergence of a minor bipole in the vicinity of a pre-existing sunspot, leading to a flare, as a reproduction of the actual active region. A key feature of this simulation is the inclusion of a corona, which allows for an eruptive flare with a magnitude equivalent to a C–class (Cheung et al., 2022). Using the R2D2 code, which covers the entire solar convection zone, Toriumi and Hotta (2019) investigated the process in which a large, deep convection cell elevates the flux tube and spontaneously generates strongly-packed bipolar sunspots (i.e. δ-spots): see Fig. 3. Magnetic flux ropes, namely complex twisted structures coiling around a relatively untwisted core, were created above the sheared PILs in the δ-spots as a consequence of sunspot rotation (Hotta and Toriumi, 2020; Kaneko et al., 2022).

In brief, understanding the formation of flare-productive active regions through a combination of observation and modeling can conceivably help predict the occurrence of flares over the course of active region evolution, from emergence to decay.

2.2. Pre-eruptive magnetic configuration and eruption onset mechanisms

The emergence and evolution of strong active region magnetic fields transports energy and magnetic flux into the solar atmosphere, reconfigures the solar corona and leads to the occurrence of solar flares and CMEs. Flares and CMEs involve an energy storage-and-release process as they are powered by the magnetic energy available due to electric currents that flow along coronal magnetic field lines (e.g. see Priest, 2014). Currents stress and distrort the magnetic field, accumulating free magnetic energy until a critical point is reached, beyond which equilibrium is lost (Forbes, 2000; Forbes et al., 2006). The system pursues relaxation, either via magnetic reconnection alone (confined flare) or via shedding helicity and energy away (CME; Low, 1994; Rust and Kumar, 1996) with the excess free magnetic energy (i.e., the difference between that of pre- and post-eruption states) converted into other forms. The timescales over which the build-up of electric currents occurs are relatively long, from less than 24 h to several days, because the pertinent photospheric driving speeds ($\lesssim 1$ km s^{-1}) are much smaller than the Alfvén speed in the corona ($\sim$1000 km s^{-1}).

In the photosphere, the most conspicuous signature of the build-up of electric currents is the presence of large, high-gradient PILs (Krall et al., 1982; Zirin and Liggett, 1987; Ambastha et al., 1993; Wang et al., 1994) where the photospheric magnetic field is highly "non-potential", meaning very different, in terms of vector orientation and strength, from the current-free magnetic field applicable to the same photospheric radial-field boundary. This often

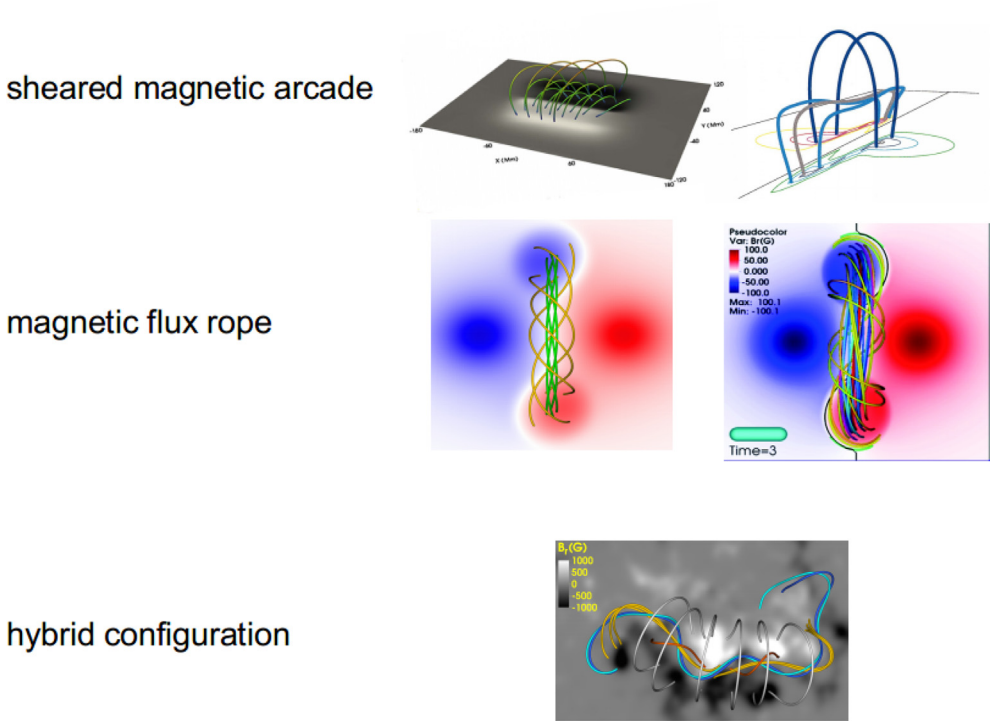

Fig. 4. Examples of pre-eruptive magnetic structures: sheared magnetic arcades (first row), magnetic flux ropes (second row) and hybrid configuration (third row). Magnetic field lines and the distribution of the normal to the photospheric magnetic field (in color contours) from MHD simulations reported by DeVore and Antiochos (2000); Titov et al. (2014); Török et al. (856(1)); Zhou et al. (2018) are shown in all panels. This Figure is a modified version taken from Patsourakos et al. (2020).

manifests as the horizontal component of the magnetic field being highly aligned to the PIL, or displaying "whirlpool" structures around sunspots. The chromospheric/coronal counterpart of a highly sheared PIL is called a filament channel, which appears as a filament or prominence when cool and dense plasma is present, filling the channel.

The build-up of currents in active region filament channels usually starts with magnetic flux emergence (e.g. Leka et al., 1996; Sun et al., 2012; Tziotziou et al., 2013). Typically, the contribution of this mechanism to the final electric current budget of the active region is not large, especially in the early stages of the flux emergence process. As soon as the PIL starts to form, much of the electric current budget is produced primarily by shearing motions around the PIL (e.g. Ambastha et al., 1993; Chintzoglou et al., 2015; Liokati et al., 2022). Strong, shear-ridden PILs exclusively feature non-neutralized (i.e., net) electric currents that seem to add decisively to their complexity and eruptive capability (Georgoulis et al., 2012; Török et al., 2014). Later on, opposite magnetic polarities around the PIL may approach each other, interact, and eventually disappear. This can be explained by the magnetic flux cancellation process (e.g. van Ballegooijen and Martens, 1989; Green et al., 2011; Yardley et al., 2018a) that reflects increased magnetic field complexity around the PIL. Another mechanism of filament channel formation is helicity condensation (Antiochos, 2013) whereby helicity is injected locally into the corona via small-scale photospheric magnetic field motions and/or flux emergence. Once injected, helicity is then transferred and condenses onto large-scale PILs.

These physical processes (e.g., flux emergence, flux cancellation, formation of non-neutralized currents, helicity condensation), not only accumulate free magnetic energy over long timescales but can also act as triggers on shorter timescales (days) to bring the pre-existing magnetic field configuration to the point of eruption. Driver mechanisms, which are ultimately responsible for the rapid expansion and upward acceleration of the erupting configuration, are limited to magnetic reconnection (Moore et al., 2001; Aulanier et al., 2010; Karpen et al., 2012), loss of equilibrium (Forbes and Isenberg, 1991) or an ideal instability (e.g. the kink or torus, see Sakurai, 1976; Török and Kliem, 2005; Kliem and Török, 2006; Kliem et al., 2014). Magnetic reconnection can form a vertical current sheet below the eruptive configuration (e.g. Moore et al., 2001), and/or in the external field above the eruptive configuration (e.g. Antiochos et al., 1999). For a full list of trigger and driver mechanisms see Table 1 in Green et al., 2018 and references therein).

A major pillar of research in solar eruptive phenomena, inspired by both CME initiation models and observations, focuses on analyzing the pre-eruptive state (e.g., see the recent reviews on various aspects of this topic by Schmieder et al., 2015; Cheng et al., 2017; Green et al., 2018; Toriumi and Wang, 2019; Georgoulis et al., 2019; Patsourakos et al., 2020). The pre-eruptive phase can be

considered complete when the ascending and eventually erupting structure reaches speeds of the order 100 km s^{-1} (Fig. 1 and related discussion in Patsourakos et al., 2020). This takes into account the kinematic behaviors of both slow and fast CMEs.

The nature of the pre-eruptive magnetic configuration has been a topic of fierce debate for many decades. Two coronal magnetic field configurations can exist prior to eruption: a sheared magnetic arcade (SMA), that can be defined as loops whose planes deviate significantly from the direction normal to the PIL on the horizontal field of view (e.g., Amari et al., 1991; Moore and Roumeliotis, 1992; Antiochos et al., 1999; Lynch et al., 2008; Wyper et al., 2017; Zhou et al., 2018), or a magnetic flux rope (MFR), namely, twisted magnetic field lines winding around a central axial field line (e.g., Forbes and Isenberg, 1991; Fan and Gibson, 2004; Manchester et al., 2004; Török and Kliem, 2007; Aulanier et al., 2010; Amari et al., 2018). The top two rows of Fig. 4 show examples of pre-eruptive SMA and MFRs from MHD simulations. Both configurations can sustain filament channels above PILs and both have occasionally been recognized as integral parts of the pre-eruptive configuration.

There is almost no debate regarding the nature of the erupting magnetic configuration, which is a MFR, that is either created during an eruption originating in a SMA or an evolving destabilized MFR, as suggested by both modeling and observations (e.g., Karpen et al., 2012; Vourlidas et al., 2013; Török et al., 856(1)). Broadly speaking, a SMA forms under the action of shearing motions at the photospheric footpoints of a magnetic arcade (e.g., Antiochos et al., 1999; DeVore and Antiochos, 2000) whereas an MFR forms in the solar atmosphere either when a twisted flux tube fully emerges from the convection zone (e.g., Fan and Gibson, 2004; MacTaggart and Hood, 2009) or by magnetic reconnection occurring in a SMA (e.g., van Ballegooijen and Martens, 1989; Aulanier et al., 2010; Archontis and Syntelis, 2019).

Given that specific conditions need to be met for a SMA to give rise to a CME, for example magnetic reconnection could occur between the SMA and an overlying magnetic null (e.g., Antiochos et al., 1999; Karpen et al., 2012), or ideal instability thresholds could be exceeded for an MFR to destabilize and give rise to a CME, such as the twist of a MFR or the decay index of the strapping magnetic field above a MFR (e.g., Török et al., 2004; Kliem and Török, 2006). Identifying the pre-eruptive magnetic configuration is an important milestone in our quest to predict CMEs with physics-based schemes. This is a formidable challenge at the same time, given several difficulties arising on both observational and modelling fronts. For example, the current lack of routine observations of vector magnetic fields above the photosphere, or models employing ad hoc initial and boundary conditions. This prompted the formation of an International Space Science Institute (ISSI) Team in order to address this issue (Patsourakos et al., 2020). A central conclusion of Patsourakos et al. (2020) was that observations and modeling could be better reconciled if a *hybrid*, time-dependent magnetic configuration encompassing both SMA and MFR segments i.e. a pre-eruptive structure that continuously evolves from a SMA to a MFR was considered (e.g., third row of Fig. 4).

2.3. Rationale and parameters for assessment of the pre-eruption state

Detailed observations and empirical knowledge on solar magnetic structures nearly coincided with pioneering applications of the Zeeman effect toward photospheric vector magnetography. This eventually led to the identification of photospheric features related to eruptive (at that time it was only flaring) active regions. Künzel (1960) noticed the formation of a common penumbra in umbrae of opposite polarities, while Severny (1964) mentioned that flares were occurring in complex active regions with enhanced linear polarization signal, meaning strong transverse magnetic fields, or strong horizontal fields near disk center. Major developments came along in the 1980s, with the concept of the δ-sunspot featuring a strong photospheric PIL (Jaeggli and Norton, 2016; Zirin and Liggett, 1987). It was then only a matter of time before such features were quantified, in the framework of sunspot classification and its probabilistic relation to flare occurrence (McIntosh, 1990; Bornmann and Shaw, 1994). An intriguing observation by Wang et al. (1994) firmly placed the shear observed invariably along flux-massive photospheric PILs into play, by showing a seemingly counter-intuitive result of shear along the PIL increasing after a major flare. Between the early 1990s and the early 2010s, an extended collection of potentially predictive photospheric parameters, predominantly referring to one component (the line-of-sight [LOS]) or the full photospheric magnetic field vector, were proposed and tested as potentially efficient flare and eruption predictors. An effort to classify these parameters was made by Georgoulis (2012) who discussed fractal (monoscale) and multifractal (multiscale), pure morphological and helioseismic parameters. More recent works in these directions include Schunker et al. (2016) for helioseismology and the photospheric electric fields of Kazachenko et al. (2014) and Fisher et al. (2020), in terms of photospheric morphology. Numerous parameters derived from vector field data were collected (mostly based on prior studies) and processed en masse by means of discriminant analysis by Leka and Barnes (2003a,b) and LaBonte et al. (2007), who found that the photospheric magnetic status of an active region at any given instant in time provides useful but limited information on the ability of the region to erupt. Still, this has led to a near-realtime flare prediction facility by using the Discriminant Analysis Flare Forecasting System (DAFFS; Leka et al., 2018). In parallel, Falconer and collaborators, in a series of papers, (Falconer, 2001; Falconer et al., 2002; Falconer et al., 2003) connected the advance prediction of CMEs, alongside flares, to photospheric magnetic field parameters

exclusively related to PILs, such as their length and gradient. Later, a similar scheme implemented as the Magnetogram Forecast (MAG4) model (Falconer et al., 2014) (there is currently another variant of the model named MagPy, a Python package that provides tools for geomagnetic data analysis) issued predictions on all flares, eruptive flares (CMEs) and SEP events.

The advent of the Helioseismic and Magnetic Imager (HMI) (Scherrer et al., 2012; Schou et al., 2012) onboard the Solar Dynamics Observatory (Pesnell et al., 2012), with its daily 1.5 TB of high-cadence, constant-quality data initiated a new era of photospheric metadata inference. The first relevant HMI data product was the HMI active region patch (HARP; Hoeksema et al., 2014) that implemented a pipeline providing timeseries of regions of interest (including active and smaller magnetic regions, lacking sunspots and hence a NOAA active region number) where the signal was strong enough to allow inversion and azimuth disambiguation of the magnetic field vector for further processing. In conjunction, a selection of Space-Weather Active Region Patch (SHARP; Bobra et al., 2014) parameters, judged from earlier works to be relevant to flare productivity (Leka and Barnes, 2007, and references therein) are provided as metadata calculated from the HARP data. A similar reasoning led to the extension into the Michelson Doppler Imager (MDI) (Scherrer et al., 1995) LOS magnetogram database onboard the Solar and Heliospheric Observatory (SOHO) and provided the Space Weather MDI Active Region Patch (SMARP; Bobra et al., 2021) pipeline that shares three parameters (out of seven in total) with the SHARPs pipeline. In this way, there are common predictive parameters (given, of course, the different instrumental specifications) extending over more than two solar cycles (23 and 24) and nearly three decades. SDO data have also been used in computer vision applications providing meaningful object and event metadata, such as the Heliophysics Events Knowledgebase (HEK; Martens et al., 2012; Hurlburt et al., 2012) that has operated since the start of the SDO mission and provides extensive sets of parameters to be used for forecasting and other purposes.

Further work has been performed in this respect, with a major effort of generating metadata parameters undertaken by the EU Flare Likelihood and Region Eruption Forecasting (FLARECAST) project. For an overview of the project and the works it spawned, see Georgoulis et al. (2021). The project generated a total of 209 parameters relying on the near-realtime HARP data products, intended for operational use. FLARECAST pledged to incorporate virtually every parameter present in the literature. As a result, on top of the SHARPs and parameters proposed independently, the FLARECAST property database (accessible via an Application Programming Interface [API]) included parameters proposed by Kontogiannis et al., 2017, 2018; Korsós et al., 2015; Park et al., 2018 Korsós et al. (2015, 2017, 2018, 293(8)) that exploit additional proxies of magnetic energy, helicity, photospheric electric currents and shear, primarily relevant to PILs.

The search for predictive parameters of solar eruptions is ongoing (see e.g., Green et al., 2018; Kontogiannis, 2023, for recent reviews). Efforts to model the morphology of the pre-eruptive state of active regions have turned to nonlinear force-free (NLFF) field extrapolations of the photospheric magnetic field (e.g., Yan et al., 2001; Canou et al., 2009; Chintzoglou et al., 2015; James et al., 2018; Woods et al., 2020) due to the difficulties in directly measuring the magnetic field in the corona. One widely adopted approach is magnetofrictional relaxation (Yang et al., 1986), which can be used to model the coronal magnetic field, either globally (e.g., Mackay and van Ballegooijen, 2006a; Mackay and van Ballegooijen, 2006b), or at active-region scales (e.g., Mackay et al., 2011; Cheung and DeRosa, 2012). The magnetofrictional approach can employ a time sequence of either line-of-sight or vector magnetograms (see e.g., Mackay et al., 2011; Gibb et al., 2014; Pomoell et al., 2019; Price et al., 2020) as the lower boundary conditions to evolve the coronal magnetic field through a continuous series of NLFF states. When used to study active regions that were a priori known to be eruptive, the models show flux rope formation resulting from the process of flux cancellation, and flux rope eruption on a timescale roughly matching that of observed CMEs (e.g., Yardley et al., 2018b; Yardley et al., 2021a). This method can differentiate eruptive configurations from non-eruptive configurations using a Lorentz force-related metric that allows an eruption early warning time of up to 16 h (Pagano et al., 2019; Pagano et al., 2019).

Another metric that has been proposed is the helicity ratio of Pariat et al. (2017). The helicity ratio is the helicity associated with the current-carrying part of the magnetic field divided by the total helicity in the volume (i.e. the relative helicity in the corona). Once a threshold in this ratio is reached, the magnetic configuration becomes ”prone” to eruption. There are several studies now on this topic including Moraitis et al. (2019); Thalmann et al. (2019); Gupta et al. (2021); Green et al. (2022) that show promise toward an enhnaced understanding of the eruption process.

Guided by the models discussed in Section 2.2, a MFR is susceptible to the torus instability if the overlying, strapping field decreases sufficiently rapidly. This has been parameterized either in terms of the decay index itself, or as the height at which a critical decay index is reached (Liu, 2008; Wang et al., 2017; Baumgartner et al., 2018; James et al., 2022). An extension of this is the r_m parameter, characterizing ratio of twist to overlying field, proposed by Lin et al. (2020), and its extensions, namly the r- and q-schemes (Lin et al., 2021). In the breakout model of Antiochos et al. (1999), magnetic reconnection occurs at a null point present in the external, overlying coronal field, allowing an SMA to erupt. The existence of coronal null points as compared to the occurrence of eruptions was considered by Ugarte-Urra et al. (2007). Finally, for an eruption to develop into a full-blown CME, as compared to a failed eruption, it may be that access to open flux is necessary, as considered by DeRosa and Barnes (2018).

Further exploration of CME initiation models using magnetofrictional and magnetohydrodynamic approaches has recently been carried out by the NASA Living with a Star Focused Science Team and is detailed in the review by Linton et al. (2023). The team investigates the roles that magnetic helicity and topology play in CME initiation via shearing, MFR formation and magnetic flux emergence. One of their main findings is that an ideal instability is not necessary for CME onset: fast flare reconnection, where the current sheet is formed due to breakout reconnection, could well be the driver mechanism responsible.

There are also ongoing efforts aiming toward an unambiguous identification of short-term observational eruption precursors. This search is mainly beyond the optical wavelengths of photospheric observations and involves EUV and soft X-ray parameters and proxies, as discussed 2.4 below.

2.4. Precursors of eruptive activity

The difference between an eruption predictor and a short-term eruption precursor is that the former can have a predictive effect of several hours, or even days, whereas the latter hints of an upcoming event within tens of minutes to a few hours. Given that the characteristic flows and respective timescales in the photosphere are much slower than those of the overlying corona, mainly due to photospheric line-tying and Alfvén time differences because of different Alfvén speeds between the photosphere and the corona, photospheric parameters are expected to be less effective in indicating an imminent eruption. In the corona, on the other hand, a number of effects have been proposed, even though virtually none unambiguously. Ambiguity stems from the fact that while proposed precursors seemingly occur before eruptions, they cannot be readily ruled out in quiescent intervals, lacking an eruption.

One of the safest precursors of a CME ascending in the corona, before it appears in the coronagraph field of view, is the transient coronal dimmings. Coronal dimmings are temporary regions of strongly reduced emission in soft X-rays and extreme-ultraviolet (EUV) wavelengths caused by expansion and evacuation of plasma associated with CMEs (e.g., Hudson et al., 1996; Thompson et al., 1997; Aschwanden et al., 2009; Tian et al., 2012). They resemble the evolution of the early CME propagation in the low corona and it was shown that characteristic properties derived from their analysis can yield useful information (e.g., Thompson et al., 2000; Harrison and Lyons, 2000; Zhukov and Auchère, 2004; Mason et al., 2016). For example, Dissauer et al. (2019) recently found strong correlations between dimming coverage and intensity with the resulting CME's mass, as well as strong correlations between the dimming dynamics and the resulting CME's speed. For flares, this is less straightforward (see, however Chen et al., 2019, for some potentially interesting results, that are subject to further evaluation).

Very recently, a large database of parameters based on 8.5 years of AIA images (specifically timeseries cut-outs centered on HMI-defined HARPs; Dissauer et al., 2023) were constructed and tested in the context of identifying pre-flare signatures (Leka et al., 2023). Employing discriminant analysis, statistical evidence showed that flare-imminent regions were brighter in E/UV images (the "big region" effect) but also that small-scale intense brightenings were frequently present in the hours prior to solar flares.

Several observations of eruptions that are preceded by weak transient brightenings at the active region's core (e.g. Moore et al., 2001; Chen et al., 2016; Xue et al., 2017) have been interpreted in terms of magnetic reconnection between sheared loops in the active region's core that creates a flux rope which subsequently erupts (Mikic and Linker, 1994; Jacobs et al., 2006). Events occurring in multipolar magnetic configurations (e.g. Ugarte-Urra et al., 2007) or involving precursor transient brightenings appearing away from the central PIL (e.g. Sterling and Moore, 2004) have been interpreted in terms of the expansion of a sheared arcade which erupts after it disrupts the overlying magnetic field by reconnection at a null point (e.g. Antiochos et al., 1999; Lynch et al., 2008).

The existence of active region flux ropes is based on several lines of observational evidence: (1) filaments showing winding threads (e.g. Xue et al., 2016) or destabilizing to straightforwardly connect to eruptive flares (Sinha et al., 2019); (2) soft X-ray sigmoids whose middle part crosses the PIL in the inverse direction (Green and Kliem, 2009; Green et al., 2011) or whose apparent end-to-end twist is very strong (Kliem et al., 2021); (3) flux-rope-like coherent hot channels or hot blobs that appear in EUV passbands (94 and 131 Å) that probe hot (~10 MK) flare plasmas, but not in passbands that probe cooler (< 2 MK), quiet coronal plasmas (e.g. Cheng et al., 2011; Cheng et al., 2012; Cheng et al., 2014; Cheng et al., 2014; Cheng et al., 2014; Zhang et al., 2012; Patsourakos et al., 2013; Nindos et al., 2015; Nindos et al., 2020; Wang et al., 2019; Yan et al., 2021). Most observations of hot channels reveal that the flux rope forms a few minutes (e.g. Zhang et al., 2012; Cheng et al., 2013; Cheng et al., 2015) to several hours (up to more than 11) prior to the eruption (e.g.] Patsourakos et al., 2013, Cheng et al., 2014b, James et al., 2018, Nindos et al., 2008 although formations during eruptions have also been reported (e.g. Song et al., 2014). Patsourakos et al. (2020) provides a list of observational signatures of pre-eruptive SMAs and MFRs, but in most cases it is difficult to identify the pre-eruptive configuration as purely consisting of a SMA or a MFR.

As explained, photospheric magnetograms contain direct information on the *morphology* of an active region and, indirectly through magnetic field modeling, on the amount of energy that is progressively stored before being released during a flare. However, such measures have limited bearing on the physical processes that happen before the eruption onset. An interesting finding was reported

recently by Liu et al. (2023), in which the local average twist parameter around the PIL showed consistent decrease in magnitude < 10 hours prior to eruptive flares, followed by an almost step-change increase immediately (1 - 2 h) thereafter. Importantly, no such behavior is seen in confined flares. While potentially hard to decipher on a case-by-case basis, this pattern warrants further investigation, both physical and operational, and might lead to a potentially viable precursor of impending eruptive flares.

Thermodynamic processes, such as changes in the temperature and density profiles of the plasma in the active region that produces the flare, are also among the phenomena that precede the onset of an event. Hence, consideration of changes in the thermodynamic environment could potentially boost the performance of flare prediction algorithms. Such improved predictive capability is particularly crucial in the case of *near-realtime* flare forecasting, where the predictive window is only a few tens of minutes and the prediction of both the size of the flare and its time of onset, need to be precise to the extent possible. In this respect, different solar data, such as EUV observations and active region emission spectra have been used in recent approaches by Nishizuka et al. (2017) and Panos and Kleint (2020), respectively.

The thermodynamic state of solar active region plasma is manifested in the intensity of spectral lines emitted by specific atomic species, each of which is formed over a relatively narrow range of temperature. Thus, thermodynamic changes can be detected through variations of multi-spectral data such as those registered by the Atmospheric Imaging Assembly on board the Solar Dynamics Observatory (SDO/AIA; Lemen et al., 2012), which has provided full–disk images of the Sun in seven different EUV wavelengths every 12 s since its launch in 2010. The intensity measured in each AIA channel ($I_i, i = 1, \ldots, 7$) is related to the Differential Emission Measure (DEM; Phillips et al., 2008) by the linear transformation

$$I_i(x, y; t) = \int \mathrm{DEM}(x, y, T; t)\, G_i(T)\, dT, \qquad (1)$$

where (x, y) are the coordinates of a specific pixel in the image plane, t is time, T is the temperature, and G_i is the temperature response function of the i-th AIA channel (although typically, six AIA channels are used, excluding the 304 Å one). Thermodynamic changes in the plasma state (and, hence, the DEM) produce variations of the intensities of each AIA channel, per Eq. 1.

A potentially promising approach for near-realtime solar flare prediction stems from Section 5 of Massa and Emslie (2022): from a datacube of AIA images this study produces a datacube of DEM inferences that can more effectively (using less space) reveal features in frequency space (e.g., changes in the characteristic size of objects in the field of view) that would be less straightforward to identify using spatial images. ML methods could play a meaningful role in this case. Another effort that uses DEM for short-term flare predictions is that of Gontikakis et al. (2020) who use statistical methods to quantify the apparent increase of the DEM prior to a major flare (Syntelis et al., 2016; Fletcher et al., 2011).

There are also multiple reports that radio observations may show a potential to identify possible precursors of eruptive activity (e.g. see the reviews by Klein et al., 2018; Vourlidas et al., 2020; Klein, 2021a, 2021b). This is because the most important drivers of space weather, CMEs and flares, produce radio emission (e.g. see Nindos et al., 2008, and references therein) in a frequency range from tens of kHz (in the vicinity of Earth) to hundreds of GHz (in the chromosphere).

Radio observations helped establish the picture that, in gradual SEP events with energies ranging from a few hundred keV to several tens of MeV, particles are primarily accelerated by CME-driven shocks traced by type II bursts (e.g. see Gopalswamy, 2022, and references therein). At higher energies (> 1 GeV), the timing of relativistic SEP events is more consistent with that of type IV bursts (i.e. radio emission by electrons trapped in large-scale loops) suggesting that coronal acceleration in the wake of the CME has a major contribution to the energies of the particles (Klein, 2021).

Practically all SEP events are associated with type III bursts generated by beams of electrons along open magnetic field lines. Type IIIs occur within minutes from the impulsive phase of the flare and their use as CME precursors has been questioned (Pohjolainen et al., 434(1),; Aurass et al., 2013). However, they may provide information about the travel path of the energetic particles and in the case of simple, short events, they may also help in the identification of the electron acceleration regions. Additionally, since type III bursts signify the presence of open magnetic field lines, their existence suggests that SEPs are possibly released from the solar corona and are injected into the interplanetary medium. As a result, the timing of Type III bursts provides an indication of the time the particles left the Sun.

Overall, identifying solar eruption precursors in multiple non-optical wavelengths is an ongoing endeavor, and spectroscopic data have an important role to play. Expectations of future EUV specroscopy missions such as the Multi-slit Solar Explorer (MUSE) mission (De Pontieu et al., 2022), for example, are such that it will be able to provide bulk and non-thermal flow maps in entire active regions at sub-arcsecond spatial scales and cadence of the order 10 s. Such observations should enlighten significantly both the pre- and post-eruptive states.

3. Prediction of solar flares and eruptions

In Section 1 it was established that different solar energetic events, from flares to CMEs to SEP events, have different spatiotemporal scales of relevance, dictating the specifics of the different prediction efforts. In this review, we discuss only prediction efforts relying on properties or

Table 1
A categorization attempt of solar flare prediction methodologies. Only methods that employ exclusively solar features and events are included. There are a few duplicate references in different sub-categories, in case multiple prediction methods are employed and used in conjunction.

Solar flares		
Prediction Method	Input Data	References (suggested)
Physics-based		
Sandpile/Avalanche models	Assimilation & synthetic data; GOES X-ray time series	Bélanger et al. (2007), Strugarek and Charbonneau (2014), Morales and Santos (2020), Thibeault et al. (2022)
Statistical		
Fractal/ Multifractal	LOS magnetograms;	McAteer et al. (2005), McAteer et al. (2010), Conlon et al. (2010)
Bayesian	Poisson probabilities; LOS magnetograms	Wheatland (2004), Wheatland (2005), Georgoulis and Rust (2007), Georgoulis (2012), Kontogiannis et al. (2017)
Discriminant Analysis	LOS magnetograms; SHARP metadata & HARP data & NOAA/SWPC metadata & GONG Dopplergrams	Leka and Barnes (2003b); Barnes et al. (2007); Leka et al. (2018); Komm et al. (2011); Welsch et al. (2009); Barnes and Leka (2006)
Superposed Epoch Analysis	LOS magnetograms	Mason and Hoeksema (2010), Reinard et al. (2010)
Best fit	Sunspot properties, HARP magnetograms, assimilation & synthetic data from avalanche/ sandpile models	Bélanger et al. (2007), Strugarek and Charbonneau (2014), Korsós et al. (2015), Korsós et al. (2020), Morales and Santos (2020), Thibeault et al. (2022)
Decision boundary	LOS magnetograms & NOAA/SWPC metadata	Huang and Wang (2013)
Poisson	Sunspot properties; NOAA/SWPC data; Forecaster in the loop	Gallagher et al. (2002), Wheatland (2004), Wheatland (2005), Berghmans et al. (2005), Bloomfield et al. (2012), Crown (2012), Lee et al. (2012), Devos et al. (2014), Murray et al. (2017), Kubo et al. (2017), McCloskey et al. (2018), Falco et al. (2019)
Timeseries/ Evolution	HMI magnetograms; SHARP metadata & HARP data & NOAA/SWPC metadata, NOAA/SWPC metadata; SHARP metadata & timeseries forest	Muranushi et al. (2015), McCloskey et al. (2018), Leka et al. (2018), Cinto et al. (2020), Ji et al. (2020) (All Clear)
Artificial Intelligence		
Machine Learning		
Supervised	LOS magnetograms; LOS magnetograms & continuum; LOS magnetograms & sunspot properties; Solar Monitor metadata; SHARP metadata; NOAA/SWPC metadata; HARP magnetograms; HARP magnetograms & AIA images; SHARP metadata & polar HMI magnetograms; IRIS data; LOS magnetograms & AIA images; SHARP metadata, HARP magnetograms & computational topology; LOS magnetograms & sunspot properties	Qahwaji and Colak (2007), Colak and Qahwaji (2009), Li et al. (2007), Song et al. (2009), Yu et al. (2009), Yuan et al. (2010), Steward et al. (2011), Steward et al. (2017), Ahmed et al. (2013), Lee et al. (2013), Bobra and Couvidat (2015), Boucheron et al. (2015), Al-Ghraibah et al. (2015), Raboonik et al. (2016), Nishizuka et al. (2017), Liu et al. (2017), Barnes et al. (2017), Florios et al. (2018), Campi et al. (2019), Domijan et al. (2019), Alipour et al. (2019), Cinto et al. (2020), Deshmukh et al. (2020), Abduallah et al. (2021), Korsós et al. (2021), Aktukmak et al. (2022), Huwyler and Melchior (2022), Sinha et al. (2022)
Hybrid (Supervised & Unsupervised)	NOAA/SWPC metadata; SHARP metadata; HARP magnetograms	Li et al. (2011), Benvenuto et al. (2018), Campi et al. (2019), Deshmukh et al. (2022)
Deep Learning		
Video Classification	HARP magnetograms	Guastavino et al. (2022)
Deep Neural Networks	LOS magnetograms; Solar Monitor metadata; HARP magnetograms & AIA images; Full-disk HMI images; HARP magnetograms & Intensity; SHARP metadata timeseries; SWPC GOES timeseries	Huang et al. (2018), Nishizuka et al. (2018), Zheng et al. (2019), Domijan et al. (2019), Yi et al. (2020), Nishizuka et al. (2020), Nishizuka et al. (2021), Abed et al. (2021), Pandey et al. (2021), Pandey et al. (2022), Chen et al. (2022), Abduallah et al. (2023)
Knowledge-informed	Magnetogram Images	Li et al. (2022)
DL model fusion	HARP magnetograms & SHARP metadata; SHARP & SMARP metadata; HMI and MDI images	Tang et al. (2021), Sun et al. (2022), Liu et al. (2022)
Long short-term memory network	SHARP metadata with or without flare history	Liu et al. (2019), Jiao et al. (2020), Wang et al. (2020)
Ensemble		
Predictor teams	LOS magnetograms	Huang et al. (2010)
Combination of probabilistic predictions from different methods	AR or full-disk probabilities & SWPC flare data;	Guerra et al. (2015), Guerra et al. (2020)

metadata from the photosphere and the lower solar corona that aim to predict these energetic events *before* they occur. Prediction of properties such as arrival time of CMEs and their potential geoeffectiveness are considered in the Cluster review of Temmer et al. (2023). In addition, efforts to predict SEP events in general are discussed in the Cluster

Table 2
Same as Table 1 but for solar flare-related prediction methodologies.

Solar flare-related		
Prediction Method	Input Data	References (suggested)
Statistical		
All Clear	SHARP metadata	Ji et al. (2020)
Flare index	SHARP metadata	Chen et al. (2021a), Zhang et al. (2022)
GOES X-ray timeseries	Solar Monitor metadata features	Higgins et al. (2011)
Validation/Evaluation of Flare Forecasts	Different methods on common data of operational methods	Barnes et al. (2016)
		Leka et al. (2019), Leka et al. (2019), Park et al. (2020)
INCLUDING CORONAL MASS EJECTIONS		
Statistical		
Discriminant Analysis	Filament descriptors; SHARP and other metadata	Barnes et al. (2017), Lin et al. (2020), Lin et al. (2021)
Best fit	LOS magnetograms; sunspot properties; flare history	Falconer (2001), Falconer et al. (2003), Falconer et al. (2012)
Machine Learning		
Supervised	Filament descriptors; SHARP and other metadata	Bobra and Ilonidis (2016), Barnes et al. (2017), Liu et al. (2020)
INCLUDING CMEs AND SEP EVENTS		
Statistical		
Bayesian	LOS magnetograms	Anastasiadis et al. (2017), Papaioannou et al. (2022)
Best fit	LOS magnetograms; SWPC flare metadata; CME properties	Falconer et al. (2014), Kahler and Ling (2015), Kahler et al. (2017), Richardson et al. (2018) (just SEP events)
Timeseries/ Evolution	SWPC flare & GOES proton data (dynamic forecasting)	Kahler and Ling (2015), Paassilta et al. (2023) (just SEP events)
Machine Learning		
Supervised	SHARP metadata; SMARP metadata; CME properties; SWPC flare metadata	Inceoglu et al. (2018), Papaioannou et al. (2022), Lavasa et al. (2021), Kasapis et al. (2022), Torres et al. (2022), Abduallah et al. (2022) (just SEP events)

review of Whitman et al. (2022) and are summarized in Section 3.3.

Here we focus on strategies and methodologies rather than on each and every one of the prediction methods, which would be impractical. These methodologies are broadly categorized into four categories:

- *Physics-based*, typically involving data-driven models constructed from first principles or empirically;
- *Statistical*, comprising different classical methods or recent variants thereof, aiming to infer a probabilistic prediction ($0 < p < 1$) by means of statistical correlations between flaring activity and photospheric information;
- *Artificial Intelligence*, comprising both ML and DL methods. ML implementations include in principle supervised (where input data is labeled, e.g., flaring or not flaring), unsupervised (where input data is not labeled) and hybrid methods. To our best understanding, there are currently no purely unsupervised ML methods applied to the prediction of space weather events. DL methods are typically based on artificial neural networks. In the case of AI strategies, the result is often binary, i.e., 1 (YES) or 0 (NO), besides the typical probabilistic predictions;
- *Ensemble*, involving the combination of different predictions or predictors. Two type of ensemble predictions can be made: single-model or multi-model ensembles.

The majority of these methodologies include data or metadata with a physical standing, constructed from first principles.

A reasonable attempt to put together all these methods under the above categorization is presented in Tables 1 and 2. Table 1 covers methodologies for solar flare prediction alone, while Table 2 covers flare-related prediction methodologies, including methodologies for CMEs and SEP events.

3.1. Solar flares

Solar flare prediction is humanity's first attempt to predict the adverse space weather. Hence, the larger number of works in Table 1 compared to Table 2 reflects efforts to predict flares in general, without distinguishing between confined and eruptive events. Flare prediction efforts are mostly probabilistic for the occurrence of a flare of certain class or above over a certain period of time. Forecast windows vary between a few hours (i.e., 6) and a few days (i.e., typically up to 3), although uncertainties increase toward both ends. At shorter forecast windows, uncertainties are due to the inherent stochasticity of the flare phenomenon (e.g., Lu and Hamilton, 1991; Vlahos et al., 1995; Vlahos and Georgoulis, 2004), owning to the unobservable spatial scales at which a flare starts. At longer forecast windows, uncertainties occur because this time span is significantly

longer than characteristic timescales of the magnetic flux evolution in active regions, that vary in the range of 10 – 20 h. This is the typical timescale of evolution within a 30 Mm supergranule (supergranules are viewed as the building blocks of active regions; Bumba and Howard, 1965; van Driel-Gesztelyi and Green, 2015) under nominal photospheric flows of the order 0.5 – 1 km/s.

Flares are nominally predicted for GOES classes C1.0 and above. Classes M1.0 and above are often characterized as major flares, while X5.0 and above (X5+) are known as great flares (Zirin and Liggett, 1987; Wang et al., 2006). Flares closer to C1.0 have much better statistics (several thousand over a typical solar cycle) but their occurrence frequencies tend to be suppressed in periods of moderate and high activity, when the GOES soft X-ray background can routinely exceed C1.0 level ($10^{-6}\ W/m^2$). Flares above X5.0 occur a few times (up to a few tens, at most) in a typical solar cycle. The relatively weak solar cycle 24 produced just five X5+ flares; cycle 23 before it produced 18. These (un) characteristically poor statistics place X5+ flares into the "black swan" category, for which methodologies such as the extreme value theory (Griffiths et al., 2022) could be a possibility.

The general methodological categories that apply to flare prediction can be divided into further sub-categories (i.e., Table 1). Physics-based methods are relatively unexplored, with the majority concentrated in exploring two-dimensional avalanche models (e.g., Morales and Santos, 2020; Bélanger et al., 2007; Abramenko et al., 2003). However, only the methods listed in Table 1 have been properly applied to observational data, resulting in predictions. On the other hand, for statistical methods, there are (roughly in terms of numbers of published papers):

- Poisson probabilities, applied to sunspot properties and data that may be coming from lookup tables (e.g. historical flaring rates) and forecasters in the loop (in a passing comment, see the seminal work of Rosner and Vaiana, 1978, on the potential origin of flares and their statistical properties);
- Curve fitting (best fit), applied to metadata properties, magnetogram- or synthetic-data-extracted parameters. In this category we have included methods dealing with synthetic data and stochastic self-organized critical (sandpile) models;
- Fractal and multifractal methods, in which the spatial and/or temporal scaling behavior of the photospheric normal-to-surface (or LOS, alternatively) magnetic field component is typically exploited;
- Bayesian methods, in which Bayes theorem, or a simplification thereof, such as Laplace's rule of succession for threshold-dependent probabilistic forecasting, are applied to either Poisson probabilities of flares or to metadata from LOS (or vector, possibly) magnetograms;
- Discriminant analysis, either linear or nonlinear, that is applied to magnetograms, metadata thereof, or the SWPC Solar Region Summary (SRS) metadata;
- Decision boundaries, that relies on a decision tree algorithm and can have both classical and ML variants;
- Superposed epoch analysis, applied to photospheric metadata, in one case referring to local helioseismology results;
- Timeseries and evolution properties, studied on magnetograms, metadata thereof and SWPC metadata, most notably the GOES soft X-ray timeseries.

The above methods typically apply to active-region data, facilitated by either the SHARP or the more recent (but corresponding mostly to solar cycle 23) SMARP data product. There are methods (particularly those employing GOES X-ray data), that refer to the entire Sun. Transforming active-region based predictions to full-Sun (i.e., full-disk) predictions is a mathematically straightforward – but often marginal in practice – problem due to the propagation of various applicable uncertainties in the local (active region-scale) probabilities. ML methodologies have also been applied to this problem (Pandey et al., 2022).

Methods that employ ML techniques can be classified in the following sub-categories:

- Supervised methods, that clearly take the lion's share in ML solar flare prediction. They apply to virtually every data or metadata available and often show promise over traditional statistical methods, although this still has to be determined robustly (see Section 4.2).
- Hybrid methods, that employ both supervised and unsupervised methodologies, the former typically for testing and the latter for training. This is a potentially appealing variant of ML methods and a number of research groups are experimenting on it.

We have not been able to find works that rely purely on unsupervised ML methodologies.

For DL methodologies, most works employ the breadth of the diverse types of deep neural networks. DL methodologies can also be implemented via long short-term memory (LSTM) networks, and these are also involved in methods pursuing a fusion of models, in which multiple DL models are combined in architectures of varying complexity. In one case (Liu et al., 2019), external knowledge in the form of prior flare history is infused into the DL method to provide a so-called knowledge-informed deep neural network for flare forecasting. In a recent study (Abduallah et al., 2023), different prediction windows are tested on a set of different flare thresholds with encouraging results, by applying a transformer-based network to SHARP metadata timeseries.

Ensemble methods for flares are believed to be capable of improving the accuracy of predictions, at the same time

providing applicable uncertainties (Knipp, 2016; Murray, 2018; Guerra et al., 2020). Multi-model methods typically combine probabilities from various other methods, statistical and/or ML, to achieve a more robust and better-constrained overall probability. Single-model methods create ensemble predictions by either perturbation of the input data or by combination of multiple predictors (i.e., multiple linear regression). Despite their potential, some ensemble methods for flare forecasting are yet to transition into operational environments. However, community-driven initiatives such as the Flare Scoreboard at the CCMC (Section 4.3) provide an excellent platform for further development, testing, and validation of these ensembles techniques.

We note that there is a handful of works that do not focus on single flare prediction of a given GOES class but, rather, on related tasks; these can be

- the All-Clear problem for solar flares, which is still a challenge to tackle (see Section 5.1);
- the flare index (Abramenko, 2005), that provides the cumulative flare productivity of a given active region; and
- the NOAA GOES X-ray timeseries (Muranushi et al., 2015), that can be then examined to detect whether a flare of interest is projected in the future.

Finally, of all flare prediction methods listed in Table 1, those that appear to be currently operational, namely, to produce forecasts in near-realtime and at regular intervals with no missing forecasts, are those validated in conjunction by Leka et al. 2019a, 2019b and Park et al. (2020). We briefly discuss the outcome of these validation efforts in Section 4.2.

In an important cautionary note, flare prediction methods applied to multi-year data should be aware of, and act on, the recent calibration note issued by NOAA (Machol et al., 2022), applicable to earlier GOES X-ray Sensor (XRS) data between GOES-1 and GOES-15. This is a significant correction as the 1–8 Å soft X-ray fluxes should be divided by a factor of 0.7. This means, for example, that a GOES-1/-15 M1.0 flare should actually be treated as a M1.4 flare, or that a respective M5.0 flare should be treated as a M7.1 one.

To our understanding, NOAA itself has started recalibrating the data, but it is important that any prediction study uses a versioning method indicating the data was accessed or whether the correction presented in Machol et al. (2022) has been applied. Versioning will facilitate reproducibility of results, although it is understood that some efforts will suffer a bias if training or testing relies on uncorrected data.

3.2. Eruptive flares: coronal mass ejections

A dominant majority of the prediction efforts pursues CME kinematic properties such as the time-of-arrival problem and the CME geoeffectiveness. These works have been captured in the Cluster review by Temmer et al. (2023). A smaller amount of works aim at predicting eruptive flares the same way as flares in general, namely, before they occur. Only a few methods that use statistical and ML methodologies for CME prediction have been published. DL has not been explored for this problem yet. Here, we briefly discuss the main methods that have been implemented in this direction.

In Statistical Methods, the curve fitting works of Falconer et al. (2002) were the first to provide quantitative forecast information on eruptive flares. This method employs the same photospheric parameter (and flare history) as for ordinary flare prediction. The most recent version of this method, MAG4/MagPy, has also been used for SEP event forecasting on top of flares and CMEs, as discussed in Section 4.3 – see also Whitman et al. (2022).

In ML methods, we were able to identify a handful or so works that deal with supervised methodologies. Some methods that also pertain to CME prediction are included in the last section of Table 2 (namely, by Anastasiadis et al., 2017; Inceoglu et al., 2018; Papaioannou et al., 2022) because this part is intended to include methods either considering all eruptive manifestations or focusing specifically on SEP events. For the CME prediction, supervised ML methods use mainly SHARP metadata as input, with exceptions using other metadata. Indeed, works such as Kontogiannis et al. (2019) and Murray et al. (2018) have shown that some parameters not included in the SHARP list, and more importantly their time variation, might provide more relevant information for the AR CME prediction.

3.3. Solar energetic particle events

3.3.1. Prediction before occurrence

Table 2 includes two types of SEP event prediction methods acting before the eruptions happen: those that include all eruption manifestations (flares, CMEs and SEP events) and those that focus only on SEP events and are indicated by the note "(just SEP events)", following each relevant reference.

Methods concerned with all eruption manifestations involve both statistical and ML components. In the statistical methodology class, Bayesian and best-fit methods rely on LOS magnetograms and metadata thereof, either from MDI or from HMI magnetograms. SWPC SRS flare metadata and potential CME properties are used in few models that are only concerned with SEP event forecasting, namely those by Kahler et al. (2015) and Richardson et al. (2018). In one particular case, a so-called "dynamic" SEP forecasting is attempted, in which the model keeps track of the evolving situation in the Sun and continuously updates the SEP event probabilities. In other solar eruption forecasting methodologies, this strategy is similar to a prediction-update rate that is significantly shorter than the prediction window.

In ML methodologies, we find only supervised methods that work with SHARP or SMARP metadata as input, as well as with metadata reflecting the CME properties. Few approaches in this category (Lavasa et al., 2021; Kasapis et al., 2022; Torres et al., 2022) focus only on the prediction of SEP events from photopsheric data without considering any CME information.

3.3.2. General prediction – a summary of Whitman et al. (2022)

The prediction of SEP events involves the monitoring or forecasting of a complex, intertwined sequence of phenomena that include, besides eruptive flares and CMEs, the suprathermal "seed" particle population near the Sun, the state of the solar wind and magnetic structures present within it that determine the magnetic connectivity and particle transport in the inner heliosphere.

The intensity of SEP events correlates with the associated soft X-ray flare characteristics and speed of the CME (Kahler et al., 1984; Cane et al., 2010), with stronger flares and faster CMEs more likely to produce a strong, energetic proton event. The development and intensity of SEP events is influenced by the magnetic connectivity to the particle source with western-located active regions more likely to result in an event at Earth (Cane and Lario, 2006; Richardson et al., 2014). Type II and III radio bursts are strongly correlated with the occurrence of SEP events (Laurenza et al., 2009; Richardson et al., 2014) and the arrival of energetic electrons at Earth are known precursors of energetic protons (Posner, 2007). While there are strong associations between solar phenomena and SEP event characteristics, individual SEP events vary widely and the occurrence of a strong flare or fast CME does not guarantee that a SEP event will be observed. Papaioannou et al. (2016) found that out of 20,429 flares $\geqslant$C1.0 over three solar cycles, 955 of which were reliably paired with CMEs, only 314 were associated with solar particle events at geospace at proton energies of 7 MeV. There remains significant difficulty in predicting SEP characteristics on an event-by-event basis which can be attributed to the complexity of the system that produces them and the rarity of the phenomena. The latter, naturally, gives ground to a significant imbalance in the datasets used for the prediction of SEP events.

Whitman et al. (2022) summarized 36 SEP prediction models that have been developed or are currently under development in the community. These SEP models employ assorted approaches and range from statistical to ML models aiming to produce fast forecasts ahead of the arrival of SEPs at Earth, instead of computationally intensive physics-based science models that aim to reproduce the complete physical picture of particle acceleration and transport to Earth. An overview of statistical, ML, and physics-based SEP prediction model approaches is provided in the introductory material of (Whitman et al., 2022), while detailed sunmaries of each model appear in the main text. The SEP models surveyed perform many types of predictions, including probability of occurrence, binary *All Clear* forecasts, and deterministic values such as threshold crossing time, peak flux, event fluence, duration, and time profiles. Due to the large number of phenomena associated with SEP events, models use one or more of a wide variety of observational inputs, aiming to capture the dominant drivers of SEP events. These observations include optical, EUV and X-ray imagery of the solar photosphere to corona: magnetograms, radio observations, coronograph images, and in situ electron and proton measurements (e.g. Posner, 2007; Laurenza et al., 2009; Marsh et al., 2015; Anastasiadis et al., 2017; Hu et al., 2017; Papaioannou et al., 2018; Sadykov et al., 2021).

Out of the 36 models, Whitman et al. (2022) identified 12 that operate in near-real time. The transition of a SEP model to operations requires more than the development of an accurate prediction algorithm. Models must be able to run continuously and robustly, ingesting only observations that are available in near-real time, and produce forecasts within an actionable, useful time period. Furthermore, validation must demonstrate that predictions satisfy the user's needs, e.g., by forecasting quantities and threshold crossings of interest to the end user. The transition from research to operations (see Sections 4 and 5 below) involves a substantial effort by both model developers and end users, as well as by data providers, because the observational data streams needed to run the models must be readily and reliably available. To achieve all this, the various institutions that hold stake in space weather forecasting must provide support.

Looking forward, SEP event prediction efforts would benefit from reductions in forecasting overhead and delays through minimizing model run times and latency in the availability of real time measurements. Likewise, continued development of science models that probe the physics of SEP event phenomena is important to identify the key physical parameters that determine the attributes of SEP events. All efforts would benefit from improved observations of the Sun and inner heliosphere with better sampling of the relevant physical systems related to SEPs, including 360 degree views of the Sun in EUV, radio, X-ray, and magnetograms, coronagraphs at multiple vantage points that observe lower down in the corona than current space-based capabilities, and in situ observations of particles and fields nearer to the Sun and distributed throughout the inner heliosphere. For a fairly detailed discussion of these issues, see Sections 5 and 6.

4. A possible framework for solar eruption prediction methodologies

4.1. Course of action

Given the immense importance different industry sectors, governments, and the scientific community assign to space weather forecasting, there is a plethora of basic research works worldwide. A cursory search, say, at the

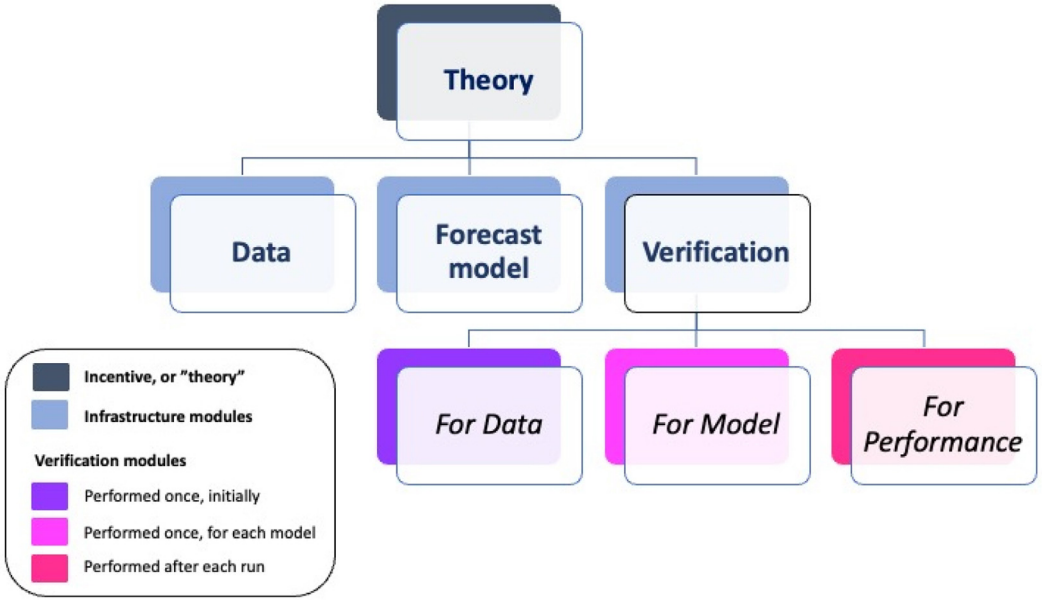

Fig. 5. A general concept applicable to space weather forecasting, starting with a hypothesis-based idea, or incentive, treated as a theory that needs data, implementation into a forecast model and a robust verification process, that includes data, model, and performance at different stages (see legend). After performance verification, a validation (i.e., comparison with similar forecast models relying on the same training and testing data) can be performed.

NASA Astrophysics Data System (ADS) will show that articles with the term 'space weather' in their abstract were in single digits in the 1950s and 1960s, double digits in the 1970s and 1980s and then started increasing exponentially to 3000 papers or more annually by 2020s. Homogenizing all this information and assimilating it in a way that allows targeted and traceable progress is a gargantuan task, particularly in cases where ML/DL methods are involved. This prompts scientific journals to take steps and issue guidelines for papers involving ML and DL methodologies to follow certain principles and be able to demonstrate tangible progress over previous works (see, for example Lugaz et al., 2021).

In the following, we discuss a possible course of action that could facilitate a practical comparison of the value of different methods, including the potential progress they bring. At the core of this proposal lies the classical notion of a theory, namely, a set of rational ideas or concepts based on observations, allowing a hypothesis, and leading to testable predictions. Hypothesizing, for example, that one or a vector of parameters has predictive value over a space weather manifestation (flares, CMEs, SEP events, or all of them) we need to test whether this can be proved quantitatively. To this purpose, we need a prediction method of any level of sophistication, as shown heuristically in Fig. 5.

The forecast model can be anything, virtually, including ML or DL. The data sets used for training and testing, however, should be well curated, following the basic principles of a benchmark data set. A benchmark dataset is an integral part of data mining (e.g., Chen et al., 1996; Roiger, 2017) and is intended for tests and comparisons between different methods or platforms on the exact same basis, making sure that they are reproducible, effective and efficient. Comparing models on different positive/ negative event samples or non-benchmarked data sets is, in fact, of little meaning (see, e.g., Nita et al., 2020, for a white-paper discussion of this issue). Benchmark data sets are well understood and tested in terms of the veracity of their event labels (e.g., flare/ no flare, etc.). Data sets of eruptive events with varying readiness levels that can be used as benchmarks have been published for flares (Barnes et al., 2016; Rotti et al., 2020; Angryk et al., 2020; Georgoulis et al., 2021, combining SOHO, SDO and NOAA/GOES databases), CMEs (Robbrecht et al., 2009; Rodriguez et al., 2022, relying on science-grade data from SOHO/LASCO and STEREO coronagraphic observations), and SEP events (Vainio et al., 2013; Crosby et al., 2015; Papaioannou et al., 2016; Rotti et al., 2022, relying on the in situ proton detectors onboard SOHO, ACE, Wind and the NOAA GOES satellites). In some cases, the event labels are combined with photospheric metadata parameters allowing methods to use directly the metadata (Angryk et al., 2020; Georgoulis et al., 2021), while in others the labels, time stamps, and photospheric magnetograms are provided for different methods to process, create their own metadata, and test predictive skills (Barnes et al., 2016; Leka et al., 2019). Near-realtime SDO/HMI data have been used for methods implemented already in, or intended for, operational settings, while definitive data are used mainly for testbed purposes and method development.

4.2. Data, model and performance verification

Following the data and the forecast model, the integral task of verification includes all three different aspects: data, model, and performance (Fig. 5). Data verification is essen-

Table 3
2×2 contingency table of a binary forecasting

		Observation		Totals
		YES	NO	
PREDICTION	YES	Hits (TP)	False Alarms (FP)	**Predicted**
	NO	Misses (FN)	True Negative (TN)	**Not Predicted**
TOTALS		**Observed**	**Not Observed**	**Grand Total (N_{tot})**

tially making sure that one has a statistically significant benchmark data set to work with, or that the event/ no-event samples are statistically significant and verified. Sufficient event sample generation is often a hurdle, given extremely class-imbalanced samples of rare events (e.g., X-class flares or SEPs).

Model verification pertains to making sure that the model works as expected. This generally implies a two-tier verification, namely, one theoretical and one practical (e.g., Thacker et al., 2004). In the theoretical aspect, one confirms that the mathematical background and/or physical laws used by the model are implemented correctly. In the practical aspect, one makes sure that the model itself and its technical and algorithmic implementations are correct. Van Horn (1971), in an early but meaningful consideration of model verification, listed the following four steps: (i) participation of domain experts in the formulation of the forecast model, (ii) testing the goodness of fit of model predictions by implementing real observations, (iii) implementation of Turing tests using real and synthetic data, and (iv) comparison of model results with the ground truth.

Performance verification examines whether a verified forecast model trained and tested on a benchmark data set performs as expected (i.e., it addresses the question *"Does it work?"*). It applies invariably to binary (YES/NO) and probabilistic ($0 < p < 1$) forecasts (see discussion in Leka et al. (2019)). To quantify performance verification, a central concept is that of the skill score (SS) (e.g., Woodcock, 1976; Murphy and Epstein, 1989)

$$SS = \frac{S_{\rm pred} - S_{\rm ref}}{S_{\rm perfect} - S_{\rm ref}} \ , \tag{2}$$

where $S_{\rm xx}; {\rm xx} \equiv \{{\rm pred}; {\rm ref}; {\rm perfect}\}$ is a metric (perceived as a score) that reflects a property for the actual prediction, a reference prediction or a perfect prediction, respectively. Common implementations of score are the mean square error (MSE) or the root mean square error (RMSE), among others, between the prediction and the ground truth, if and when available. A positive skill score ($SS > 0$) corresponds to an overall performance across the set of forecasts being evaluated as better than the set of reference forecasts. A negative skill score ($SS < 0$) is performance worse than the reference, and a zero skill score is performance equal to the reference. Typically, the reference prediction is a "naive" or moderately educated one, against which the prediction method of interest is tested. In the case of the evaluating scores being the MSE or RMSE, $SS_{\rm perfect} = 0$ (no error), hence a very common form of the skill score in this case is

$$SS = 1 - \frac{S_{\rm pred}}{S_{\rm ref}} \ . \tag{3}$$

In binary (YES/NO) forecasting and the simplest case of a two-category prediction (for example, flares of GOES class M and above vs. flares below GOES M-class or no flares) one can summarize the prediction outcome by populating the contingency table (or confusion matrix) of Table 3. This matrix identifies the possible outcome as hits or true positives (TP; predicted *and* observed); false alarms or false positives (FP; predicted *but not* observed); misses or false negatives (FN; not predicted *but* observed); and true negatives (TN; not predicted *and not* observed). The sums of the two rows give the numbers of positive predictions and negative predictions, respectively, while the sums of the two columns provide the numbers of positive observations (event) and negative observations (no event), respectively. The sum of all entries of the confusion matrix gives the total number N_{tot} of times the prediction method was applied.

The simple matrix of Table 3 gives rise to a wealth of metrics, such as probabilities of detection and non-detection, accuracy, false alarm ratio and rate, threat score, equitable threat score, etc. The reader is referred to the treatise of Jolliffe and Stephenson (2011) for the various definitions, as well as to the excellent online resource of the Joint Working Group on Forecast Verification Research of the World Climate Research Program, available at https://www.cawcr.gov.au/projects/verification/verif_web_page.html. ESA, on the other hand, has issued a Technical Note on the Common Validation of its Space Weather Service Network products (Tsagouri et al., 2020).

Let us now describe briefly some notable skill scores and statistical metrics stemming from Table 3, with particular applicability to the solar eruption prediction problem:

- The Heidke skill score (HSS; Heidke, 1926), in which the reference forecast is randomness, i.e. the method is tested against correct prediction due to random chance. A convenient form of this skill score is,

$$HSS = \frac{(TP + TN) - N_{tot} R_{HSS}}{N_{tot}(1 - R_{HSS})} \ , \tag{4}$$

where,

$$R_{HSS} = \frac{(TP + FN)(TP + FP) + (TN + FN)(TN + FP)}{N_{tot}} \ . \tag{5}$$

This flows directly from the definition of the skill score of Eq. 2, where the perfect score (the accuracy $(TP+TN)/N_{tot}$) is 1, i.e., when the number of true predictions equals N_{tot}.

- The Appleman skill score (ApSS; Appleman, 1960), in which the reference forecast is climatology, i.e. the mean event rate in the evaluated period. This is expressed as (Barnes et al., 2016),

$$R_{ApSS} = \begin{cases} \frac{TN+FP}{N_{tot}} & if \quad TP+FN < TN+FP \\ \\ \frac{TP+FN}{N_{tot}} & if \quad TP+FN > TN+FP \end{cases}.$$

The first form of the reference occurs when the number of event observations is smaller than the number of no-event observations (that is a rule in statistically significant data sets of rare events), while the second form occurs in the opposite case. The forecast parameter then being the accuracy $(TP+TN)/N_{tot}$, the perfect forecast is, again, 1. Applying Eq. 2, we obtain,

$$ApSS = \frac{(TP+TN) - N_{tot}R_{ApSS}}{N_{tot}(1-R_{ApSS})}. \quad (6)$$

An additional metric, which is not a skill score but a discriminant (known as the Hanssen & Kuipers Discriminant; Bloomfield et al., 2012; Barnes et al., 2016) and also known as the True Skill Statistic (TSS), compares the probability of detection with the probability of false detection, namely (Bloomfield et al., 2012),

$$TSS = \frac{TP}{TP+FN} - \frac{FP}{FP+TN}. \quad (7)$$

This metric penalizes false detections and is particularly robust in class-imbalanced samples (Bloomfield et al., 2012; Ahmadzadeh et al., 2021), which is a valuable trait, unlike the behavior of HSS and ApSS.

In probabilistic forecasting, besides a forecast probability $p_i, i \equiv \{1,\ldots N_{tot}\}$, one has the ground-truth observation $o_i = 1$ (event) or $o_i = 0$ (no event). The MSE between p_i and o_i provides the Brier Score (BS; Brier, 1950),

$$BS = \frac{1}{N_{tot}}\sum_{i=1}^{N_{tot}}(p_i - o_i)^2. \quad (8)$$

In case of a perfect probabilistic forecasting, $o_i = p_i$ and p_i becomes a binary (0/1), rather than a probability. Therefore, perfect performance means $SS_{\rm perfect} = 0$ in this framework. The Brier skill Score (BSS) is then,

$$BSS = 1 - \frac{BS}{BS_{ref}}, \quad (9)$$

in which case the reference is taken as,

$$BS_{\rm ref} = \frac{1}{N_{tot}}\sum_{i=1}^{N_{tot}}(p_i - \bar{o})^2, \quad (10)$$

where $\bar{o} = \sum_{i=1}^{N_{tot}} o_i$ is the average of the binary event occurrences (i.e., the test period's climatology). In practice, the, BSS addresses the question of how close the probabilistic prediction is to a binary prediction, penalizing probabilities far from 0 or 1, along with erroneous 0 or 1.

While traditionally the flare forecasting research community has been using skill scores for performance verification, in recent years there has been a shift towards other visual measures more commonly used in operational terrestrial weather forecasting (Sharpe and Murray, 2017). For example, probabilistic forecasts allow the construction of a so-called reliability diagram that correlates the forecast probabilities $\mathbf{f} = \{f_j\}$ with the observed frequencies $\mathbf{o} = \{o_j\}$ under a suitable binning $j \equiv \{1,\ldots,N_{\rm bin}\}$ with $N_{\rm bin}$ number of bins. Reliability diagrams typically accompany Relative Operating Characteristic (ROC) curves, plotting probabilities of detection versus probabilities of false detection by creating different contingency tables (Table 3) for different probability thresholds. Departures above the ROC diagonal imply better performance, with differences at each probability threshold giving the TSS values as a function of threshold. This is a practical way of translating a probabilistic forecasting into a threshold-based binary forecasting. The area under [the ROC] curve (AUC) also provides a useful measure of success of the prediction, with a perfect prediction giving AUC = 1 and a perfectly random forecast giving AUC = 0.5 (also implying TSS = 0). Directly stemming from the AUC is the Gini coefficient, $GC = 2\times AUC - 1$ that ranges between [-1, 1] for $AUC \in [0,1]$. For a purely random forecast of AUC = 0.5, GC = 0. Negative GC values ($AUC < 0.5$) imply a possibility to invert the outputs of the prediction classifier, gaining forecasting skill in this respect.

There is also a rich statistical background stemming from the reliability diagram, in which case a perfect probabilistic forecast is achieved when all points fall on the diagonal. Note that a perfect probabilistic forecast does *not* imply a perfect Brier Score ($BSS = 1$) if points are scattered along the diagonal, as explained before. The classical skill score of Murphy and Epstein (1989) using MSE or RMSE as scores can quantify the departure of the probabilistic forecast from the diagonal (SS = 1 in case of perfect alignment, in spite of $BSS \neq 1$).

New evaluation methods can pinpoint performance in a particular circumstance. For example, flare forecasting methods routinely fail the "first flare/ last flare" challenge, meaning the capability to predict when an evolving active region will produce its first/ last significant flare. A new graphics-based metric using radar plots was developed to elucidate forecasting performance in this context (Park et al., 2020). Invoking this new evaluation strategy can help models identify and mitigate a large source of forecast errors of both types.

Ongoing research on prediction assessment sometimes adopts the idea that false alarms preceding actual events may be more tolerable than false alarms occurring amidst

consecutive non-event days/ periods. On the other hand, missing isolated events may have a greater impact, or value, than missing a single specific event that is part of a chain of consecutive ones (Mylne, 2002). First applications of value-weighted skill scores for binary prediction of flares with ML seem to perform better than quality-weighted approaches, particularly for the forecasting of M- and X-class flares (Guastavino et al., 2022).

4.3. Ongoing efforts and initiatives

The metrics described in the previous section (along with many more) have been used widely by the community in verifying the performance of flare and eruption forecasting methods, either in pioneering statistical or ML/DL studies or in collaborative works (Balch, 2008; Crown, 2012; Bobra and Couvidat, 2015; Barnes et al., 2016; Bobra and Ilonidis, 2016; Kubo et al., 2017; Sharpe and Murray, 2017; Leka et al., 2019; Leka et al., 2019; Park et al., 2020). Some works optimise their forecasts to a particular metric, and ensemble techniques are particularly useful in this case to tailor forecast outputs to specific end-user needs (Guerra et al., 2020). Moving forward, whatever technique is used, it is crucial for new methods to be compared and evaluated consistently using the *exact same* data sets (including event / no event samples), time periods, and verification metrics, to maintain a clear view of the concurrent state-of-the-art (see Section 4.1). Leka et al. (2019) provided a useful starting point for this by comparing operational (defined as "providing a forecast on a routine, consistent basis using only data available prior to the issuance time") flare forecasts for the first time against a 120-day prior climatological rate. It is clear from the results of this recent comparison study and other operational performance evaluations (e.g., Crown, 2012; Devos et al., 2014; Murray et al., 2017) that the current performance of operational methods is sub-optimal, barely outperforming climatology and requiring a human "forecaster-in-the-loop" (FITL) to use their expertise to adjust automated outputs as necessary before issuing forecasts intended for end users.

The first systematic comparison of the performance of a small subset of the methods outlined in Section 3 was undertaken by Barnes et al. (2016). This study highlighted the need for the use of consistent data sets in making meaningful comparisons, and demonstrated that, when such comparisons are made, the variation in the performance across a wide range of methods is comparatively small; that is, no one method clearly outperforms the others. The work identified that a major factor in this is the correlation among parameters, including ones that are not readily related in a physical or mathematical sense, such as parameters characterizing the strong-gradient PILs and ones characterizing the coronal magnetic connectivity. These unexpected correlations likely limit the ability of even highly sophisticated prediction methods to successfully determine when an event (a flare in this case) is likely to occur.

This initial comparison was expanded upon by Leka et al. (2019); Leka et al. (2019); Park et al. (2020), who focused on operational flare forecasting methods. In addition to comparing the overall performance of a variety of different methods (Leka et al., 2019), this investigation also tried to determine the factors that were most important in determining when a flare is imminent. The findings on overall performance of the methods were similar to Barnes et al. (2016), with no method clearly outperforming the others and, by most metrics, showing moderate positive skill. Leka et al. (2019) concluded that there was weak evidence to support the idea that including prior flaring history (persistence) and having a human FITL improved forecasting performance in comparison with methods that did not include either. It was also found that, in an operational setting, the best results are obtained when methods are not restricted to producing forecasts near disk center (in the sense that they will not issue forecasts on targets far from the central solar meridian and closer to the solar limbs). Park et al. (2020) further identified and quantified one particular failure mode common to most methods – the challenges of the first flare and/or last flare. That is, methods are more likely to miss predicting the first flare in a sequence of flares and/or give a false alarm for the interval following the final flare in a sequence when compared with forecasting a flare in the middle of a sequence, or a flare-quiet time not immediately following a flare.

There is significant pondering in the community over how method development and comparison could be streamlined and implemented to work better together to improve upon the current state-of-the-art. Cinto et al. (2020) proposed a framework in which flare prediction systems can be designed, trained, and verified/validated. Modularity is key to this task, so that it allows different data and/or models to be digested and processed/tested. Engell et al. (2017) are implementing the SPRINTS (Space Radiation Intelligent System) that aims to contribute to SEP event forecasting starting all the way from the solar sources, namely going through all the nominal course of events, from flares, to CMEs to SEP events. The framework works with the MAG4 model of Falconer et al. (2014) and its MagPy extension. Involving solar sources is an important course of action, self-consistent and physically sound that, however, must deal with the immense span of spatial and temporal scales (Fig. 1) and the lack of advance warning in flares, contrary to CMEs and SEP events. Solar-source driven SEP forecast efforts also include FORSPEF (Forecasting of Solar Particle Events and Flares; Anastasiadis et al., 2017) and PROSPER (Probabilistic Solar Particle Event Forecasting; Papaioannou et al., 2022) that tap into databases and near-realtime results from flare and CME prediction metrics from ESA's A-EFFort (Athens Effective Solar Flare Forecasting; Georgoulis et al., 2016) and FLARECAST (Georgoulis et al., 2021). These efforts have

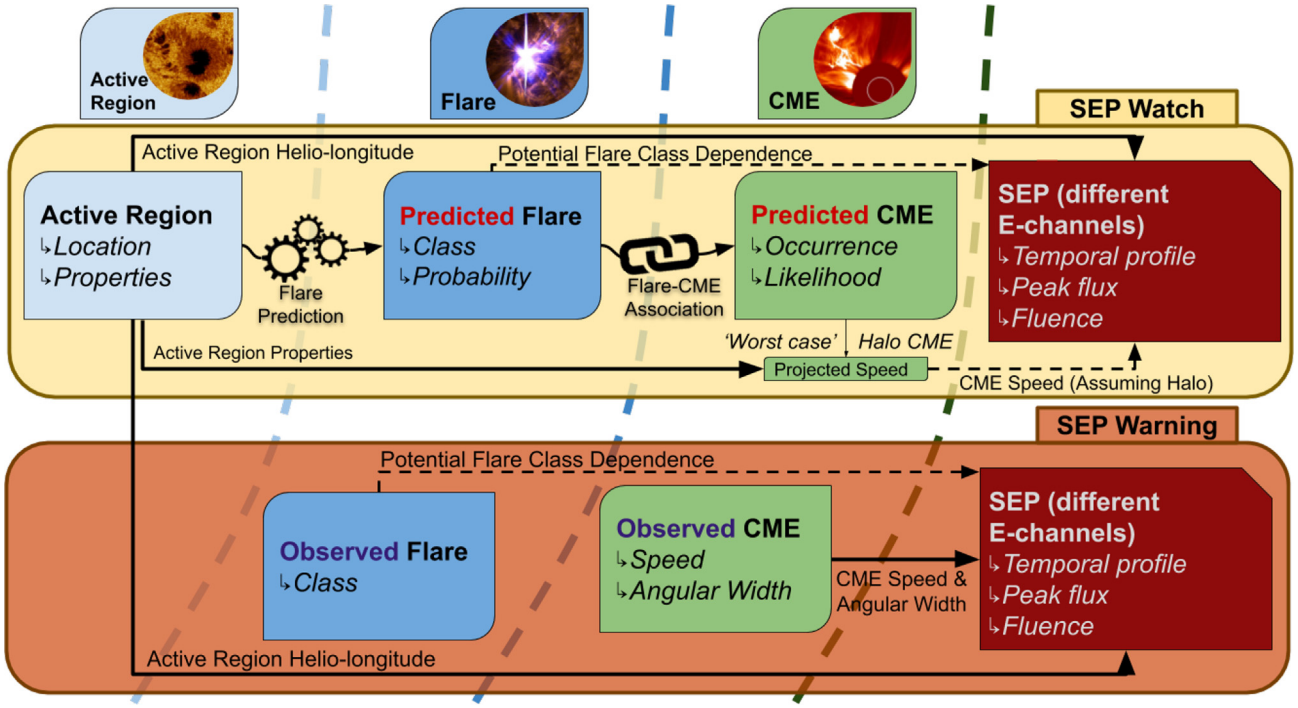

Fig. 6. Two-tier (i.e., Watch and Warning) SEP forecasting concept involving activity sources and repercussions from the Sun's photosphere to geospace. Credit: Georgia State University/ Data Mining Lab (DMLab).

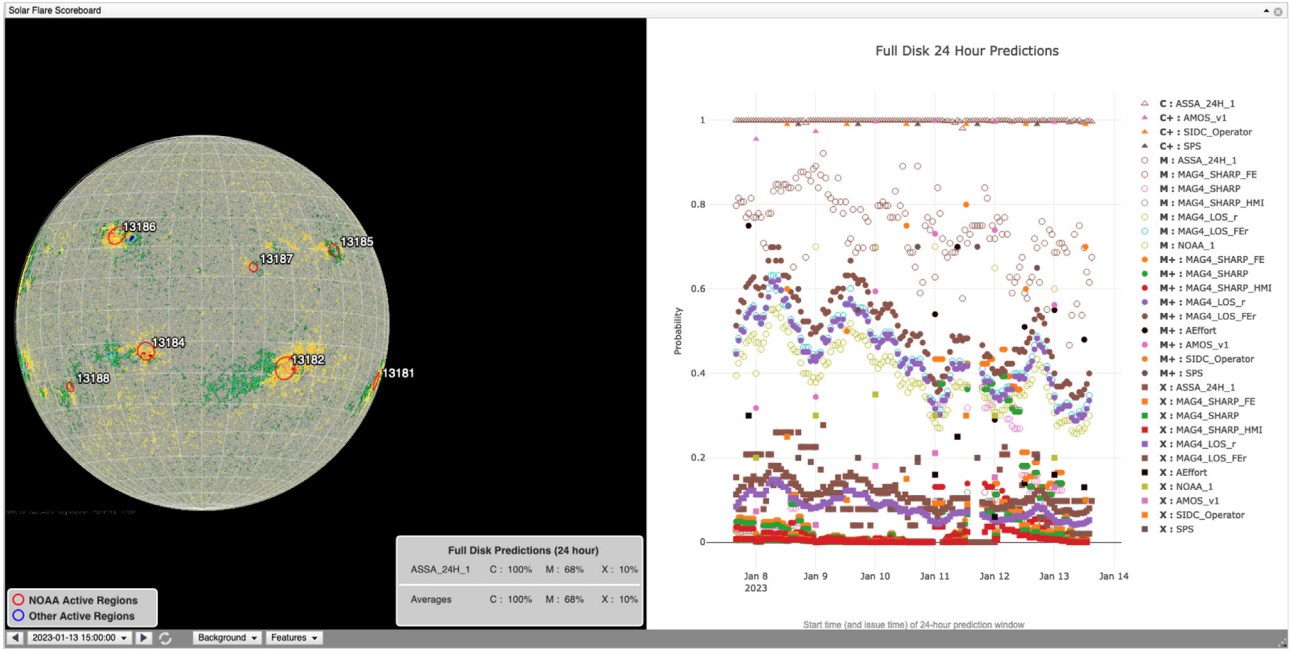

Fig. 7. The CCMC Flare Scoreboard frontend from January 13, 2023 at 15:00 UT. Shown are (left) the most important NOAA active regions and average predicted 24-h full-disk probabilities for flares of GOES classes C, M, and X (the background image is a full-disk solar magnetogram); and (right) detailed results and progression over the previous 5 days of the tens of operational flare prediction methods included in the Scoreboard and providing their results on a regular basis.

both forecasting and nowcasting components when CMEs are involved. A SEP forecast concept by the Georgia State University's Data Mining Lab (DMLab) looks into the problem of flare/ CME/ SEP event forecasting via a two-tier approach (Fig. 6) that accounts for a "SEP Watch" module (in case the conditions are ripe for a SEP-bearing eruption) and an "SEP Warning" module, indicating that an eruption is on its way and projecting its repercussions

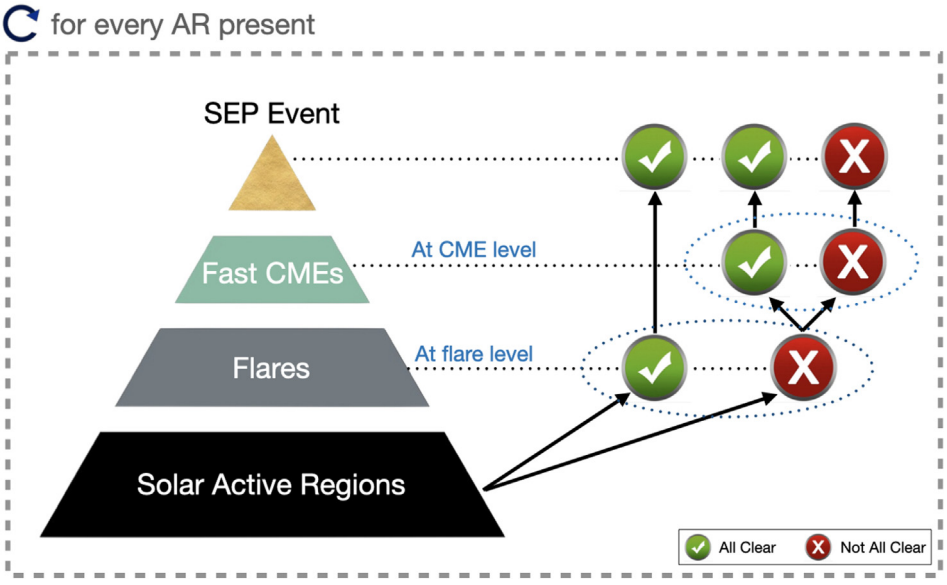

Fig. 8. A potential logic for predicting All Clear for the full visible solar disk. Variants of this scheme would be either the targeted prediction of the negative (no event) class at flare or CME level, or the prediction of the positive class (event), with low event forecast probability or NO binary outcome, implying All Clear. The pyramidal shape implies the degree of rarity from active regions to flares, to fast CMEs to SEP events at a certain heliospheric location with the given view of the solar disk (nominally geospace). Actions within the dashed box are to be repeated for all solar active regions present in the visible (nominally earthward) solar hemisphere.

at geospace. The SEP Warning module incorporates nowcasting information such as flare magnitude, CME speed and angular width.

NASA's Community Coordinated Modeling Center (CCMC) plays an important, grassroots role involving an as wide as possible part of the global space weather forecasting community. Central among CCMC tasks are the Scoreboard initiatives, aiming to collect all operational forecasts in a uniform format that, first, allows viewing of collective near-realtime results and, second, facilitates seamless validation efforts at suitable times in the future. Besides providing API access to all different results, the Scoreboards aim to provide insightful visual information, also in near-realtime. The first such scoreboard is the Flare Scoreboard (accessible at https://ccmc.gsfc.nasa.gov/scoreboards/flare/ - see also Fig. 7) while soon thereafter the CME Scoreboard (accessible at https://ccmc.gsfc.nasa.gov/scoreboards/cme/) and the SEP Scoreboard (accessible at https://ccmc.gsfc.nasa.gov/scoreboards/sep/) followed. A very recent development is the planned Interplanetary Magnetic Field (IMF) Bz Scoreboard that will become accessible at https://ccmc.gsfc.nasa.gov/scoreboards/imf-bz/ and will aim to collect results forecasting the geoeffectiveness of CMEs propagating in the inner heliosphere. There is little doubt that more scoreboards will follow in the future, fostering improved community efforts in modeling and verification.

5. Present challenges and objectives

Here we provide a condensed discussion of the most important challenges, problems and caveats marring the efforts for solar eruption forecasting. For some of them, proposed or envisioned remedies can be found in Section 6.

5.1. Predicting All Clear

The exact opposite to the prediction of a solar event is All Clear prediction, namely, when a solar energetic manifestation is *not* predicted to occur. An All Clear prediction would imply either a binary YES or a high All Clear probability P_{AC} above a threshold, allowing a sufficiently low complementary probability for an event. Considering a solar event category of space-weather interest (flare, CME, or SEP), All Clear could be the immediate target of the prediction (see, e.g.,Ji et al., 2020, for flares), in which case P_{AC} is the main outcome, or it could be a by-product, where $P_{AC} = 1 - P_{FD}$, when P_{FD} is the full-disk event probability. In case of different P_{AC_i} for different solar sources $i \equiv \{1, \ldots, N_{source}\}$, the full-disk All Clear probability is aggregated as expected, i.e.,

$$P_{AC} = 1 - \prod_{i=1}^{N_{source}} (1 - P_{AC_i}) \, . \tag{11}$$

If the prediction target is P_{FD}, then the aggregated probability of Eq. (11) applies equivalently for P_{FD_i}. This is the theoretical inference of the probability; in practice, though, the propagation of uncertainties on these probabilities may render the scheme of Eq. (11) impractical or infeasible. In case of binary YES/NO All Clear forecasting, a full-disk All Clear would be YES if all sources i have a YES All Clear. The presence of a single NO for a given source i would imply an overall NO All Clear.

Fig. 8 provides an abstract visualization of the level of complexity present in the All Clear problem: if a given active region on the solar disk has an All Clear in effect over a certain time interval for flares of a certain size, then no fast CMEs are expected for this interval and the All Clear can be propagated all the way to SEP events from this source, namely $P_{AC_i} \simeq 1$ (ignoring, in this case, the possible flare-accelerated SEP events, short-lived and impulsive, that would require magnetic connectivity information to predict (e.g.,Reames, 2015, and references therein)). If a flare All Clear is not the case, then the target shifts to whether there is an All Clear for fast CMEs. In this case (All Clear for fast CMEs), the same $P_{AC_i} \simeq 1$ could be imposed for SEP events; otherwise, not All Clear for fast CMEs would imply a not All Clear for SEP events, too ($P_{AC_i} < 1$ or $P_{AC_i} \ll 1$).

In practice, the main goal of an All Clear prediction is to minimize risk to tolerable levels for the interested stakeholder. A practical way to achieve this is by minimizing the number of missed events while keeping the number of false alarms low. While the objective is the same with that of the classical problem of event prediction, it may well be infeasible to present it as the exact reverse problem. The higher focus on missed events can result in the modification of the cost function, which is minimized for the forecast. Because many statistical and ML prediction algorithms can be fine-tuned relative to a particular cost function, All Clear prediction may require retraining the entire algorithm from scratch.

The first systematic validation effort of flare prediction methods, undertaken by Barnes et al. (2016), was originally intended for an All Clear prediction but there was no consensus on what All Clear should entail, hence the paper was devoted to validation of flare prediction methods instead. Investigation of ML capabilities on the flare benchmark data set of Angryk et al. (2020) demonstrated better performance of the Time Series Forest classifier compared to other ML methods, such as decision trees, logistic regression, and support vector machines for flare All Clear (Ji et al., 2020). That model was recently extended to a SEP All Clear (Ji et al., 2021). Investigation of the potential of a ML-driven algorithm to predict SEP events over solar cycle 24 and the corresponding All Clear demonstrated ability to capture all SEP events using statistical properties of soft X-rays (Sadykov et al., 2021). However, in this case the false positive rate reaches about 40% of the true negative rate (~500 daily false alarms for ~1200 non-SEP days in the test data set). A different approach was followed by Torres et al. (2022) to predict SEP events from properties of the preceding CMEs. Investigation of the false prediction cases indicated that some false predictions could be caused by inaccurate CME records assigned to the SEP or by the cases representing weak or doubtful SEP events.

The comprehensive Whitman et al. (2022) review of the SEP prediction models indicated that several other models could potentially extend their capabilities to the All Clear prediction (e.g., Núñez, 23). The SEP Scoreboard (Section 4.3) could also contribute meaningfully to this objective.

Because (i) the missed instances and false alarm instances are treated unequally in the All Clear prediction problem, and (ii) the prediction models are often tuned with respect to specific assessment metrics, dedicated training and assessment strategies may be required for All Clear prediction. As an example, the daily probabilistic forecasts of solar proton events by the SWPC (Bain et al., 2021) result in satisfactory values of the BSS, TSS or HSS. However, Sadykov et al. (2021) noted that the same forecasts had missed 14 of the solar proton events' 101 days in solar cycle 24, issuing very low probabilities for these days. Sometimes there is no possibility to adjust the probabilistic thresholds of event forecasts for All Clear ones. For the forecast assessment, Sadykov et al. (2021) proposed the Weighted True Skill Statistic (WTSS) metric that aims to achieve an adjustable weighting indicating the ratio of penalties for missed events and false alarms. Differentiating between the two, as mentioned above, may spearhead All Clear prediction efforts.

Summarizing, on the antipodes of event prediction, practical All Clear forecasting may well require separate attention. Similar to the event prediction, however, All Clear periods are subject to the definition and timing properties initiated by the demand of each particular operator (see Section 5.4 below). For example, operators interested in spacecraft charging and human spaceflight safety may have different requirements for the energies, fluxes, and All Clear time SEP event windows. With constantly refined requirements on the detection and impact of solar eruptions, operational All Clear becomes crucial and, above all, it remains a challenge.

5.2. Class imbalance, climatology, timeseries and the like: hurdles for training and testing

Existing forecast models face serious challenges impeding their performance. These are discussed briefly below, along with some efforts to address them:

5.2.1. Class imbalance

Increasing sizes of eruption thresholds for forecasting makes the prediction problem increasingly more class-imbalanced, given the increasingly dominant negative sample over the shrinking positive sample. For ML modeling, this is a major issue to tackle. More specifically, class imbalance refers to the situation where there is an imbalance (skew) between the number of instances of different classes. For example, the ratio between the flaring (class M+) and non-flaring active region samples in the benchmark data set of Angryk et al. (2020) is approximately 60:1.

In performance verification, class imbalance invalidates some well known metrics, such as the accuracy of forecasts $(TP + TN)/N_{tot}$ (Table 3). If the number of true negatives is

overwhelmingly large ($TN \simeq N_{tot}$), then accuracy $\simeq 1$, namely perfect performance that, however, is an artifact (e.g., Leka et al., 2019). The HSS (Eq. 4) is also biased by class imbalance, with often unreliable results. This is not the case with TSS (Eq. 7) that is generally unbiased, which adds to its appeal for forecasting rare events (Bloomfield et al., 2012; Ahmadzadeh et al., 2021; Lavasa et al., 2021). However, care should still be exercised because each minority class event (or no-event if "quiet" times are the rare class) will have increasing influence on the overall TSS value as the degree of class imbalance grows.

For ML methodologies, class imbalance is also a pressing problem that has been thoroughly investigated in the computer science community (see, e.g., Kubat and Matwin, 1997; Japkowicz, 2000; He and Garcia, 2009; Krawczyk, 2016). The space weather forecasting community is catching up over recent years, with a number of treatments discussed in, e.g., flare prediction (see, e.g., Ahmadzadeh et al., 2021; Nita et al., 2022; Ahmadzadeh et al., 2019; Ahmadzadeh et al., 2019), with some potentially promising approaches proposed in general (Chen et al., 2021b; Ahmadzadeh et al., 2023) and for the prediction of SEP events (see Lavasa et al., 2021, and references therein). Nonetheless, class imbalance directly affects the obtained performance of a predictive model (i.e. the false alarm rate) for SEPs (Stumpo et al., 2021).

Generally there are methods to augment the training sample via oversampling (i.e., replicating) of the positive sample, undersampling (i.e., cropping) of the negative sample, or misclassification weighting, that penalizes with larger weights the misclassification of the (minority) positive sample. The latter seems to hold better promise (Ahmadzadeh et al., 2021). Regardless of the training sample manipulation, however, the testing sample must be kept untouched (i.e., class-imbalanced) in any case, as manipulating it totally invalidates the performance verification process. Manipulating the testing sample is a rather common mistake in a number of studies.

Another way to overcome the class imbalance is to naturally increase sampling of larger flares by involving longer periods of time. Many prediction tools rely on availability of vector magnetograms. The most recent solar cycle 24 was relatively weak with few large flares, though it is the only solar cycle in which consistent time-sequence vector magnetograms have been available from SDO/HMI. LOS magnetograms are available from SOHO/MDI in active solar cycle 23 with many large flares. Jiang et al. (2023) developed a new deep learning method to learn from combined LOS magnetograms, B_x and B_y taken by SDO/HMI along with H-alpha images, and to generate vector components for MDI data. This development has potential to provide synoptic vector magnetograms covering periods from 1996 to present.

Finally, it is possible to design algorithms that generate balanced training sets of active regions accounting for the flare class rates associated to a specific solar phase (Guastavino et al., 2022). The training of ML and DL algorithms based on the exploitation of such sets is primarily intended for operational settings.

5.2.2. Varying climatology

Predicting solar energetic events via training and testing on different sub-samples implies that these samples have a statistical significance appropriate for the performance verification at hand. To achieve statistical significance, one uses sizable fractions of the solar cycle for training (on the order of several months or a few years), and typically less for testing. However, training on one part of the solar cycle and testing on another implies that training and testing occur in different climatology conditions, as shown clearly in Fig. 2 of Leka et al. (2019). In other words, the mean occurrence frequency of eruption instances changes significantly, impeding the models that should ideally train and test on similar climatology conditions. While one might think of remedies to this problem for proper training practices (see Section 5.2.4), the data used for performance verification should be carefully selected in order to approach the true performance of the method in actual, near-realtime operational settings.

5.2.3. Temporal coherence

Solar flares and eruptions eruptions occur above a continuously varying background of solar activity evolving every magnetic feature in the Sun's atmosphere at different timescales. A dominant majority of the eruption prediction methods of Tables 1 and 2 exercise "point-in-time" forecasting; namely, they collect apparent conditions at a given instant and translate them into a forecasting over a certain forecast window. A number of methods, however, indicated separately in Tables 1 and 2, perform their forecasts using timeseries as input. The part of the timeseries used to sample the concurrent condition of the system is often called the observation window. For example, a point-in-time forecasting takes place at time t_0 evaluating the snapshot conditions at time $\lesssim t_0$ for a prediction window $\Delta T_{\rm pred}$ with or without latency $\Delta t_{\rm lat}$, which specifies in how much time does the specific forecast become effective (for $\Delta t_{\rm lat} = 0$, it is effective immediately at t_0; otherwise, it becomes effective at $t_0 + \Delta t_{\rm lat}$). A timeseries forecasting at time t_0 incorporates information over the time interval $t_0 - \Delta t_{\rm obs}$, with $\Delta t_{\rm obs}$ being the observation window, and issues a forecast for an interval $\Delta T_{\rm pred}$, again with or without latency $\Delta t_{\rm lat}$.

Timeseries forecasting is challenging particularly in case the refresh time $\Delta t_{\rm refr}$ (i.e., the time until the next application of the prediction method) is significantly shorter than the observation window $\Delta t_{\rm obs}$. In this case, the timeseries used to assess the conditions of the system at times t_0 and $t_0 + \Delta t_{\rm refr}$ are largely identical. For $\Delta t_{\rm obs} = 12$ hours and $\Delta t_{\rm refr} = 1$ hour, for example, the two timeseries are identical for $\Delta t_{\rm obs} - \Delta t_{\rm refr} = 11$ hours or $\sim$92% of their length. While this may secure continuity and constrain

erratic behavior in the forecasts, it is problematic for events (e.g., flares) that have typical timescales $< \Delta t_{\mathrm{refr}}$, let alone the observation window. In this case, regardless of the forecast method, the forecasts will not change. Ahmadzadeh et al. (2021) have shown that this practice incurs an artificial clustering in the predictive parameter space (Fig. 3 of that work) that may well mislead the prediction method. Furthermore, complications can arise in verification of forecast systems that have refresh time scales shorter than their forecast windows because each resulting forecast is not independent (a key tenet to many of the verification metrics and skill scores). Note that this is not unique to timeseries forecasting and applies equally to "point-in-time" forecasting as well.

Again, some potential remedies are discussed in Section 5.2.4 but this is a problem that needs to be tackled in a systematic way. This is yet to be achieved decisively.

5.2.4. Proper training and testing practices

Performance verification of models, assuming that data and model verification are complete (Fig. 5), is the last and arguably most important part of the decision process on whether a given prediction method should be transitioning to operations.

The choice of proper verification metrics is crucial, as explained in the previous sections. Even with the right metrics in place, however, one should make sure that training and testing abide by certain standards; otherwise, the values of these metrics may be misleading.

First and foremost, there should be no overlapping between training and testing samples. A method cannot test on a sub-sample on which it has been trained on previously. This has led to some superficially high performance verification metrics in the literature, particularly in case ML methods are involved, because in this case the method does not learn; it simply memorizes. Transitioning such a trained method to operations will lead to very different results when enough near real-time forecasts will be collected to enable the first operational verification.

The process of randomizing the training and testing samples at different times is risky, too. For example, having a series of data from an active region (magnetograms, EUV/X-ray images) and using different days (24-h blocks) of the same active region for training and testing will also very likely result in memorizing. In the series of studies on which validation of operational flare forecasting methods was performed (Barnes et al., 2016; Leka et al., 2019a, 2019b; Park et al., 2020) different time intervals and event/no-event instances were implemented, similarly for all methods. Campi et al. (2019) further showed the impact of artificially leveraging the training process by training and testing on samples of different active regions (or HARP series) to show that verification results are more realistic (lower) in this case compared to when different time intervals of the same active regions are used. Solar flare and eruption prediction focusing on active regions facilitates this practice given the different NOAA or HARP numbers, although this is harder for HARPs as the near-realtime (NRT) data product does not guarantee fixed HARP numbers.

In case of multiparametric prediction, statistical or ML regardless, it is meaningful to ensure that the different indices highlight complementary, rather than similar, insight of the training subject. In Barnes et al. (2016), for example, it was shown that different metrics from the validated methods were highly correlating with each other, some with correlation coefficients in excess of 0.9. Selecting which parameters to use in a prediction method is an important task that relies both on physical understanding of these parameters and on numerical testing with the method(s) of choice. It has been shown using multi-variable discriminant analysis (Leka and Barnes, 2007) and by feature ranking in several supervised ML cases (e.g., Bobra and Couvidat, 2015; Florios et al., 2018; Campi et al., 2019) that the values of performance verification metrics tend to saturate after more than a handful, or up to ~10, predictive parameters are used. In today's capabilities of scores of predictive parameters (the FLARECAST project made available 209 of them, for example, at different cadences), this feature ranking should be performed systematically and comprehensively. This is also a question of the event definition (or the prediction method per se), as there are cases (e.g., Campi et al., 2019) in which feature ranking for different event definitions (i.e., different flare classes) is significantly different. One needs a sufficient number of parameters to identify patterns, find the few most consistent ones and use them with the method of choice thereafter. To our knowledge, this task is yet to be performed but can lead to a valuable physical interpretation, particularly in case of ML models (see Section 5.5 for further discussion).

The interplay between training and testing in supervised methods can be systematically addressed by introducing score-oriented loss (SOL) functions (Marchetti et al., 2022). From a formal viewpoint, these functions can be designed by using probabilistic confusion matrices and can be applied in the training phase of ML and DL algorithms to automatically and a priori maximize specific skill scores.

Concluding, the training of ML methods, in particular, entails a number of important tasks and challenges. While a detailed discussion lies beyond the scope of the current review, several works included in Tables 1 2 cite the importance of correctly tuning hyper-parameters used in the prediction schemes. This could conceivably help both physical understanding (as tuning may rely on important physics of the problem at hand) and operational efficiency, in case physics-inspired tuning leads to an improved or optimized performance.

5.3. Missing data and 'photospheric-only' forecasts

Photospheric magnetic fields are inferred from polarized light, and are influenced by numerous radiative transfer effects and assumptions applied during the data reduction.

For LOS magnetographs, such as the MDI onboard SOHO and the HMI line-of-sight data products, the LOS component increasingly deviates from the radial component, especially in very inclined regions such as sunspot penumbrae (Leka et al., 2017). Obvious problems become visible at 40^o – 45^o EW in central meridian distance, as the $cos(\theta)cos(\phi)$ correction factor from LOS to the local radial direction under the assumption that all fields are radially directed (θ, ϕ being the central meridian distance and heliographic latitude, respectively), is significant. Some conservative approaches (e.g., Falconer et al., 2006) limit analysis to within $\pm 30^o$ from central meridian. Other methods that employ LOS magnetic fields utilize different approaches that do not make the radial-field assumption, in order to mitigate the projection effects (Leka et al., 2018).

For vector magnetographs, such as HMI onboard SDO, the situation is somewhat less adverse as one can deproject the full magnetic field vector to that of the heliographic reference system (Gary and Hagyard, 1990; Thompson, 2006) once the inherent 180° ambiguity has been resolved (Hoeksema et al., 2014). Even in this case, though, second-order curvature and foreshortening effects appear after 50^o – 55^o, inhibiting the diagnostic capability of these magnetograms (see, for example, Section 3.2 of Gary and Hagyard, 1990). The HMI data become hardly usable after 70^o EW, as explained by Bobra and Couvidat (2015) (Section 2.1) – see also Falconer et al. (2016). Given that an active region stays on the visible solar disk for approximately 14 days rotating a typical $\sim 14^o$ per day, approximately 22% of this time (or ~ 3 days) the active region magnetograms are totally inaccessible. One should add to this another 3 days when the active region will be in the 50^o – 70^o EW zone to realize that approximately 43% of the time the active region rotates in the earthward solar hemisphere, its magnetograms are either compromised or simply non-existent. Numerous major flares and eruptions have occurred when their source active regions were on or close to the limbs, or ever slightly beyond them to the Sun's farside. Among them, the strongest flare of the space age (or since the start of the NOAA records) of GOES class X28 on October 28, 2003 (e.g., Manchester et al., 2004; Jackson et al., 2006), the September 10, 2017 GOES X8.2 flare (e.g., Yang et al., 2017; Yardley et al., 2022), and even very recently, on January 5, 2023, a flare classified as GOES X1.2 observed when its source region (NOAA AR 13182) was partially beyond the eastern limb. We note that in Park et al. (2020) an example of poor performance of flare forecasting models is shown for flaring regions near the limb due to limitations of magnetic field data as model input. Currently there is no solution to this problem other than potentially employing proxies from other wavelengths (Section 2.4) or simply maintaining (i.e., "freezing") the forecasts from before the active region entered the problematic zone, assuming that it rotates as a solid body, without evolving. This oversimplification does not apply to active regions rotating from the eastern solar limb; to those moving toward the western limb, even pure translational rotation increases the probability of an acute SEP event. The solution of continuous, operationally-oriented observations beyond the Sun-Earth line and even on the farside of the Sun is discussed in Section 6.2.

In another recent development, the exclusive photospheric nature of predictive parameters due to their reliance on magnetograms was investigated by Korsós et al. (2020), who performed potential-field extrapolations above the photosphere and considered flare prediction on previously tested parameters (Korsós et al., 2019) at different levels using the extrapolated fields. They concluded that at altitudes between $1 - 1.8$ Mm above the apparent $\tau = 1$ photospheric layer, they could improve the predictions' lead time by $2 - 8$ hours. This is a potentially interesting finding, as flares and eruptions occur slightly above the photosphere, and points to a potentially promising combination between photospheric or extrapolated magnetic field-based metadata and proxies from other wavelengths to further boost predictive capabilities. The use of extrapolated magnetic field information from higher atmospheric layers in eruption prediction was also explored by Pagano et al., (2019a,b). They used a data-driven magnetofrictional model to calculate a time- and space-dependent eruption metric which is a combination of the magnetic field configuration (i.e. presence and location of magnetic flux ropes) and the integral of the vertical component of the Lorentz force acting outwards on the flux ropes as these are responsible for triggering eruption onset. Aiming to adapt their method to operational CME forecasting, they build on this metric by including not only observed but projected magnetograms as the lower boundary condition in the magnetofrictional simulations, to provide a good indication whether there is the risk of an eruption occurring over the next $10 - 16$ hours. Finally, NLFF field extrapolations of photospheric magnetograms were used by Lin et al. (2020) to determine the ratio of the magnetic flux associated with high twist to that of the overlying magnetic flux. The proposed quantity had limited predictive potential, since it was also based on information of magnetic ribbons to constrain the area related to flaring.

Another recent promising development was the advent of EUV spectroscopic diagnostics, which supply access to the magnitude of the magnetic field in the corona (e.g. for an application to EIS/Hinode observations for a small flare, Landi et al., 2021). Advanced data inversion methods, benchmarked with sophisticated MHD simulations, showed that the anticipated uncertainty in the coronal magnetic field for strong-field regions (> 250 G) from the novel diagnostic could be around 18% (Martínez-Sykora et al., 2022). Application of these novel diagnostics to observations should shed light into their predictive capabilities.

5.4. Customizable forecasts for different stakeholder communities and Research-to-Operations

Following a series of grassroots community meetings, it became clear that different sectors have different needs and

hence "one size does not fit all" in terms of space weather forecasts. One of the first such meetings took place in 2009 at the premises of NWRA/ CoRA (NorthWest Research Associates/Colorado Research Associates) in Boulder Colorado, USA, shortly after the former NOAA Space Environment Center had evolved into the current Space Weather Prediction Center (SWPC; 2007). The topic of the workshop was "Forecasting the All Clear" (Barnes et al., 2016) and was attended by experts of the aviation industry and the defense sector, among others. There was no consensus on what an "All Clear" means, but it became clear that different space weather repercussions had different weights for each of these sectors, and that there are sectors less resilient (i.e., more vulnerable) to forecast misses (False Negatives) contrary to others that are less resilient to false alarms (False Positives; see Table 3). In the course of the FLARECAST project there were two Stakeholders' Workshops organized that were hosted by the Met Office, UK and the European Space Weather Week, respectively (see Sections 6.2, 6.3 and Appendix B of Georgoulis et al., 2021). Ground-based, aviation, defense and satellite industry representatives were present. On top of reiterating the earlier finding of the 2009 NWRA/CoRA workshop, it was revealed that different sectors need an actual person to guide them through the details and, very often, the jargon of the forecasts. The consensus was that the actual end-users of the space weather forecasts were professional forecasters themselves. The need (and, at certain cases, noted improvement of forecasts) for human FITL was one of the conclusions of the Flare Prediction Workshop organized at Nagoya University, Japan (Leka et al., 2019). It is worth noting that FITL may apparently limit or restrict the complete automation of forecasts, unless FITL only play a role in interpreting the automated forecasts. This is a topic that remains to be resolved in the future.

Another key finding of the FLARECAST Stakeholders' Workshops, encapsulated in a FLARECAST user survey organized by the Met Office, was that the three most significant factors of successful forecasts, invariably for all sectors, were, in decreasing order of significance: "timeliness of data"; "accuracy"; "ease of use/ understanding". Perhaps not surprisingly, the least important factor out of 11 possibilities, was "scientific detail". A rather puzzling finding, possibly due to limited response statistics, was that "ability to tailor forecasts" scored toward the bottom in terms of importance. Immediately following the three most significant factors was "information on forecast uncertainty".

Transforming basic-research solar eruption forecasting attempts into operational products or services (also known as Research-to-Operations [R2O]) is a major task that must be dealt with by the scientific community with the help of all interested sectors and partners. All the issues discussed in the previous subsections of Section 5, namely, missing data and lack of crucial observations, pertain squarely to this problem. In addition, operational forecasts imply operational missions, namely, missions that are either devoted to near-realtime data provision (with known caveats, artifacts and the higher uncertainty of non-definitive data) or have solar coverage at suitable spatial resolution and cadence to be helpful to operations. SOHO and SDO were flagship missions not a priori devoted to space weather but effectively serving the need for near-realtime, high-cadence and constant-quality observations. Parker Solar Probe and Solar Orbiter are not such missions, even though their data could crucially help future operational missions. A discussion of future missions and concepts that have a stated objective to assist in space weather forecasting efforts is provided for completeness in Appendix A.

Steenburgh et al. (2013) provide a practical guide of the R2O transition that, besides all of the above factors, includes a platform hosting one (or more) prediction models, visualization and specification tools. Visualization combined with near-realtime coverage allows for expedient decision-making, while specification tools are used for inferring eruption (CME, most notably) parameters and deducing correlations between parameters in near-realtime. This is another potential significance of FITL in space weather forecasting. Moreover, Merceret et al. (2013) describes the R2O transition drawing an analog from terrestrial weather to space weather, given the century-long experience and expertise of terrestrial weather forecasting against the near-infancy stage of space weather forecasting. Virtually all metrics discussed in Section 4.2 were first established for terrestrial weather forecasting purposes and extremes thereof. Merceret et al. (2013) also describes that the transition implements a "Valley of Death", where models that do not survive performance verification and validation end up. As noted by Merceret et al. (2013), however, this has been described elsewhere (Robinson, 2012) as a "Valley of Opportunity", given the new capabilities for improvement via an osmosis of expertise, collaboration and partnership.

The reverse process, known as Operations to Research (O2R) refers to the benefits of operational results for leading to an improved physical understanding of the problem at hand. And then perhaps using this understanding for a new R2O iteration, more efficient than the previous. This could potentially optimize the forecasting process and push the state-of-the-art envelope. The challenge is most prominent in ML and particularly DL applications, whose interpretation is currently an active research task. This topic is briefly discussed below.

5.5. Understanding: physical interpretation and interpretable machine learning

A growing, important topic in AI is explainable, interpretable models. For example, the neighboring field of atmospheric science and weather prediction has seen a large investment from NSF, under the relatively new vehicle of the NSF AI Institute for Research on Trustworthy AI in Weather, Climate, and Coastal Oceanography (AI2ES, https://www.ai2es.org). Nevertheless, a criticism

often encountered in the use of AI for forecasting and, eventually, decision making, is the opaque, black-box nature of ML and, in particular, DL models. By relying on millions of learned parameters, these models offer no physical intuition on how and why a model gives a certain prediction, or suggests a certain course of action. An interpretable model is one that is deemed to be human intelligible. The archetype of interpretability is perhaps linear regression, where the coefficients associated with each input feature have a natural interpretation as the relative importance of these inputs. The more complex a model becomes, the less interpretable it is, so one is often posed with a trade-off between interpretability, accuracy, simplicity, and speed (Ivezić et al., 2014). When the number of features becomes sufficiently large, or when they are derived in a data-driven way, possibly as a nonlinear combination of physical quantities (as is often the case in Generalized Linear Models), a straightforward interpretation of the model is often not possible.

One class of interpretable models are decision or classification trees. Indeed, these can be analyzed in terms of simple "if-then" rules and the final outcome can be easily tracked back in terms of input–output relationships. However, when decision trees are used in a more performance-oriented way, possibly as weak learners in an ensemble model, such interpretability is lost. From the viewpoint of achieving reliable space weather prediction without completely losing control of the underlying decision process, explainable models might be more appealing. By this one means using a number of techniques that can help a posteriori to decipher and understand the inner mechanisms of a ML model. This helps understanding if the model is guided by information that has a physical meaning, or whether, for instance, a good prediction was merely due to coincidence.

Two popular techniques to extract information about the inner workings of a ML model are Local Interpretable Model-Agnostic Explanation (LIME) (Ribeiro et al., 2016) and SHapley Additive exPlanations (SHAP) (Lundberg et al., 2017). Both methods aim to estimate the relative importance of each individual feature (i.e., quantities used as inputs for a ML model). SHAP uses the concept of the Shapley value, introduced in a game theory context as the value that each player contributes to an outcome when they are part of a team (Winter, 2002). SHAP provides a very intuitive explanation that is additive, meaning that the sum of SHAP values of all features adds up to 100%. On the other hand, LIME builds a local (i.e. valid only within a small neighborhood of input values) approximation of the underlying model that is less complex and more interpretable than the global model (for instance, a linear model). Both LIME and SHAP have become extremely popular tools and off-the-shelf Python libraries have made their implementation exceptionally straightforward. Eventually, the aim of both interpretable and explainable models is to learn what physical quantities or processes are the most important (or perhaps solely important) ones in order to devise an accurate prediction model. In turn, this leads to a better understanding of the underlying physics, hence it can be seen as a data-driven approach to improve our understanding.

Another set of tools to interpret the results of ML models such as convolutional neural networks, which use image data as an input, include attribution methods (e.g. Springenberg et al. (2014)). These methods identify spatial features of an image and have the greatest impact on the model output. Sun et al. (2022); Lv and Liu (2022); Bhattacharjee et al. (2020); Yi et al. (2021) all used attribution methods for solar flare forecasting. Some attribution methods deliberately eliminate a portion of the input image to see how the missing data affects performance (e.g. occlusion methods). Others use the differences between a reference image and real input data to identify how the change in data affects performance (e.g., integrated gradients and DeepLIFT; Shrikumar et al., 2017). Other examples of interpretable models for solar flare forecasting include, e.g., Sun et al. (2021); Jarolim et al. (2022).

Yet another set of promising interpretability tools include physics-informed neural networks (PINNs), or physics-informed ML, in general (Raissi et al., 2019; Karniadakis et al., 2021). A very appealing feature of physics-informed ML is its applicability to problems including partial differential equations; the MHD equations dictating the evolution on the photosphere and above are nothing but that. This methodology is yet to be implemented in the forecasting of solar eruptions. The preliminary work of Jarolim et al. (2023), is our only known example of a first attempt to use PINNs as solvers of the force-free magnetic field equations. Such efforts, however (see also the very recent physics-enhanced deep surrogate

Table 4
Measurement and knowledge gaps and approaches to improve the prediction of solar eruptive activity

Gaps	Measurement Approach	Derived Quantities
Quantify the pre-eruption energy accumulation and distribution over the PIL	SEL Multi-height vector B, off-SEL EUV Imaging + photospheric vector B	Magnetic Energy, Helicity
Separate triggers from pre-cursor activity	Imaging of hot (> 10 MK) plasmas, Multi-wavelength EUV imaging	Sigmoids, MFRs
Understand energy release via magnetic reconnection	Imaging spectropolarimetry of PILs, off-SEL SXR irradiance	free energy proxies, AR flaring history, ML/AI training

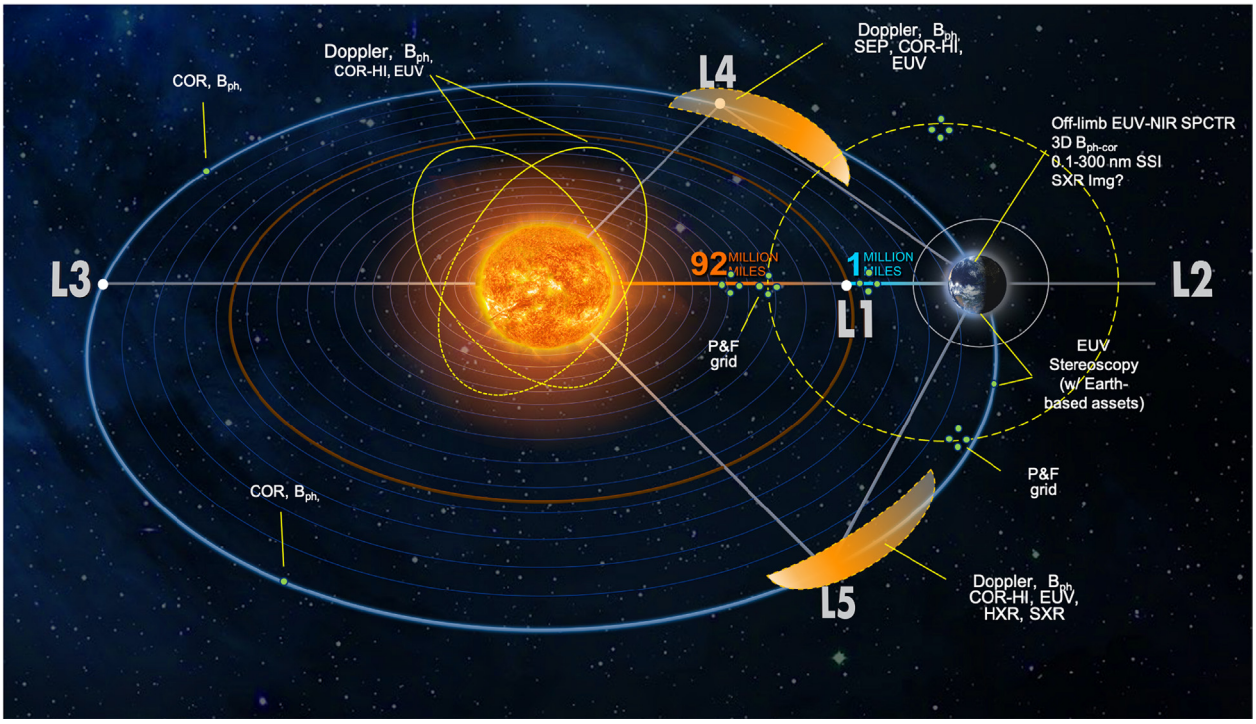

Fig. 9. Graphic representation of the results of the NASA gap analysis with respect to solar and heliospheric observational gaps.'P&F grid' represents multipoint measurements of 'particles and fields' that make up the in situ solar wind. Credit: Applied Physics Laboratory (APL)/ A. Vourlidas.

(PEDS) method for partial differential equations Pestourie et al., 2023), need to mature further to determine whether tangible results can be achieved.

6. Future needs and outlook

6.1. Data gaps

Major solar flares and eruptions are the main agents of severe-to-extreme Space Weather. As such, the prediction of eruptive activity features is prominently among the top concerns of the providers and users of space weather forecasts. Flare and CME prediction is primarily relevant to medium-term (defined as hours to days) forecasting (e.g. Vourlidas, 2021), although flare forecasting is currently used to estimate SEP levels after an eruption with some success (e.g. Laurenza et al., 2009; Kahler and Ling, 2018; Anastasiadis et al., 2019; Papaioannou et al., 2022).

It is well understood that solar eruptions comprise the aftermath of the impulsive release of magnetic energy accumulated in the corona over a PIL. The key to the accurate prediction of an eruption, therefore, lies in better understanding how the magnetic energy is stored in the corona and in measuring the distribution of that energy in space and time so that the system (e.g. an active region) can be monitored as it approaches the threshold to eruption. Many of these issues were recently reviewed by Patsourakos et al. (2020) from a research perspective and the topic was revisited from a more space weather-focused perspective in the recent NASA Observational Gap Analysis Report (Vourlidas et al., 2021).

The above report and analysis therein identified several observing gaps and candidate measurement approaches for closing them, in order to make eruption prediction viable for operations. Table 4 provides a top-level summary of those findings and shows that the problem of eruption prediction can be decomposed to just three high-level knowledge and measurement gaps. All three revolve around the physical understanding and measurement of the magnetic energy flow from the photosphere to the corona. The path forward requires multi-height magnetic field measurements along the Sun-Earth line (SEL), to capture the flow and buildup of energy but also of helicity in the corona. However, SEL measurements are of use over a rather short observing window of about 10 days (roughly the time an active region spends within $\pm 60^{\circ}$ from the central meridian, when vector magnetograms are most reliable). To expand this window, and hence the horizon for prediction, off-SEL magnetic and EUV observations are required to uninterruptedly trace the evolution of an AR from emergence to eruption and to constrain the 3D structure of the magnetic field (e.g., overall benefits shown in Fig. 10 of Posner et al., 2021).

6.2. Solar observations beyond the Sun-Earth line

The measurement approaches in Table 4 flow naturally into mission architectures at the Sun-Earth Lagrangian L4 and L5 points or thereabouts, as discussed in the recent

LWS Architecture Committee Report (see online report at Cohen et al., 2022) and shown graphically in Fig. 9. For an L4 mission, the emphasis is on predicting SEP-productive eruptions from magnetically-connected ARs to primarily protect astronauts in the cislunar space (e.g. Vourlidas, 2015; Posner et al., 2021). This space weather concern drives the need for reliable short- to medium-term forecasting while an L5 mission will be primarily focused on the lifetime and eruptive history of an AR rotating towards Earth and hence medium-term forecasting. A more efficient and effective strategy would require the development of a tightly-coupled L1-L5-L4 mission system, as originally suggested by Vourlidas (2015) and further emphasized in the Gap Analysis and LWS Architecture reports.

Given that the above ideas address only short-to-medium term forecasting needs, can we move past the hour-to-day horizon and into creating meaningful eruption forecasts for weeks, or even months, ahead? This capability may sound overly ambitious but it is possible by mapping and quantifying magnetic flux *before* it emerges on the solar surface as magnetic flux tubes rise from the tachocline. Already, we can create coarse maps of those magnetic bundles using helioseismology (e.g. Braun and Lindsey, 2001) although a relationship between subsurface structures as inferred from helioseismology and future flaring activity is largely lacking, with only few attempts in this direction (Reinard et al., 2010; Komm et al., 2011; Braun, 2016). The lack of multi-point helioseismology measurements hinders further progress on this issue. These measurements are required to increase the spatial resolution of sub-surface mapping and to allow sampling deeper into the convection zone. Both global and local helioseismology techniques must be implemented and hence measurements must be distributed in both longitude and latitude.

The best way to acquire those measurements, while also tracing the magnetic field above the surface, is through the deployment of a multi-spacecraft constellation that provides a full, so-called 4π coverage of the solar surface and atmosphere (Gibson et al., 2018; Vourlidas et al., 2018; Vourlidas, 2021). The 4π mission requires a minimum of four spacecraft and can be designed in various configurations, i.e. all four or only two spacecraft in high inclination orbits, depending on programmatic resources. A detailed mission design study for a science-driven 4π concept, called Firefly, was recently performed (Raouafi et al., 2022). Other mission designs envisioning solar stereoscopic exploration (Yang et al., 2023) with the Solar Polar-orbit Observatory (Deng et al., 2023) and the Solar Ring mission (Wang et al., 2023), forming holistic observations of the Sun, have also been proposed. The LWS Architecture Report considered a similar but more space weather-focused concept while the Gap Analysis concluded that the 4π coverage of the Sun will lead several open operational and primarily knowledge gaps to closure.

The above are indeed supported by scientific, technological and policy advances over the past twenty years. These have shown the importance and timeliness of monitoring, ideally, the whole Sun and its surrounding magnetic and plasma structures, not just those parts that can be viewed from locations on the ground or in near-Earth space. The value of observations off the SEL has been demonstrated by several missions, in particular by the STEREO mission (Kaiser et al., 2007). This has now provided observations from all solar longitudes relative to Earth, despite the loss of STEREO-B in 2014. Those observations have led to a wealth of scientific results, including how off-SEL imaging can improve measurements of CME velocity, acceleration and deceleration, as well as the value of monitoring farside regions to enhance awareness of active regions that will soon start to affect Earth. These results have driven studies to look at future off-SEL missions, both for new science and as steps towards operational monitoring. The ESA Vigil mission to L5 (Palomba and Luntama, 2022, see also https://www.esa.int/Space_Safety/Vigil) is one concrete output of these studies, with the mission now moving towards construction phase (phase C in the jargon of satellite projects). Hopefully others will follow, e.g. missions to L4. These are all excellent steps forward that will improve our ability to monitor solar activity. But the long-term goal should be to establish whole-Sun monitoring, not to trade off between views from L1, L4, L5 and other locations. The insights gained from these different locations must be combined to provide robust monitoring of our star. In particular, whole-Sun monitoring will bring two strategic benefits:

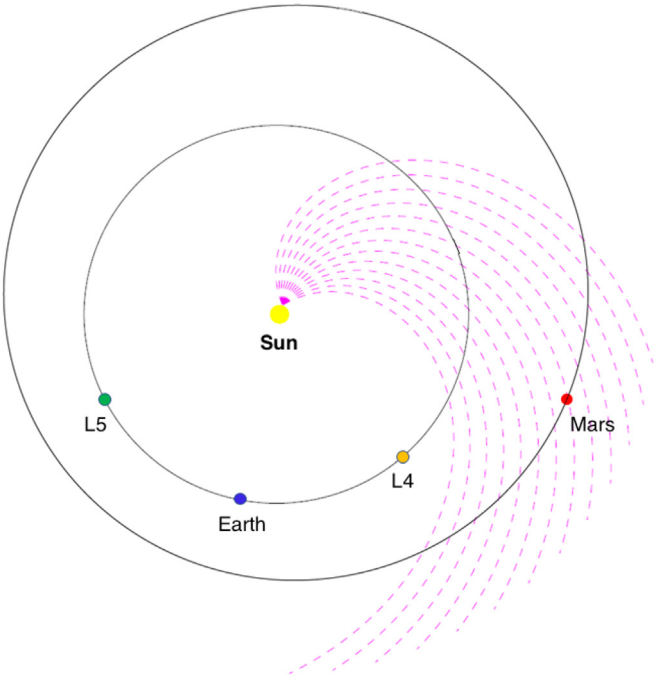

Fig. 10. The elliptical orbits of Earth and Mars around the Sun (yellow). Here Mars (red) is ahead of the Earth (blue) and is exposed to SEPs originating in an active region 90° further west in solar longitude (as expected for a Parker spiral field). In this case the active region is not visible from Earth or Mars or either of the L4 (orange) and L5 (green) Lagrange points.

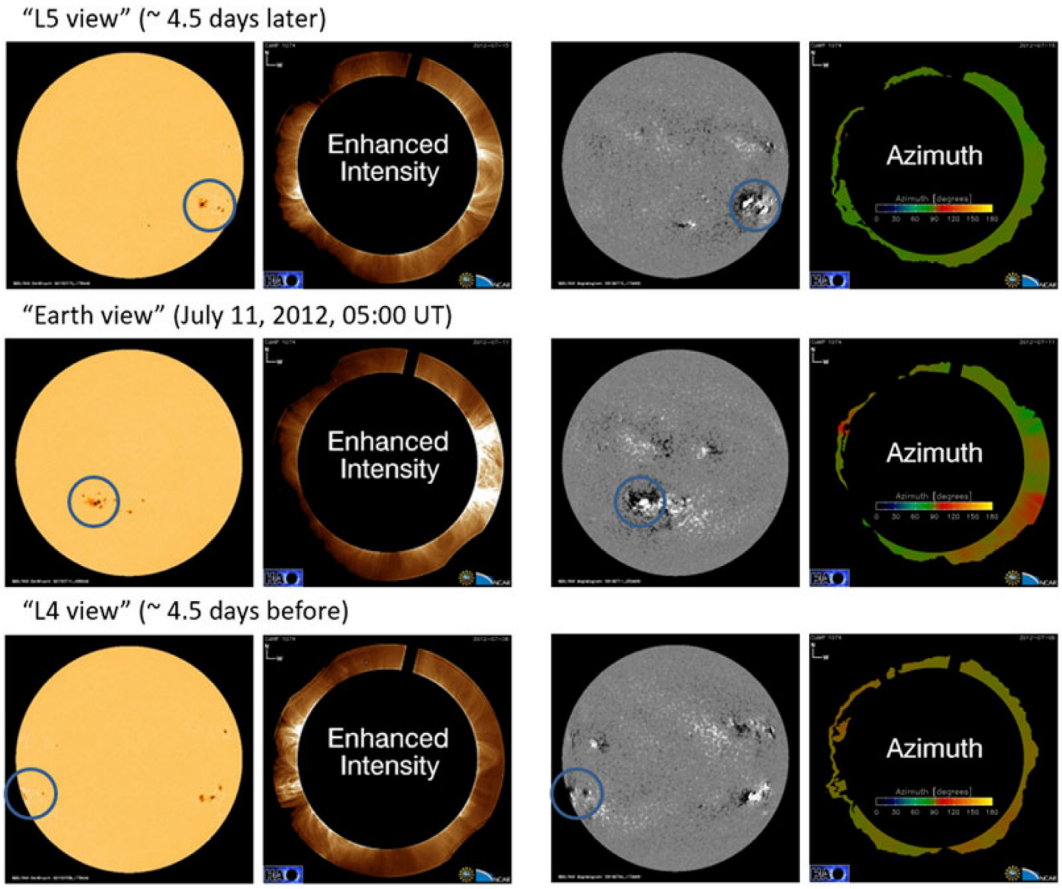

Fig. 11. Emulation of observations of an active region from three different viepoints, namely L1 (middle), L5 (top) and L4 (bottom). Shown are the photospheric continuum (leftmost column), coronagraphic EUV images (second from left), photosphetic magnetograms (second from right) and azimuth measurements for inferring the coronal magnetic field vector (rightmost column). Adapted from Bemporad (2021).

- It will reduce the risk of abrupt changes in forecasts of solar activity when new regions come into view, especially if those regions have complex magnetic structures. Such abrupt changes can confuse both forecasters and end users and, most importantly, they could reduce user confidence in forecasts. Whilst this might be partially mitigated by reaching out to users to keep them better informed, the best solution is to produce high quality forecasts that evolve gradually and justifiably in response to changing conditions everywhere on the Sun.
- Whole Sun monitoring will be essential when humans travel to Mars, which now seems likely in the next few decades. Space weather is an important factor for human travel to Mars as discussed by Hapgood (2019). Whilst good spacecraft design can reduce radiation doses (e.g. from the background flux of very high energy cosmic rays), the crew will also need more heavily shielded sheltering when the spacecraft is exposed to intense bursts of solar energetic particles. Thus the mitigation provided by good design must be complemented by forecasts of eruptive activity that is likely to affect the spacecraft. The crew can then reconfirm that the shelter is ready for use, and be prepared to retreat when an event is imminent, e.g. when onboard monitors detect relativistic electrons ahead of radiation storm protons (Posner, 2007). However, the monitoring of solar active regions with potential to erupt towards the spacecraft requires a set of monitors that can cover all solar longitudes and also provide system-level resilience (e.g. robustness against the loss of one or two spacecraft). It cannot rely on observations from Earth, L1, L4 and L5, or on the spacecraft itself. As an example, Fig. 10 shows a worst case scenario where Mars is visible from Earth, but magnetically connected to a farside active region. An eruption here will endanger astronauts at or near Mars, but will not be visible from Earth, Mars, L4 or L5.

Complementarity in terms of crucial space weather observations that would allow both a consistent study of the heliospheric propagation of solar eruptive transients and an improved fundamental understanding of the Sun also calls for twin spacecraft for L4 and L5, as proposed by Bemporad (2021). The concept of stereoscopic helioseismology could help in the advance prediction of active region emergence in the photosphere while stereoscopy can also lead to increased reliability in the measurement of coronal magnetic fields. Potentially interesting geometri-

cal configurations, such as relative or quasi-quadrature could greatly assist monitoring and operations, if both spacecraft are equipped with identical in situ and remote sensing instruments. Fig. 11 shows an emulation example of photospheric and coronal observations from identical instruments at L1, L4 and L5: in this example, three different lines of sight observe the Sun in both local (i.e., active region) and global spatial scales.

In summary, given the above discussion and building on ideas noted by Schrijver et al. (2015), there is a long-term, pressing need to develop and establish a resilient system of whole-Sun monitoring: to protect societal activities on and near Earth, to advance the science behind that protection, and also to support future human missions to Mars.

Appendix A provides a brief account of future missions that can have a transformative effect on the achievement of the above goals, either by directly facilitating operational forecasting or by providing key observations for modeling in this direction. We note in passing that we focus exclusively on space missions here as the only alternative baseline for a minimal (i.e., with the above caveats and more) R2O plan on space weather forecasting is global ground-based networks such as the existing GONG (Hill, 2018) and the envisioned SAMNet (Erdelyi et al., 2022).

7. Conclusions

In this review we have aimed to provide a contemporary summary and cross-cut of solar eruption prediction methods since the COSPAR/ ILWS roadmap paper by Schrijver et al. (2015). In these closing remarks, we aim to list (i) the progress made since this landmark collaborative work, (ii) some reasonably short-term (i.e., within the next 5 years) recommendations, (iii) long-term recommendations (i.e., within the next 10 + years) and, finally, some of the key challenges that lie ahead, intercepting this path to progress.

7.1. Current progress

In brief, the following progress has been achieved since Schrijver et al. (2015):

- *Soaring public interest*. Global interest in solar energetic phenomena and their prediction has skyrocketed and is expected to increase further, as it has entered the everyday, wider-public online media and tabloids. Dynamical solar manifestations seem to cause a public sensation that is further fueled by the anticipated crewed exploration of the Moon in the USA, Europe and China, and even more by the ultimate phase of the NASA/ ARTEMIS program that foresees the first humans on Mars. It is in the community's realm to ride this "wave of excitement" and to communicate its progress responsively to the public because public attention can lead to increased funding for basic research, on top of operations.
- *Increased community awareness toward synergistic and collaborative studies*. Albeit at a preliminary level, there are clear signs that the solar and heliophysics communities have come closer to organizing joint comparisons and validation of various prediction methodologies, roughly along the lines of Section 4. These actions are summarized in Section 4.3 and refer mostly to flare prediction in this review, with similar efforts on CME and SEP event prediction discussed in the Cluster reviews of Temmer et al. (2023) and Whitman et al. (2022), respectively. These activities have led to the realization that the current state-of-the-art is still lagging over what the community would have wished. As synergies highlight the needs that we must address, it is synergies that will signify progress, when it is achieved.
- *Enhancement of interdisciplinarity*. The scientific community itself has further embraced space weather and its forecasting. In Schrijver et al. (2015), the approximately 900 papers per year with "space weather" present in their abstract have more than tripled nowadays. This is not necessarily due to an increase in the size of the heliophysics community (which may indeed be the case to some extent) but, rather, due to the involvement of a significant part of the much larger data and computer science community. This interdisciplinarity, mainly bringing ML methods into the prediction problem, is a much needed development. It was heralded since 2007 for flares with the first application by Qahwaji and Colak (2007) and was further brought into spotlight by the computer vision effort of Martens et al. (2012). It is in the community's best interests that such collaborations be further fostered and enhanced. We hope that by this and previous reviews it has become clear that the prediction of solar energetic phenomena is too important a topic to be left to heliophysicists alone.
- *Deep learning into play*. The number of ML papers in solar eruption forecasting have indeed increased precipitously, but the new development since 2015 is the advent of DL methodologies into the problem. As explained in Section 1, it is still an open question whether DL methods are applicable to the "data-starved" problems of solar events forecasting, despite a good number of attempts already (Tables 1, 2). So far we have not witnessed a transformative effect from the application of DL methods and it remains to be seen whether this will continue to be the case.
- *Existing and envisioned dedicated space weather missions*. As discussed in Section 6.2 and Appendix A, various space agencies worldwide are now seriously contemplating building and launching missions with space weather forecasting firmly in their core objectives. In the case of China's ASO-S (A.2), the mission is already launched and its data are widely anticipated. ISRO's Aditya-L1 (A.3) was launched in September 2023, while ESA's Vigil L5 mission is currently in the stage of payload selection. The notion of a spacecraft constellation beyond the SEL (Sun-Earth line) and above/below the

ecliptic has also matured and there are multiple mission concepts pursuing these ideas. These elements largely shape our recommendations for the next 10 + years.

7.2. Short-term recommendations (next 5 years)

A tentative list of short-term recommendations is as follows:

- *Streamline prediction research; enhance transparency and openness*. To develop a common, end-to-end framework for forecasting solar eruptions, predicted either separately (i.e., for flare, CME, or SEP event forecasting), or in tandem, with the latter being preferable. The framework should serve for the development of new, and the improvement of existing, methods. The framework should not be dependent on the actual prediction problem and its specifics, but should be general and clear enough to be easily digested by the community. Fig. 5 and pertinent discussion makes such a case. Such an action naturally calls for (i) creating open-access, comprehensive benchmark data sets for a systematic training and testing of methods; (ii) developing standard training–testing practices; and (iii) defining a set of common (i.e., by community's consensus) verification/ validation metrics for each problem. The CCMC Scoreboards (Section 4.3) is an initiative heading clearly in this direction. Benchmark data should abide by contemporary requirements, such as the FAIR set of principles (Findable, Accessible, Interoperable, and Reusable; Wilkinson et al., 2016). Methods have different specifications and all methods may not be able to accommodate all metrics. They should, at least, use a subset of these metrics to allow direct comparison on identical training and testing samples of positive (event) and negative (no event) instances.
- *Clear the scientific journal landscape*. Related to the previous item, scientific journals should aim to control the mounting influx of submitted manuscripts on solar event prediction topics, particularly those employing AI techniques, by issuing guidelines for publication acceptance. Given the increased interest, the influx is inevitable. However, these methods and results should be able to demonstrate tangible progress over existing methods, hopefully by aligning to a framework such as the one discussed above. Journals are not agnostic to this issue and there is already one such set of guidelines (Lugaz et al., 2021). More should follow and this motion should be supported.
- *Facilitate space weather forecasting as a Sun-to-Earth endeavor*. Namely, establish the notion that forecasting solar energetic events is a Sun-to-Earth, rather than an inner-heliospheric, problem. Naturally there are challenges (Fig. 1), but the artificial splitting of the heliospheric "system of systems" into different subsystems deprives methods of crucial information to assimilate and increases the impact of artificial "boundaries", besides impeding physical understanding in some cases. The understanding of the processes and the operational demands should go hand-in–hand. In this respect, inner heliospheric modeling frameworks discussed in the Cluster review of Temmer et al. (2023) are the designated solution given the lack of inner heliospheric remote-sensing and scarce in situ data. How these methods connect with the models and results in the lower solar atmosphere as boundary and initial conditions, or as educated guesses at least, is a challenge that we need to overcome. In the medium-to-long-term future, one envisions a Sun-to-Earth forecasting framework that addresses all partial problems (initiation, propagation, geoeffectivenes) supported by data from multiple vantage points. Given the momentum, the seeds for this process can be placed in the next five years.
- *Determine applicability of deep learning methodologies*. This is a straightforward task to envision, albeit a formidable one to pursue. The question seems clear: are there enough positive samples for DL methods to be used for a credible prediction of solar events? Given the high spatial resolution, constant quality and high cadence of even present solar observations, DL methods seem able to train on negative samples. Will they be able to determine an instance of the positive sample when they process it? Will synthetic data or manual oversampling of the positive training sample be viable remedies or recipes? Answers to these questions, however tentative, should become available in the next few years.
- *Interpret unsupervised machine learning and deep learning*. The interpretability issue is discussed at some detail in Section 5.5 and it impedes progress in physical understanding and, equally importantly, in the envisioned achievement of O2R in Section 5.4. The R2O leg, if successful, will manage to provide forecast results to stakeholders, who are less interested in scientific accuracy in any case. However, O2R will not be feasible via these methods unless interpretability is boosted, so that one can see a successful, converging R2O - O2R loop toward optimal forecasts. In ML, hybrid techniques may be able to show progress in this direction but the question on a large part of DL methods remains wide open. Recent developments on knowledge-informed or physics-informed machine learning provide hope but they are still at their infancy (or perhaps, not even there) for space weather forecasting applications.
- *Achieve customized, and customizable, space weather forecasts*. This demand has emerged in multiple occasions and it would be a meaningful practice for the community to start experimenting in this direction. This is mentioned here because it also helps elaborate on R2O, by means of diversification into the needs of different sectors and due to the additional research we need to devote into performance verification for this. This important task cannot be achieved without the help of space weather forecasting agencies; SWPC, ESA Space

Safety Network, MOSWOC, ISES, NICT, KSWC, etc. whose role, as demonstrated broadly in multiple meetings, is to interface between stakeholders and the scientific community.

7.3. Long-term recommendations (10 + years)

These are largely shaped by the discussion in Section 6. We provide a summary of the main points below:

- *Homogenize/ streamline prediction for the full set of problems*. Assuming that the previous steps of streamlining research and enhancing transparency are successful, we should be considering bringing all problems concerned with Sun-induced space weather under a common framework. This implies flare, CME and SEP prediction, CME propagation in the inner heliosphere, time of arrival, as well as geoeffectiveness. Modularity is key in this respect because such a framework will have its testbeds and breadboards for the development, testing, and/ or inclusion of new modules devoted to different problems of the set. More such frameworks may appear worldwide, but the adoption of generally accepted streamlining rules will result in all of them sharing largely similar (albeit not identical) principles such as, say, the winning technologies prevalent in commodities such as aircraft, cars, or boats.
- *Achieve observations beyond the Sun-Earth line and the ecliptic*. Missions to L4 and L5, in conjunction with L1, should be implemented and launched in order to achieve continuous operations-grade data beyond the Sun-Earth line. Given existing legacies of space observatories in orbit and at L1, one does not expect that missions dedicated to operations should entail new technology developments for their payloads. In addition, a significant part of the community already believes that the data of these missions will also be science-grade and enable major leaps in physical understanding, at the same time facilitating a successful R2O. Observations beyond the ecliptic and at changing geometries should be facilitated via the Firefly Constellation. The scientific gain of non-space weather missions such as Parker Solar Probe and Solar Orbiter, along with Ulysses in the past, is evidence enough of the dual benefit of such mission concepts, in terms of both cutting-edge science and facilitating future operations.
- *Expand from terrestrial to planetary space weather*. Given ARTEMIS, with its lunar and martian phases, MoonVillage, and even robotic exploration toward solar system worlds featuring liquid oceans, the next decade should see the foundations of a planetary space weather forecasting network. Such a need is already envisioned and well documented (Plainaki et al., 2016). Provided that short-term recommendations about streamlining and homogenization are successful, along with the multi-messenger observations from different vantage points of the previous item, expanding circumterrestrial and cislunar forecasting to deep space should not be, or feel, like re-discovering the wheel. One or more modular space weather forecasting systems should be able to provide forecasts beyond 1 AU, albeit exclusively via modeling, as all our solar observers will be within, at the limit, or slightly beyond, the inner heliosphere. Placing space weather-oriented missions beyond 1 AU could be considered as a (much) longer-term task, or accommodated to some degree alongside future solar system exploration missions.

Declaration of Competing Interest

The authors declare that they have no known competing financial interests or personal relationships that could have appeared to influence the work reported in this paper.

Acknowledgments

We are grateful to the two anonymous referees who read the manuscript with extreme care and suggested revisions that improved the manuscript significantly. COSPAR Panel on Space Weather's International Space Weather Action Teams (ISWAT) program has been facilitating and coordinating this series of roadmap papers in which this work belongs to. M.K.G. and co-authors are grateful for the opportunity to participate and contribute to this collective work by the community. M.K.G. acknowledges the National Committee for Space Research of the Academy of Athens that approved his participation in this work. He also acknowledges the European Union's projects SoME-UFo (grant agreement ID: 268245), FLARECAST (grant agreement ID: 640216), and SWATNET (grant agreement ID: 955620), ESA Space Safety Network's A-EFFort service (product code S.124), and the New Generation Visiting Program of the Georgia State University in Atlanta, GA, USA for partial support on research cited in this work. S.L.Y. is grateful to the Scientific Technology and Facilities Council for their support via the consolidated grant (STFC ST/V000497/1) and for the award of an Ernest Rutherford Fellowship (ST/X003787/1). A.V.'s participation in the ISWAT activities is supported by NASA grant 80NSSC22K0970. The Gap Analysis work was funded under ARDES II Contract 80MSFC20D0004. ASO-S is supported by the Strategic Priority Research Program on Space Science, Chinese Academy of Sciences (Grant No. 15320000). A.N.Z. thanks the Belgian Federal Science Policy Office (BELSPO) for the provision of financial support in the framework of the PRODEX Programme of the European Space Agency (ESA) under contract number 4000136424. S.A.M. is involved with the European Union Horizon Europe Project No. 101082164 (ARCAFF). G.B. was supported by NASA grant 80NSSC19K0087. A.G.E. and P.M. were supported by NASA Kentucky under NASA award number

80NSSC21M0362. A.G.E. was also supported by NASA award number 80NSSC23M0074, the NASA Kentucky EPSCoR Program and the Kentucky Cabinet for Economic Development. A.A. acknowledges support by the NSF's OAC grant (2209912). Io.K. acknowledges support by grant KO 6283/2-1 of the Deutsche Forschungsgemeinschaft (DFG). A. N. and S. P. acknowledge support by the ERC Synergy Grant (810218) "The Whole Sun", and E.U.'s SWATNET grant (grant agreement ID: 955620). S.-H.P. was supported by basic research funding from the Korea Astronomy and Space Science Institute (KASI2024185002). S.T. was supported by JSPS KAKENHI Grant Nos. JP20KK0072 (PI: S. Toriumi), JP21H01124 (PI: T. Yokoyama), JP21H04492 (PI: K. Kusano).

Appendix A. Mission outlook

A.1. Firefly: The Need for a Wholistic View of the Sun and its Environment

Critical knowledge gaps (see Fig. 12) exist in our understanding of how magnetic fields control solar (and, by extension, stellar) activity on timescales from minutes to years; filling these gaps will require a transformative observational approach of the Sun and its environment. We know that solar activity drives space weather as the result of dynamic magnetic fields that form in the solar interior and evolve continuously until reaching levels of complexity in the atmosphere that trigger eruptions. However, we do not fully understand how solar and, more generally, stellar magnetic fields are generated, or how they evolve through the eruptive states.

Firefly is an innovative mission concept designed to close these long-standing knowledge gaps in heliophysics. A constellation of spacecraft will provide both remote sensing and in situ observations of the Sun and heliosphere from a full 4π-steradian field of view. This mission implements a holistic observational philosophy that extends from the Sun's interior, to the photosphere, through the corona, and into the solar wind, simultaneously with multiple spacecraft at multiple vantage points, optimized for continual global coverage over much of a solar cycle. The mission constellation includes two spacecraft in the ecliptic plane and two flying above 70° solar latitude. The overarching goal of the Firefly mission concept is to understand the global structure and dynamics of the Sun's interior, the generation of solar magnetic fields, the origin of the solar cycle, the causes of solar activity, and the structure and dynamics of the corona as it creates the heliosphere. To advance the scientific knowledge needed to characterize the heliosphere, the Firefly mission concept has defined four fundamental science objectives: (1) Understand how surface and sub-surface flows combined with toroidal magnetic field instabilities produce the cyclic solar dynamo, the root cause of solar activity; (2) Understand the conditions leading to solar eruptive activity and the role of the large-scale magnetic field; (3) Determine how solar wind conditions vary with latitude and longitude both in response to changing global solar conditions and throughout the solar cycle; and (4) Understand how and where energetic particles are accelerated and transported through the heliosphere.

The Firefly constellation offers ample opportunities for cross-disciplinary science from viewpoints not accessible before. It will provide significant insight into the dust structure of the zodiacal cloud, near-Earth hazardous objects, comets, and objects inside 1 AU. The down-view of the solar system from high latitudes beyond the ecliptic plane is critical to all these research topics. Previous observations could only offer a single viewpoint, that often suffers from effects (e.g., projection, timeliness, and continuity of the observations) that curtail access to important information about not only space weather but also about cometary objects and stealth asteroids in the inner heliosphere. This information to be offered by Firefly and changing observation geometries is equally critical with space weather for Earth's safety. In addition, observing the solar planetary system from different viewpoints offers essential information about planetary alignment or misalignment to the path of propagating solar transients. This is essential for our understanding of exo-planetary space weather.

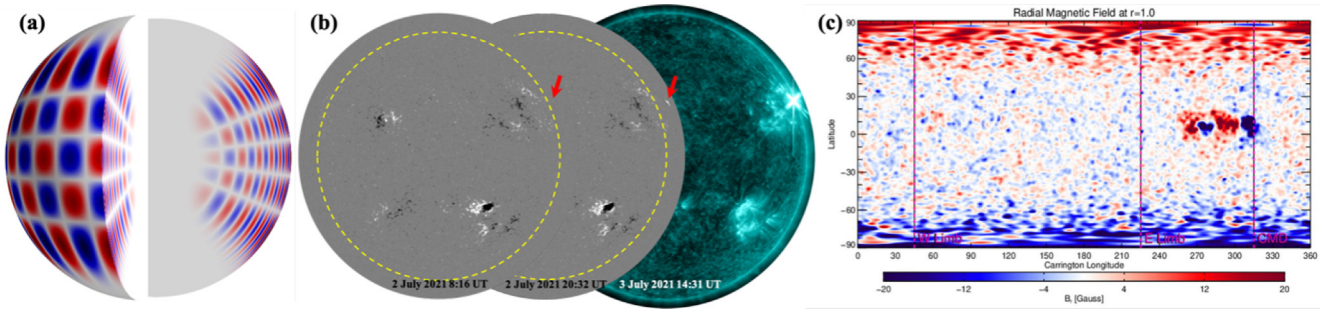

Fig. 12. Example of the major knowledge gaps in our understanding of the Sun and the Heliosphere. (a) Global helioseismic modes that are insensitive to conditions at high latitudes. (b) Example of the failure of Sun-Earth line magnetograms to capture a newly emerging active region near the limb. This active region emerged within 12 h and produced an X1.5-class flare that could not be forecast due to lack of magnetic field data. The yellow dashed line shows the S/N limit for magnetogram data away from disk center. (c) Photospheric radial magnetic field daily-update "synoptic map" built using measurements taken over a 27-day "Carrington Rotation" (CR) during CR 2217 and 2218. Note that the polar regions are extrapolated and distorted due to low signal-to-noise above 60^o latitude and lack of visibility. Courtesy: Predictive Sciences Inc. (PSI)/ Cooper Downs.

A.2. The Advanced Space-Based Observatory – Solar (ASO-S) mission

The ASO-S (Chinese nickname Kuafu-1, Gan et al., 2019; Gan et al., 2022; Gan et al., 2023) mission was launched in October 2022. It is the first Chinese comprehensive solar-dedicated observatory in space and aims at exploring the relationship and physics between solar magnetic fields, solar flares and CMEs. Besides scientific objectives, the mission is commissioned to provide operational data support for forecasts of solar eruptions, especially CMEs. To fulfill these major objectives, ASO-S has three payloads onboard: the Full-disk vector MagnetoGraph (FMG), the Hard X-ray Imager (HXI), and the Lyman-alpha Solar Telescope (LST) dedicated to observe vector magnetic fields, flares, and CMEs, respectively.

The space weather tasks of the ASO-S mission include the development of an image browsing system for the ASO-S observations, automatic detection and tracking of solar eruptions, predictions of CME arrival time, flare forecasts, etc (Feng et al., 2020, for detailed information). Major emphasis is placed on the CME arrival time predictions (Alobaid et al., 2022). To enable such predictions, the mission prioritizes the downlink of the LST coronagraph (Solar Corona Imager, SCI) data. SCI observes the corona from 1.1 to 2.5 $R_{\odot}$ in both white light and the H I Lyman-α line. If the instrument works well, the classification of coronagraph images with or without a CME could be done with the inflight triggering algorithm of the SCI event mode (Lu et al., 2020). The images with a CME will be distributed to different space weather prediction centers in China for further processing and forecasts once the Science Operation and Data Center (SODC) of ASO-S receives the data from the Science Mission Operation Center (SMOC). The automatic detection and tracking (Wang et al., 2019), and three-dimensional (3D) reconstructions of CMEs are implemented to calculate the 3D CME parameters used as the inputs for the CME propagation models (e.g. Wang et al., 2018). Solar flare forecasting is still a challenging task, given also the difficulty to locate an efficient precursor. Huang et al. (2018) applied a deep learning method to automatically extract forecasting patterns from the line-of-sight magnetograms of active regions and soft X-ray observations. The magnetograms are planned to be provided by FMG. Supplemental information can be acquired by HXI and LST.

A.3. The Aditya-L1 Solar Observatory

The Aditya-L1 mission is India's first solar space mission, which recently launched in September 2023 (Seetha and Megala, 2017). Aditya-L1 is a comprehensive solar observatory, to be located at L1, which carries seven payloads geared towards observing the origin of solar dynamic activity and its manifestations at near-Earth space environment. Four payloads are remote sensing instruments while three instruments focus on in situ measurements of solar wind and transients. The nominal mission lifetime is envisaged to be 5 years, but an extension is possible over the completion of solar cycle 25 and into cycle 26.

The Solar Ultraviolet Imaging Telescope (SUIT; Ghosh et al. (2016, 2017)) onboard Aditya-L1 will observe solar dynamics (at the 200–400 nm wavelength range) from near the photosphere to through the chromosphere in order to understand the coupling of the solar atmosphere and energy flow from the photosphere to the corona, as mediated by magnetic fields and radiation. The instrument will return full-disk images of the Sun across various layers of the solar atmosphere. The Variable Emission Line Coronagraph (VELC; Raghavendra Prasad et al. (2017)) instrument will observe the dynamics of the solar corona in visible and infra-red channels and has capabilities for spectroscopy, imaging and magnetic field measurements for coronal magnetometry. The goals of VELC are to understand coronal heating, the initiation mechanisms and kinematics of CMEs and to constrain the magnetic structure of the corona. With a targeted field of view between $1.05R_{\odot}$ and $3R_{\odot}$, VELC has the ambitious goal of capturing the early initiation dynamics of CMEs in the inner corona. The Solar Low Energy X-ray Spectrometer (SoLEXS) and High Energy L1 Orbiting X-ray Spectrometer (HEL1OS) will study the origin and dynamics leading to solar flares, will characterize flare emission and will probe the flare-associated acceleration mechanisms of solar energetic particles (Sankarasubramanian et al., 2011; Sankarasubramanian et al., 2017).

Other than these remote sensing instruments, there are three in situ plasma and magnetic field diagnostics instruments for the solar wind, transients, and CME flux ropes before they impact Earth. The Aditya Solar Wind Particle Experiment (ASPEX; Goyal et al. (2018)) and Plasma Analyzer Package for Aditya (PAPA; Thampi et al. (2014)) will measure the solar wind speed, constrain its physical properties including its composition and particle distribution. The Aditya Magnetometer Experiment (Yadav et al., 2018) will characterize the magnetic field properties of the solar wind, transient structures and CMEs at L1.

Taken together, it is expected that the suite of instruments on the Indian Space Research Organisation (ISRO) Aditya-L1 mission will continue and enhance the legacy of great observatories such as ESA's Solar and Heliospheric Observatory (SOHO) and NASA's Solar Dynamics Observatory (SDO). Specifically, the combination of remote imaging, spectroscopy and in situ observations are envisaged to generate transformative information and knowledge on the genesis and near-Earth impact of space weather (Nandy et al., 2020).

A.4. Next-generation Solar-observing Satellite (SOLAR-C)

SOLAR-C (Shimizu et al., 2020: target launch in late 2020s) is JAXA's next-generation solar-observing satellite, designed to answer the question of "How does the interplay of magnetic fields and plasma drive solar activity?"

with its onboard telescope EUVST (EUV High-throughput Spectroscopic Telescope). The two primary science objectives of SOLAR-C are:

- Understand how fundamental processes lead to the formation of the solar atmosphere and the solar wind.
- Understand how the solar atmosphere becomes unstable, releasing the energy that drives solar flares and eruptions.

Solar flare studies are frequently based on the magnetic field measurements in the photosphere and on coronal field extrapolations due to the instrumental and technological constraints (see discussion in Section 5.3). However, to truly understand how magnetic energy is accumulated in the corona and initiates magnetic reconnection that triggers the flare, it is critical to obtain information on the active-region atmosphere and quantify its characteristics. To this end, a sub-objective of SOLAR-C aims at understanding the fast magnetic reconnection process that explains flare eruptions by temporally and spatially resolving the evolution of flare reconnection. Another sub-objective seeks to understand the large-scale evolution of flare-productive active regions over days by monitoring the active-region atmosphere and identifying appropriate spectroscopic signatures such as non-thermal upflows, which may indicate the energy buildup. To achieve these science objectives, SOLAR-C will take the following approaches:

A. Seamlessly and simultaneously observe all the temperature regimes of the solar atmosphere from the chromosphere to the corona ($\log(T/[\mathrm{K}]) = 4$–7),
B. Resolve elemental structures of the solar atmosphere with high spatial resolution and cadence to track their evolution (0.4 arcsec and 0.5 s), and,
C. Obtain spectroscopic information on the dynamics of elementary processes taking place in the solar atmosphere (EUV spectroscopy).

By taking full advantage of its spatial, temporal, and spectral resolution, SOLAR-C measures the velocity field around the flare-triggering site in active region at multiple temperatures (i.e., multiple heights). Such observables help to clarify the physical conditions and MHD instability modes in flare eruptions, which may contribute to the flare prediction, probably through comparisons with state-of-the-art numerical simulations. In this regard, one of the mission outcomes of SOLAR-C is defined to extend our understanding to building the algorithms of flare prediction and estimating the flare impact on terrestrial environment.

SOLAR-C is a mission of international cooperation led by Japan (JAXA) with participation from US (NASA) and Europe (the European Space Agency and the space agencies of Germany, France, Italy, and Switzerland). In April 2020, SOLAR-C was downselected at ISAS/JAXA for the 4th Competitively-chosen Middle-class mission, to be launched by the Epsilon S launch vehicle. SOLAR-C passed the mission definition review in July 2022 and, in November 2022, JAXA SOLAR-C Pre-Project Team was officially established.

A.5. The Polarimeter to UNify the Corona and Heliosphere (PUNCH)

The PUNCH mission (DeForest et al., 2022) is an in-development Small Explorer mission to image the Sun's outer corona and the inner heliosphere, in 3D, as a single unified system. PUNCH comprises four smallsats in low Earth orbit, each carrying one primary instrument: one "Narrow Field Imager" (NFI), a coronagraph whose field of view spans from roughly 6 $R_\odot$ to 30 $R_\odot$ on the sky; and three "Wide Field Imagers" (WFIs), each of which is a heliospheric imager whose field of view extends from roughly 20 $R_\odot$ to 45^o from the Sun. The four instruments are synchronized and operate together as a single suite. PUNCH images contain full linear polarization information, enabling direct 3D imaging of space weather relevant phenomena from a single vantage point (DeForest et al., 2013; Howard et al., 2013). The mission is scheduled to launch in 2025.

PUNCH data have the potential to greatly improve near-term space weather forecasting, both by tracking CMEs and providing updated estimates of arrival time and impact angle, and also by delivering direct measurements of the internal 3D structure (chirality) of their associated flux ropes (DeForest et al., 2016). Chirality is an indicator of the sign of the north/south component of the magnetic field (B_z) at the leading edge of the CME. B_z direction is the single strongest indicator of CME geoeffectiveness, and is difficult to measure remotely with current instrumentation (Möstl et al., 2014). Forecasting of CME arrival currently requires direct extrapolation (modeling) from coronagraph images (e.g., Webb et al., 2009; Gressl et al., 2014), and major sources of uncertainty arise both from ambiguities in 3D determination from unpolarized imaging, and from the not-well-characterized physics of CME propagation in the inner heliosphere. By eliminating the need to extrapolate from the corona itself across 0.8 AU to Earth, PUNCH and similar instruments will greatly improve prediction of arrival time and geoeffectiveness once an event has occurred on the Sun, benefiting forecasting on the time scale of 1–4 days.

A.6. The ASPIICS coronagraph onboard the PROBA-3 mission

PROBA-3 (PRoject for On-Board Autonomy) is a technology demonstration mission of the European Space Agency (ESA). It consists of two spacecraft flying in a precise formation. The main spacecraft will host a telescope, and the smaller spacecraft will carry a circular occulter. Together the two spacecraft will form a giant solar coron-

agraph called ASPIICS (Association of Spacecraft for Polarimetric and Imaging Investigation of the Corona of the Sun, see Lamy et al., 2010; Galano et al., 2018). The separation between the spacecraft, approximately 144 m, will allow observing the corona from around 1.1 $R_\odot$ with very low straylight (e.g. Shestov et al., 2021). The launch is scheduled in the second quarter of 2024.

ASPIICS will observe the solar corona between 1.1 $R_\odot$ and 3 $R_\odot$ in three spectral passbands. The main white-light passband of 5350–5650 Å is dominated by the green Thomson-scattered continuum and does not contain strong spectral lines. The two narrow passbands centered on the Fe XIV line at 5304 Å (coronal "green line") and on the He I D_3 line at 5877 Å will be used to image the emission of the hot (around 2 MK) corona and cold (a few tens of thousand Kelvin) prominences respectively. The main white-light passband will also be used for polarimetric observations made with three linear polarizers oriented at 60° with respect to each other. The spatial resolution is 2 arc sec per pixel (in the unvignetted zone), and the nominal synoptic cadence is 1 min (Galano et al., 2018).

ASPIICS will not be used for real-time space weather monitoring due to its duty cycle (on average, two orbits per week will be dedicated to solar coronagraphy and observations will be made during 6 h out of the 19.6 h orbit) and data latency (days to weeks). However, besides technology demonstration aspects, ASPIICS will give crucial scientific insight into the physics of CMEs. The ASPIICS observations will provide information on the CME initiation in the low corona, and on CME-driven shocks that will be often forming within the ASPIICS field of view. ASPIICS will measure the increase of the height of prominences during their slow rise, which is an important eruption precursor (e.g. Filippov and Den, 2001). The morphological evolution of coronal cavities, in particular their "necking" that correlates with the CME eruption (Gibson et al., 2006), will be observed by ASPIICS as well.

The precise formation flying technology of the PROBA-3 mission may be used in the future for improving the design of coronagraphs dedicated to CME monitoring. In particular, this could allow extending the coronagraph field of view to lower heights without increasing the straylight. This is important also for obtaining information on the CME initiation in white light (i.e. showing the density structure) virtually down to the CME source region, and for providing seamless observations of the CME initiation and propagation from low to high corona using a single telescope.

A.7. Envisioning the Solar Stereoscopic Exploration

Solar Stereo Exploration (Yang et al., 2023) is envisioned with the Solar Polar-orbit Observatory (SPO, Deng et al. (2023)) to directly image the solar polar regions conjugated with two spacecraft in an unprecedented way by traveling around 1-AU distance in a large solar inclination angle ($\geqslant$80 degrees) and a small ellipticity, and Solar Ring (SOR, Wang et al. (2023)) deploying three 120°-separated spacecraft on the 1-AU orbit, or three spacecraft locating at Sun-Earth Lagrangian points L3, L4, and L5 (Yang et al., 2023), to monitor and study the Sun and inner heliosphere from a full 360^o perspective on the ecliptic plane.

Solar magnetic fields and related solar activity largely determine the characterization of the heliospheric environment and shape space weather. The polar magnetic fields of the Sun and its dynamic processes are especially vital in the aspects of manifesting the internal dynamo of the Sun, and shaping magnetic fields in the heliosphere for the space weather and space climate. Up to now, almost all solar observations have been limited in the vicinity of the ecliptic plane, with the exception of Solar Orbiter that has a slanted angle toward the solar poles later in the mission and Ulysses that, however, had no remote-sensing observations. Due to projection effects, the polar regions remain the least-known territories of the Sun.

Based on multi-band remote-sensing and in situ measurements, SPO (Deng et al., 2023) aims to achieve breakthroughs on the following top-level scientific objectives: (1) provide decisive observations to reveal the origin of the solar magnetic activity that shapes the solar eruptivity, space weather and space climate; (2) provide direct observational support for unveiling the origin, mechanism, and effect of the "primitive" high-speed solar wind that connects the Sun and celestial bodies in the solar system; (3) provide the necessary, complete, and self-consistent initial and boundary conditions for creating a data-driven global heliospheric numerical model that serves as the foundation for space weather prediction.

SOR has its first spacecraft located 30° upstream of the Earth, the second spacecraft 90° downstream, and the third one 120° apart (Wang et al., 2023). In Solar Stereo Exploration three spacecraft located at Sun-Earth Lagrangian points L3, L4, and L5 have been proposed (Yang et al., 2023). With necessary science instruments, (e.g., the Doppler-velocity and vector magnetic field imager, wide-angle coronagraph, and in situ instruments), either mission from a full 360° perspective in the ecliptic plane will allow us to establish unprecedented capabilities: (1) provide simultaneous Doppler-velocity observations of the whole solar surface to understand the solar interior, (2) provide vector magnetograms of the whole photosphere—the inner boundary of the solar atmosphere and the heliosphere, (3) provide information on the full-lifetime evolution of solar featured structures, and (4) provide a holistic view of solar transients and their space weather repercussions in the inner heliosphere.

The Solar Stereoscopic Exploration missions can overcome the limitation of single-view observation, and access to omni-directional & multi-element physical data, thus contributing to finding solutions for major scientific problems in solar physics and space weather. By orbiting the ecliptic and the omni-dimensional exploration of polar

regions, Solar Stereo Exploration realizes solar detection from five vantage points, with the ability to detect the Sun in all directions. The missions will provide high-quality data for scientific research and space weather forecasting. The achievements will advance knowledge of the Sun's internal structure and the origin of **the** solar magnetic field, the mechanism of solar activities and full heliospheric space weather effects, at the same time boosting and facilitating novel space weather forecasting models.

Appendix B. Acronym List

See Table B.5.

Table B.5
A full list of acronyms used throughout this paper.

Acronym	Meaning
A-EFFort	Athens Effective Solar Flare Forecasting
AAS	American Astronomical Society
ACE	Advanced Composition Explorer
ADS	Astrophysics Data System
AI	Artificial Intelligence
AI2ES	National Science Foundation Artificial Intelligence Institute for Research on Trustworthy Artificial Intelligence in Weather, Climate, and Coastal Oceanography
AIA	Atmospheric Imaging Assembly
API	Application Programming Interface
ApSS	Appleman Skill Score
ARCAFF	Active Region Classification and Flare Forecasting
ARDES	Aerospace, Research, Development, and Engineering Support Services
ASO-S	Advanced Space-Based Observatory - Solar
ASPEX	Aditya Solar Wind Particle Experiment
ASPIICS	Association of Spacecraft for Polarimetric and Imaging Investigation of the Corona of the Sun
AUC	Area Under Curve
BELSPO	Belgian Federal Science Policy Office
BS	Brier Score
BSS	Brier Skill Score
CCMC	Community Coordinated Modeling Center
CME	Coronal Mass Ejection
CoRA	Colorado Research Associates
COSPAR	Committee on Space Research
CSHKP	Carmichael, Sturrock, Hirayama, Kopp, Pneuman
DAFFS	Discriminant Analysis Flare Forecasting System
DeepLIFT	Deep Learning Important FeaTures
DEM	Differential Emission Measure
DL	Deep Learning
DMLab	Data Mining Laboratory
EIS	Extreme-ultraviolet Imaging Spectrometer
EOP	Emergency Operation Plans
ESA	European Space Agency
EUHFORIA	EUropean Heliospheric FORecasting Information Asset
EUV	Extreme Ultraviolet
EUVST	Extreme-ultraviolet High-throughput Spectroscopic Telescope
EW	East–West
FITL	Forecaster in the loop
FLARECAST	Flare Likelihood And Region Eruption foreCASTing
FMG	Full-disk vector MagnetoGraph
FN	False Negative
FORSPEF	Forecasting of Solar Particle Events and Flares
FP	False Positive
GC	Gini coefficient
GOES	Geostationary Operational Environmental Satellite
GONG	Global Oscillations Network Group
HARP	Helioseismic and Magnetic Imager Active Region Patches
HEL1OS	High Energy Lagrange 1 Orbiting X-ray Spectrometer
HMI	Helioseismic and Magnetic Imager
HSS	Heidke Skill Score
HXI	Hard X-ray Imager
ILWS	International Living With a Star
IMF	Interplanetary Magnetic Field
IRIS	Interface Region Imaging Spectrograph
ISAS	Institute of Space and Astronautical Science
ISES	International Space Environment Service
ISRO	Indian Space Research Organisation
ISSI	International Space Science Institute
ISWAT	International Space Weather Action Teams
JAXA	Japan Aerospace Exploration Agency
KSWC	Korean Space Weather Center
L (1/4/5)	Lagrange
LASCO	Large Angle and Spectrometric Coronagraph
LIME	Local Interpretable Model-Agnostic Explanation
LOS	Line-of-sight
LST	Lyman-alpha Solar Telescope
LSTM	Long Short-Term Memory Networks
LWS	Living With a Star
MAG4	Magnetogram forecast model
MagPy	Python package that provides tools for geomagnetic data analysis
MDI	Michelson Doppler Imager
MFR	Magnetic Flux Rope
MHD	Magnetohydrodynamic
ML	Machine Learning
MOSWOC	Met Office Space Weather Operations Centre
MSE	Mean Squared Error
MURaM	Max Planck University of Chicago Radiative Magnetohydrodynamic Model
MUSE	Multi-Slit Solar Explorer
NASA	National Aeronautics and Space Administration
NFI	Narrow Field Imager
NICT	National Institute of Information and Communications Technology
NLFF	Nonlinear force-free
NOAA	National Oceanic and Atmospheric Administration
NRC	National Research Council
NRT	Near-realtime
NSF	National Science Foundation
NWRA	NorthWest Research Associates
O2R	Operations-to-Research
PAPA	Plasma Analyzer Package for Aditya
PEDS	Physics-Enhanced Deep Surrogate
PIL	Polarity Inversion Line
PINN	Physics-Informed Neural Network

(continued on next page)

Table B.5 (*continued*)

Acronym	Meaning
PROBA	PRoject for On-Board Autonomy
PROSPER	Probabilistic Solar Particle Event Forecasting
PUNCH	Polarimeter to UNify the Corona and Heliosphere
R2O	Research-to-Operations
RMSE	Root Mean Squared Error
ROC	Relative Operating Characteristic
SAMNet	Solar Acvivity Monitor Network
SCI	Solar Corona Imager
SDO	Solar Dynamics Observatory
SEL	Sun-Earth line
SEP	Solar Energetic Particle
SHAP	SHapley Additive exPlanations
SHARP	Space Weather Helioseismic and Magnetic Imager Active Region Patches
SMA	Sheared Magnetic Arcade
SMARP	Space Weather Michelson Doppler Imager Active Region Patch
SMOC	Science Mission Operation Center
SODC	Science Operation and Data Center
SOHO	Solar and Heliospheric Observatory
SoLEXS	Solar Low Energy X-ray Spectrometer
SOR	Solar Ring
SPO	Solar Polar-orbit Observatory
SPRINTS	Space Radiation Intelligent System
SRS	Solar Region Summary
SS	Skill Score
STEREO	Solar Terrestrial Relations Observatory
STFC	Science and Technology Facilities Council
SUIT	Solar Ultraviolet Imaging Telescope
SWATNET	Space Weather Awareness Training Network
SWPC	Space Weather Prediction Center
SXR	Soft X-ray
TN	True Negative
TP	True Positive
TSS	True Skill Statistic
UK	United Kingdom
USA	United States of America
VELC	Variable Emission Line Coronagraph
WFI	Wide Field Imager
WSA	Wang Sheeley Arge
WTSS	Weighted True Skill Statistic
XRS	X-ray Sensor

References

Abduallah, Y., Jordanova, V.K., Liu, H., Li, Q., Wang, J.T.L., Wang, H., 2022. Predicting solar energetic particles using sdo/hmi vector magnetic data products and a bidirectional LSTM network. Astrophys. J. Suppl. Ser. 260 (1), 16. https://doi.org/10.3847/1538-4365/ac5f56.

Abduallah, Y., Wang, J.T.L., Nie, Y., Liu, C., Wang, H., 2021. DeepSun: machine-learning-as-a-service for solar flare prediction. Res. Astron. Astrophys. 21 (7), 160. https://doi.org/10.1088/1674-4527/21/7/160.

Abduallah, Y., Wang, J.T.L., Wang, H., Xu, Y., 2023. Operational prediction of solar flares using a transformer-based framework. Scient. Rep. 13, 13665. https://doi.org/10.1038/s41598-023-40884-1.

Abed, A.K., Qahwaji, R., Abed, A., 2021. The automated prediction of solar flares from SDO images using deep learning. Adv. Space Res. 67 (8), 2544–2557. https://doi.org/10.1016/j.asr.2021.01.042.

Abramenko, V.I., 2005. Relationship between magnetic power spectrum and flare productivity in solar active regions. Astrophys. J. 629 (2), 1141–1149. https://doi.org/10.1086/431732.

Abramenko, V.I., Yurchyshyn, V.B., Wang, H., Spirock, T.J., Goode, P. R., 2003. Signature of an Avalanche in solar flares as measured by photospheric magnetic fields. Astrophys. J. 597 (2), 1135–1144. https://doi.org/10.1086/378492.

Ahmadzadeh, A., Aydin, B., Georgoulis, M.K., Kempton, D.J., Mahajan, S.S., Angryk, R.A., 2021. How to train your flare prediction model: Revisiting robust sampling of rare events. Astrophys. J. Suppl. Ser. 254 (2), 23. https://doi.org/10.3847/1538-4365/abec88.

Ahmadzadeh, A., Aydin, B., Kempton, D.J., Hostetter, M., Angryk, R. A., Georgoulis, M.K., Mahajan, S.S., 2019. Rare-event time series prediction: A case study of solar flare forecasting. In: 2019 18th IEEE International Conference On Machine Learning And Applications (ICMLA), pp. 1814–1820. https://doi.org/10.1109/ICMLA.2019.00293.

Ahmadzadeh, A., Hostetter, M., Aydin, B., Georgoulis, M.K., Kempton, D.J., Mahajan, S.S., Angryk, R., 2019. Challenges with extreme class-imbalance and temporal coherence: A study on solar flare data. In: 2019 IEEE International Conference on Big Data (Big Data), pp. 1423–1431. https://doi.org/10.1109/BigData47090.2019.9006505.

Ahmadzadeh, A., Kempton, D.J., Martens, P.C., Angryk, R.A., 2023. Contingency space: A semimetric space for classification evaluation. IEEE Trans. Pattern Anal. Mach. Intell. 45 (2), 1501–1513. https://doi.org/10.1109/TPAMI.2022.3167007.

Ahmed, O.W., Qahwaji, R., Colak, T., Higgins, P.A., Gallagher, P.T., Bloomfield, D.S., 2013. Solar flare prediction using advanced feature extraction, machine learning, and feature selection. Sol. Phys. 283 (1), 157–175. https://doi.org/10.1007/s11207-011-9896-1.

Aktukmak, M., Sun, Z., Bobra, M., Gombosi, T., IV, W.B.M., Chen, Y., Hero, A., 2022. Incorporating polar field data for improved solar flare prediction. Front. Astron. Space Sci., 9. URL: https://doi.org/10.3389/fspas.2022.1040107. doi:10.3389/fspas.2022.1040107.

Al-Ghraibah, A., Boucheron, L., McAteer, R., 2015. An automated classification approach to ranking photospheric proxies of magnetic energy build-up. Astron. Astrophys. 579, A64. https://doi.org/10.1051/0004-6361/201525978.

Alipour, N., Mohammadi, F., Safari, H., 2019. Prediction of flares within 10 days before they occur on the sun. Astrophys. J. Suppl. Ser. 243 (2), 20. https://doi.org/10.3847/1538-4365/ab289b.

Alobaid, K.A., Abduallah, Y., Wang, J.T.L., Wang, H., Jiang, H., Xu, Y., Yurchyshyn, V., Zhang, H., Cavus, H., Jing, J., 2022. Predicting CME arrival time through data integration and ensemble learning. Front. Astron. Space Sci. 9, 1013345. https://doi.org/10.3389/fspas.2022.1013345.

Amari, T., Canou, A., Aly, J.-J., Delyon, F., Alauzet, F., 2018. Magnetic cage and rope as the key for solar eruptions. Nature 554 (7691), 211–215. https://doi.org/10.1038/nature24671.

Amari, T., Démoulin, P., Browning, P., Hood, A., Priest, E., 1991. The creation of the magnetic environment for prominence formation in a coronal arcade. Astron. Astrophys. 241 (2), 604–612.

Ambastha, A., Hagyard, M.J., West, E.A., 1993. Evolutionary and flare-associated magnetic shear variations observed in a complex flare-productive active region. Sol. Phys. 148, 277–299. https://doi.org/10.1007/BF00645091.

Anastasiadis, A., Lario, D., Papaioannou, A., Kouloumvakos, A., Vourlidas, A., 2019. Solar energetic particles in the inner heliosphere: status and open questions. Philos. Trans. Royal Soc. A: Math., Phys. Eng. Sci. 377 (2148), 20180100. https://doi.org/10.1098/rsta.2018.0100.

Anastasiadis, A., Papaioannou, A., Sandberg, I., Georgoulis, M., Tziotziou, K., Kouloumvakos, A., Jiggens, P., 2017. Predicting flares and solar energetic particle events: The FORSPEF tool. Sol. Phys. 292 (9). https://doi.org/10.1007/s11207-017-1163-7.

Angryk, R.A., Martens, P.C., Aydin, B., Kempton, D., Mahajan, S.S., Basodi, S., Ahmadzadeh, A., Cai, X., Boubrahimi, S.F., Hamdi, S.M., Schuh, M.A., Georgoulis, M.K., 2020. Multivariate time series dataset for space weather data analytics. Scientific Data 7 (1). https://doi.org/10.1038/s41597-020-0548-x.

Antiochos, S.K., 2013. Helicity Condensation as the Origin of Coronal and Solar Wind Structure. Astrophys. J. 772 (1), 72. https://doi.org/10.1088/0004-637X/772/1/72, arXiv:1211.4132.

Antiochos, S.K., DeVore, C.R., Klimchuk, J.A., 1999. A model for solar coronal mass ejections. Astrophys. J. 510 (1), 485–493. https://doi.org/10.1086/306563, arXiv:astro-ph/9807220.

Appleman, H.S., 1960. A fallacy in the use of skill scores. Bull. Am. Meteorol. Soc. 41 (2), 64–67. https://doi.org/10.1175/1520-0477-41.2.64.

Archontis, V., Syntelis, P., 2019. The emergence of magnetic flux and its role on the onset of solar dynamic events. Philos. Trans. Roy. Soc. London Ser. A 377 (2148), 20180387. https://doi.org/10.1098/rsta.2018.0387, arXiv:1904.06274.

Aschwanden, M.J., Nitta, N.V., Wuelser, J.-P., Lemen, J.R., Sandman, A., Vourlidas, A., Colaninno, R.C., 2009. First measurements of the mass of coronal mass ejections from the EUV Dimming Observed with STEREO EUVI A+B Spacecraft. Astrophys. J. 706, 376–392. https://doi.org/10.1088/0004-637X/706/1/376.

Aulanier, G., Török, T., Démoulin, P., DeLuca, E.E., 2010. Formation of torus-unstable flux ropes and electric currents in erupting sigmoids. Astrophys. J. 708 (1), 314–333. https://doi.org/10.1088/0004-637X/708/1/314.

Aurass, H., Holman, G., Braune, S., Mann, G., Zlobec, P., 2013. Radio evidence for breakout reconnection in solar eruptive events. Astron. Astrophys. 555, A40. https://doi.org/10.1051/0004-6361/201321111.

Bain, H.M., Steenburgh, R.A., Onsager, T.G., Stitely, E.M., 2021. A summary of national oceanic and atmospheric administration space weather prediction center proton event forecast performance and skill. Space Weather 19 (7). https://doi.org/10.1029/2020SW002670, e2020SW002670.

Balch, C.C., 2008. Updated verification of the space weather prediction center's solar energetic particle prediction model. Space Weather 6 (1). https://doi.org/10.1029/2007sw000337, n/a–n/a.

Barnes, G., 2007. On the relationship between coronal magnetic null points and solar eruptive events. Astrophys. J. 670, L53–L56. https://doi.org/10.1086/524107.

Barnes, G., Leka, K., Schumer, E., Della-Rose, D., 2007. Probabilistic forecasting of solar flares from vector magnetogram data. Space Weather 5 (9). https://doi.org/10.1029/2007SW000317.

Barnes, G., Leka, K.D., 2006. Photospheric magnetic field properties of flaring versus flare-quiet active regions. III. Magnetic charge topology models. Astrophys. J. 646 (2), 1303–1318. https://doi.org/10.1086/504960.

Barnes, G., Leka, K.D., Schrijver, C.J., Colak, T., Qahwaji, R., Ashamari, O.W., Yuan, Y., Zhang, J., McAteer, R.T.J., Bloomfield, D.S., Higgins, P.A., Gallagher, P.T., Falconer, D.A., Georgoulis, M.K., Wheatland, M.S., Balch, C., Dunn, T., Wagner, E.L., 2016. A comparison of flare forecasting methods. I. Results from the "All-Clear" Workshop. Astrophys. J. 829 (2), 89. https://doi.org/10.3847/0004-637X/829/2/89, arXiv:1608.06319.

Barnes, G., Schanche, N., Leka, K.D., Aggarwal, A., & Reeves, K. (2017). A Comparison of Classifiers for Solar Energetic Events. In M. Brescia, S.G. Djorgovski, E.D. Feigelson, G. Longo, & S. Cavuoti (Eds.), Astroinformatics (pp. 201–204). volume 325. doi:10.1017/S1743921316012758.

Baumgartner, C., Thalmann, J.K., Veronig, A.M., 2018. On the factors determining the eruptive character of solar flares. Astrophys. J. 853, 105. https://doi.org/10.3847/1538-4357/aaa243.

Bélanger, E., Vincent, A., Charbonneau, P., 2007. Predicting solar flares by data assimilation in avalanche models. Sol. Phys. 245 (1). https://doi.org/10.1007/s11207-007-9009-3, 141–165.

Bemporad, A., 2021. Possible advantages of a twin spacecraft heliospheric mission at the sun-earth lagrangian points l4 and l5. In: Front. Astron. Space Sci., p. 8. https://doi.org/10.3389/fspas.2021.627576.

Benvenuto, F., Piana, M., Campi, C., Massone, A.M., 2018. A hybrid supervised/unsupervised machine learning approach to solar flare prediction. Astrophys. J. 853 (1), 90. https://doi.org/10.3847/1538-4357/aaa23c.

Berghmans, D., van der Linden, R.A.M., Vanlommel, P., Warnant, R., Zhukov, A., Robbrecht, E., Clette, F., Podladchikova, O., Nicula, B., Hochedez, J.F., Wauters, L., Willems, S., 2005. Solar activity: nowcasting and forecasting at the SIDC. Ann. Geophys. 23 (9), 3115–3128. https://doi.org/10.5194/angeo-23-3115-2005.

Bhattacharjee, S., Alshehhi, R., Dhuri, D.B., Hanasoge, S.M., 2020. Supervised convolutional neural networks for classification of flaring and nonflaring active regions using line-of-sight magnetograms. Astrophys. J. 898 (2), 98. https://doi.org/10.3847/1538-4357/ab9c29.

Bloomfield, D.S., Higgins, P.A., McAteer, R.T.J., Gallagher, P.T., 2012. Toward reliable benchmarking of solar flare forecasting methods. Astrophys. J. Lett. 747 (2), L41. https://doi.org/10.1088/2041-8205/747/2/L41, arXiv:1202.5995.

Bobra, M.G., Couvidat, S., 2015. Solar flare prediction using SDO/HMI vector magnetic field data with a machine-learning algorithm. Astrophys. J. 798 (2), 135. https://doi.org/10.1088/0004-637X/798/2/135, arXiv:1411.1405.

Bobra, M.G., Ilonidis, S., 2016. Predicting coronal mass ejections using machine learning methods. Astrophys. J. 821 (2), 127. https://doi.org/10.3847/0004-637X/821/2/127, arXiv:1603.03775.

Bobra, M.G., Sun, X., Hoeksema, J.T., Turmon, M., Liu, Y., Hayashi, K., Barnes, G., Leka, K.D., 2014. The Helioseismic and Magnetic Imager (HMI) Vector Magnetic Field Pipeline: SHARPs - Space-Weather HMI Active Region Patches. Sol. Phys. 289 (9), 3549–3578. https://doi.org/10.1007/s11207-014-0529-3, arXiv:1404.1879.

Bobra, M.G., Wright, P.J., Sun, X., Turmon, M.J., 2021. SMARPs and SHARPs: Two solar cycles of active region data. Astrophys. J. Suppl. Ser. 256 (2), 26. https://doi.org/10.3847/1538-4365/ac1f1d.

Bornmann, P.L., Shaw, D., 1994. Flare rates and the McIntosh active-region classifications. Sol. Phys. 150, 127–146. https://doi.org/10.1007/BF00712882.

Boucheron, L.E., Al-Ghraibah, A., McAteer, R.J., 2015. Prediction of solar flare size and time-to-flare using support vector machine regression. Astrophys. J. 812 (1), 51. https://doi.org/10.1088/0004-637X/812/1/51.

Braun, D.C., 2016. A helioseismic survey of near-surface flows around active regions and their association with flares. Astrophys. J. 819, 106. https://doi.org/10.3847/0004-637X/819/2/106.

Braun, D.C., Lindsey, C., 2001. Seismic imaging of the far hemisphere of the sun. Astrophys. J. 560 (2), L189. https://doi.org/10.1086/324323.

Brier, G.W., 1950. Verification of forecasts expressed in terms of probability. Mon. Weather Rev. 78 (1), 1–3. https://doi.org/10.1175/1520-0493(1950)078<0001:vofeit>2.0.co;2.

Brown, D.S., Nightingale, R.W., Alexander, D., Schrijver, C.J., Metcalf, T.R., Shine, R.A., Title, A.M., Wolfson, C.J., 2003. Observations of Rotating Sunspots from TRACE. Sol. Phys. 216 (1), 79–108. https://doi.org/10.1023/A:1026138413791.

Bumba, V., Howard, R., 1965. A Study of the Development of Active Regions on the Sun. Astrophys. J. 141, 1492. https://doi.org/10.1086/148237.

Campi, C., Benvenuto, F., Massone, A.M., Bloomfield, D.S., Georgoulis, M.K., Piana, M., 2019. Feature ranking of active region source properties in solar flare forecasting and the uncompromised stochasticity of flare occurrence. Astrophys. J. 883 (2), 150. https://doi.org/10.3847/1538-4357/ab3c26.

Camporeale, E., 2019. The challenge of machine learning in space weather: Nowcasting and forecasting. Space. Weather 17 (8), 1166–1207. https://doi.org/10.1029/2018sw002061.

Cane, H.V., 2000. Coronal mass ejections and forbush decreases. Space Sci. Rev. 93, 55–77. https://doi.org/10.1023/A:1026532125747.

Cane, H.V., Lario, D., 2006. An Introduction to CMEs and Energetic Particles. Space Sci. Rev. 123 (1–3), 45–56. https://doi.org/10.1007/s11214-006-9011-3.

Cane, H.V., Richardson, I.G., von Rosenvinge, T.T., 2010. A study of solar energetic particle events of 1997–2006: Their composition and associations. J. Geophys. Res. 115 (A8), A08101. https://doi.org/10.1029/2009JA014848.

Canou, A., Amari, T., Bommier, V., Schmieder, B., Aulanier, G., Li, H., 2009. Evidence for a pre-eruptive twisted flux rope using the themis vector magnetograph. Astrophys. J. Lett. 693 (1), L27–L30. https://doi.org/10.1088/0004-637X/693/1/L27.

Chen, A., Ye, Q., Wang, J., 2021a. Flare index prediction with machine learning algorithms. Sol. Phys. 296 (10), 1–17. https://doi.org/10.1007/s11207-021-01895-1.

Chen, H., Zhang, J., Li, L., Ma, S., 2016. Tether-cutting reconnection between two solar filaments triggering outflows and a coronal mass ejection. Astrophys. J. Lett. 818 (2), L27. https://doi.org/10.3847/2041-8205/818/2/L27, arXiv:1602.00378.

Chen, J., Li, W., Li, S., Chen, H., Zhao, X., Peng, J., Chen, Y., & Deng, H. (2022). Two-stage solar flare forecasting based on convolutional neural networks. Space: Science & amp Technology, 2022, 1–10. URL: https://doi.org/10.34133/2022/9761567. doi:10.34133/2022/9761567.

Chen, M., Mao, S., Liu, Y., 2014. Big data: A survey. Mobile Networks and Applications 19 (2), 171–209. https://doi.org/10.1007/s11036-013-0489-0.

Chen, M.-S., Han, J., Yu, P.S., 1996. Data mining: an overview from a database perspective. IEEE Transactions on Knowledge and data Engineering 8 (6), 866–883. https://doi.org/10.1109/69.553155.

Chen, Y., Kempton, D.J., Ahmadzadeh, A., & Angryk, R.A. (2021b). Towards synthetic multivariate time series generation for flare forecasting. In International Conference on Artificial Intelligence and Soft Computing (pp. 296–307). Springer, Cham. doi:10.1007/978-3-030-87986-0_26.

Chen, Y., Manchester, W.B., Hero, A.O., Toth, G., DuFumier, B., Zhou, T., Wang, X., Zhu, H., Sun, Z., Gombosi, T.I., 2019. Identifying solar flare precursors using time series of SDO/HMI images and SHARP parameters. Space Weather 17 (10), 1404–1426. https://doi.org/10.1029/2019sw002214.

Cheng, X., Ding, M.D., Fang, C., 2015. Imaging and Spectroscopic Diagnostics on the Formation of Two Magnetic Flux Ropes Revealed by SDO/AIA and IRIS. Astrophys. J. 804 (2), 82. https://doi.org/10.1088/0004-637X/804/2/82, arXiv:1502.07801.

Cheng, X., Ding, M.D., Guo, Y., Zhang, J., Vourlidas, A., Liu, Y.D., Olmedo, O., Sun, J.Q., Li, C., 2014. Tracking the Evolution of a Coherent Magnetic Flux Rope Continuously from the Inner to the Outer Corona. Astrophys. J. 780 (1), 28. https://doi.org/10.1088/0004-637X/780/1/28, arXiv:1310.6782.

Cheng, X., Ding, M.D., Zhang, J., Srivastava, A.K., Guo, Y., Chen, P.F., Sun, J.Q., 2014. On the Relationship Between a Hot-channel-like Solar Magnetic Flux Rope and its Embedded Prominence. Astrophys. J. Letters 789 (2), L35. https://doi.org/10.1088/2041-8205/789/2/L35, arXiv:1406.4196.

Cheng, X., Ding, M.D., Zhang, J., Sun, X.D., Guo, Y., Wang, Y.M., Kliem, B., Deng, Y.Y., 2014. Formation of a Double-decker Magnetic Flux Rope in the Sigmoidal Solar Active Region 11520. Astrophys. J. 789 (2), 93. https://doi.org/10.1088/0004-637X/789/2/93, arXiv:1405.4923.

Cheng, X., Guo, Y., Ding, M., 2017. Origin and Structures of Solar Eruptions I: Magnetic Flux Rope. Science China Earth Sciences 60, 1383–1407. https://doi.org/10.1007/s11430-017-9074-6, arXiv:1705.08198.

Cheng, X., Zhang, J., Ding, M.D., Liu, Y., Poomvises, W., 2013. The Driver of Coronal Mass Ejections in the Low Corona: A Flux Rope. Astrophys. J. 763 (1), 43. https://doi.org/10.1088/0004-637X/763/1/43, arXiv:1211.6524.

Cheng, X., Zhang, J., Liu, Y., Ding, M.D., 2011. Observing flux rope formation during the impulsive phase of a solar eruption. Astrophys. J. Letters 732 (2), L25. https://doi.org/10.1088/2041-8205/732/2/L25, arXiv:1103.5084.

Cheng, X., Zhang, J., Saar, S.H., Ding, M.D., 2012. Differential Emission Measure Analysis of Multiple Structural Components of Coronal Mass Ejections in the Inner Corona. Astrophys. J. 761 (1), 62. https://doi.org/10.1088/0004-637X/761/1/62, arXiv:1210.7287.

Cheung, M.C.M., DeRosa, M.L., 2012. A method for data-driven simulations of evolving solar active regions. Astrophys. J. 757 (2), 147. https://doi.org/10.1088/0004-637X/757/2/147, arXiv:1208.2954.

Cheung, M.C.M., Martínez-Sykora, J., Testa, P., De Pontieu, B., Chintzoglou, G., Rempel, M., Polito, V., Kerr, G.S., Reeves, K.K., Fletcher, L., Jin, M., Nóbrega-Siverio, D., Danilovic, S., Antolin, P., Allred, J., Hansteen, V., Ugarte-Urra, I., DeLuca, E., Longcope, D., Takasao, S., DeRosa, M.L., Boerner, P., Jaeggli, S., Nitta, N.V., Daw, A., Carlsson, M., Golub, L., The, 2022. Probing the Physics of the Solar Atmosphere with the Multi-slit Solar Explorer (MUSE). II. Flares and Eruptions. Astrophys. J. 926 (1), 53. https://doi.org/10.3847/1538-4357/ac4223, arXiv:2106.15591.

Cheung, M.C.M., Rempel, M., Chintzoglou, G., Chen, F., Testa, P., Martínez-Sykora, J., Sainz Dalda, A., DeRosa, M.L., Malanushenko, A., Hansteen, V., De Pontieu, B., Carlsson, M., Gudiksen, B., McIntosh, S.W., 2019. A comprehensive three-dimensional radiative magnetohydrodynamic simulation of a solar flare. Nature Astronomy 3, 160–166. https://doi.org/10.1038/s41550-018-0629-3.

Chintzoglou, G., Patsourakos, S., Vourlidas, A., 2015. Formation of magnetic flux ropes during a confined flaring well before the onset of a pair of major coronal mass ejections. Astrophys. J. 809 (1), 34. https://doi.org/10.1088/0004-637X/809/1/34, arXiv:1507.01165.

Chintzoglou, G., Zhang, J., 2013. Reconstructing the Subsurface Three-dimensional Magnetic Structure of a Solar Active Region Using SDO/HMI Observations. Astrophys. J. Lett. 764 (1), L3. https://doi.org/10.1088/2041-8205/764/1/L3, arXiv:1301.4651.

Cinto, T., Gradvohl, A., Coelho, G., da Silva, A., 2020. Solar flare forecasting using time series and extreme gradient boosting ensembles. Sol. Phys. 295 (7), 1–30. https://doi.org/10.1007/s11207-020-01661-9.

Cinto, T., Gradvohl, A.L.S., Coelho, G.P., da Silva, A.E.A., 2020. A framework for designing and evaluating solar flare forecasting systems. Mon. Not. R. Astron. Soc. 495 (3), 3332–3349. https://doi.org/10.1093/mnras/staa1257.

Cliver, E.W., Schrijver, C.J., Shibata, K., Usoskin, I.G., 2022. Extreme solar events. Living Rev. Sol. Phys. 19 (1). https://doi.org/10.1007/s41116-022-00033-8.

Cohen, C.M.S., Berger, T., Desai, M.I., Duncan, N., Ho, G.C., Maruyama, N., Pulkkinen, T., Szabo, A., Vourlidas, A., Zesta, E., & Zhang, Y. (2022). Living with a star architecture committee report. https://science.nasa.gov/science-pink/s3fs-public/atoms/files/LWS-Architecture-Committee-Report_08-26-2022_FINAL.pdf.

Colak, T., Qahwaji, R., 2009. Automated solar activity prediction: a hybrid computer platform using machine learning and solar imaging for automated prediction of solar flares. Space Weather 7 (6). https://doi.org/10.1029/2008SW000401.

Conlon, P.A., McAteer, R.T.J., Gallagher, P.T., Fennell, L., 2010. Quantifying the Evolving Magnetic Structure of Active Regions. Astrophys J 722 (1), 577–585. https://doi.org/10.1088/0004-637X/722/1/577.

Crosby, N., Heynderickx, D., Jiggens, P., Aran, A., Sanahuja, B., Truscott, P., Lei, F., Jacobs, C., Poedts, S., Gabriel, S., et al., 2015. Sepem: A tool for statistical modeling the solar energetic particle environment. Space Weather 13 (7), 406–426. https://doi.org/10.1002/2013SW001008.

Crown, M.D., 2012. Validation of the NOAA space weather prediction center's solar flare forecasting look-up table and forecaster-issued probabilities. Space Weather 10 (6). https://doi.org/10.1029/2011sw000760, n/a–n/a.

De Mauro, A., Greco, M., & Grimaldi, M. (2015). What is big data? a consensual definition and a review of key research topics. In AIP conference proceedings (pp. 97–104). American Institute of Physics volume 1644. doi:10.1063/1.4907823.

De Pontieu, B., Testa, P., Martínez-Sykora, J., Antolin, P., Karampelas, K., Hansteen, V., Rempel, M., Cheung, M.C.M., Reale, F., Danilovic, S., Pagano, P., Polito, V., De Moortel, I., Nóbrega-Siverio, D., Van Doorsselaere, T., Petralia, A., Asgari-Targhi, M., Boerner, P.,

Carlsson, M., Chintzoglou, G., Daw, A., DeLuca, E., Golub, L., Matsumoto, T., Ugarte-Urra, I., McIntosh, S.W., & the MUSE Team (2022). Probing the Physics of the Solar Atmosphere with the Multi-slit Solar Explorer (MUSE). I. Coronal Heating. The Astrophysical Journal, 926(1), 52. doi:10.3847/1538-4357/ac4222. arXiv:2106.15584.

DeForest, C., Howard, T., Webb, D., Davies, J., 2016. The utility of polarized heliospheric imaging for space weather monitoring. Space Weather 14 (1), 32–49. https://doi.org/10.1002/2015SW001286.

DeForest, C., Killough, R., Gibson, S., Henry, A., Case, T., Beasley, M., Laurent, G., Colaninno, R., Waltham, N., 2022. Polarimeter to unify the corona and heliosphere (PUNCH): Science, status, and path to flight. In: In 2022 IEEE Aerospace Conference (AERO). IEEE, pp. 1–11. https://doi.org/10.1109/AERO53065.2022.9843340.

DeForest, C.E., Howard, T.A., Tappin, S.J., 2013. The Thomson Surface. II. Polarization. Astrophys J 765 (1), 44. https://doi.org/10.1088/0004-637X/765/1/44, arXiv:1207.5894.

Deng, Y., Zhou, G., Dai, S., Wang, Y., Feng, X., He, J., Jiang, J., Tian, H., Yang, S., Hou, J., Yan, Y., Gan, W., Bai, X., Li, L., Xia, L., Li, H., Su, Y., Xiong, M., Zhang, Y., Zhu, C., Lin, J., Zhang, H., Chen, B., He, L., Feng, L., Zhang, H., Sun, M., Zhang, A., Chen, L., Tan, B., Zhang, Z., Yang, J., Yang, M., Wang, J., 2023. 太阳极轨天文台 (solar polar-orbit observatory). Chin. Sci. Bull. 68 (4), 298–308. https://doi.org/10.1360/TB-2022-0674.

DeRosa, M.L., Barnes, G., 2018. Does nearby open flux affect the eruptivity of solar active regions? Astrophys J 861, 131. https://doi.org/10.3847/1538-4357/aac77a.

Deshmukh, V., Berger, T.E., Bradley, E., Meiss, J.D., 2020. Leveraging the mathematics of shape for solar magnetic eruption prediction. J. Space Weather Space Clim. 10, 13. https://doi.org/10.1051/swsc/2020014.

Deshmukh, V., Flyer, N., Van Der Sande, K., Berger, T., 2022. Decreasing false-alarm rates in CNN-based solar flare prediction using SDO/HMI data. Astrophys. J. Suppl. Ser. 260 (1), 9. https://doi.org/10.3847/1538-4365/ac5b0c.

DeVore, C.R., Antiochos, S.K., 2000. Dynamical Formation and Stability of Helical Prominence Magnetic Fields. Astrophys J 539 (2), 954–963. https://doi.org/10.1086/309275.

Devos, A., Verbeeck, C., Robbrecht, E., 2014. Verification of space weather forecasting at the Regional Warning Center in Belgium. J. Space Weather Space Clim. 4, A29. https://doi.org/10.1051/swsc/2014025.

Dissauer, K., Leka, K., Wagner, E.L., 2023. Properties of Flare-Imminent versus Flare-Quiet Active Regions from the Chromosphere through the Corona I: Introduction of the AIA Active Region Patches (AARPs). Astrophys J 942, 83. https://doi.org/10.3847/1538-4357/ac9c06, arXiv:2212.11251.

Dissauer, K., Veronig, A.M., Temmer, M., Podladchikova, T., 2019. Statistics of Coronal Dimmings Associated with Coronal Mass Ejections. II. Relationship between Coronal Dimmings and Their Associated CMEs. Astrophys J 874 (2), 123. https://doi.org/10.3847/1538-4357/ab0962, arXiv:1810.01589.

Domijan, K., Bloomfield, D.S., Pitié, F., 2019. Solar flare forecasting from magnetic feature properties generated by the solar monitor active region tracker. Sol. Phys. 294 (1), 1–19. https://doi.org/10.1007/s11207-018-1392-4.

van Driel-Gesztelyi, L., Green, L.M., 2015. Evolution of active regions. Living Rev. Sol. Phys. 12 (1), 1–98. https://doi.org/10.1007/lrsp-2015-1.

Eastwood, J.P., Biffis, E., Hapgood, M.A., Green, L., Bisi, M.M., Bentley, R.D., Wicks, R., McKinnell, L.-A., Gibbs, M., Burnett, C., 2017. The economic impact of space weather: Where do we stand? Risk Anal. 37 (2), 206–218. https://doi.org/10.1111/risa.12765.

Erdelyi, R. et al., 2022. The Solar Activity Monitor Network – SAMNet. J. Space Weather Space Clim. 12, 2. https://doi.org/10.1051/swsc/2021025.

Engell, A.J., Falconer, D.A., Schuh, M., Loomis, J., Bissett, D., 2017. SPRINTS: A framework for solar-driven event forecasting and research. Space Weather 15 (10), 1321–1346. https://doi.org/10.1002/2017sw001660.

EOP, 2016. The national artificial intelligence research and development strategic plan.

EOP (2019). The national artificial intelligence research and development strategic plan: 2019 update, a report by the select committee on artificial intelligence of the national sciences & technology council. https://www.hsdl.org/?view&did=831483.

European Commission, Joint Research Centre, Krausmann, E., Andersson, E., Murtagh, W., & Gibbs, M. (2016). Space weather & critical infrastructures – Findings and outlook. Publications Office, Luxembourg. doi:doi/10.2788/152877.

Falco, M., Costa, P., Romano, P., 2019. Solar flare forecasting using morphological properties of sunspot groups. J. Space Weather Space Clim. 9, A22. https://doi.org/10.1051/swsc/2019019.

Falconer, D.A., 2001. A prospective method for predicting coronal mass ejections from vector magnetograms. J. Geophys. Res. 106 (A11), 25185–25190. https://doi.org/10.1029/2000JA004005.

Falconer, D.A., Moore, R.L., Barghouty, A.F., Khazanov, I., 2012. Prior flaring as a complement to free magnetic energy for forecasting solar eruptions. Astrophys J 757 (1), 32. https://doi.org/10.1088/0004-637X/757/1/32.

Falconer, D.A., Moore, R.L., Barghouty, A.F., Khazanov, I., 2014. MAG4 versus alternative techniques for forecasting active region flare productivity. Space Weather 12 (5), 306–317. https://doi.org/10.1002/2013sw001024.

Falconer, D.A., Moore, R.L., Gary, G.A., 2002. Correlation of the Coronal Mass Ejection Productivity of Solar Active Regions with Measures of Their Global Nonpotentiality from Vector Magnetograms: Baseline Results. Astrophys J 569 (2), 1016–1025. https://doi.org/10.1086/339161.

Falconer, D.A., Moore, R.L., Gary, G.A., 2003. A measure from line-of-sight magnetograms for prediction of coronal mass ejections. Journal of Geophysical Research (Space Physics) 108 (A10), 1380. https://doi.org/10.1029/2003JA010030.

Falconer, D.A., Moore, R.L., Gary, G.A., 2006. Magnetic Causes of Solar Coronal Mass Ejections: Dominance of the Free Magnetic Energy over the Magnetic Twist Alone. Astrophys J 644 (2), 1258–1272. https://doi.org/10.1086/503699.

Falconer, D.A., Tiwari, S.K., Moore, R.L., Khazanov, I., 2016. A New Method to Quantify and Reduce the net Projection Error in Whole-solar-active-region Parameters Measured from Vector Magnetograms. Astrophys. J. Lett. 833 (2), L31. https://doi.org/10.3847/2041-8213/833/2/L31, arXiv:1612.01948.

Fan, Y., Gibson, S.E., 2004. Numerical Simulations of Three-dimensional Coronal Magnetic Fields Resulting from the Emergence of Twisted Magnetic Flux Tubes. Astrophys J 609 (2), 1123–1133. https://doi.org/10.1086/421238.

Fan, Y., Zweibel, E.G., Linton, M.G., Fisher, G.H., 1999. The Rise of Kink-unstable Magnetic Flux Tubes and the Origin of δ-Configuration Sunspots. Astrophys J 521 (1), 460–477. https://doi.org/10.1086/307533.

Fang, F., Fan, Y., 2015. δ-Sunspot Formation in Simulation of Active-region-scale Flux Emergence. Astrophys J 806 (1), 79. https://doi.org/10.1088/0004-637X/806/1/79, arXiv:1504.04393.

Feng, L., Gan, W., Liu, S., Wang, H., Li, H., Xu, L., Zong, W., Zhang, X., Zhu, Y., Wu, H., Chen, A., Cui, Y., Dai, X., Guo, J., He, H., Huang, X., Lu, L., Song, Q., Wang, J., Zhong, Q., Chen, L., Du, Z., Guo, X., Huang, Y., Li, H., Li, Y., Xiong, S., Yang, S., Ying, B., 2020. Space Weather Related to Solar Eruptions with the ASO-S Mission. Frontiers in Physics 8, 45. https://doi.org/10.3389/fphy.2020.00045.

Filippov, B.P., Den, O.G., 2001. A critical height of quiescent prominences before eruption. J. Geophys. Res. 106 (A11), 25177–25184. https://doi.org/10.1029/2000JA004002.

Fisher, G.H., Kazachenko, M.D., Welsch, B.T., Sun, X., Lumme, E., Bercik, D.J., DeRosa, M.L., Cheung, M.C.M., 2020. The PDFI_SS Electric Field Inversion Software. Astrophys. J. Suppl. Series 248 (1), 2. https://doi.org/10.3847/1538-4365/ab8303, arXiv:1912.08301.

Fletcher, L., Dennis, B.R., Hudson, H.S., Krucker, S., Phillips, K., Veronig, A., Battaglia, M., Bone, L., Caspi, A., Chen, Q., Gallagher, P., Grigis, P.T., Ji, H., Liu, W., Milligan, R.O., Temmer, M., 2011. An observational overview of solar flares. Space Sci. Rev. 159 (1–4), 19–106. https://doi.org/10.1007/s11214-010-9701-8.

Florios, K., Kontogiannis, I., Park, S.-H., Guerra, J.A., Benvenuto, F., Bloomfield, D.S., Georgoulis, M.K., 2018. Forecasting solar flares using magnetogram-based predictors and machine learning. Sol. Phys. 293 (2), 1–42. https://doi.org/10.1007/s11207-018-1250-4.

Forbes, T.G., 2000. A review on the genesis of coronal mass ejections. J. Geophys. Res. 105 (A10), 23153–23166. https://doi.org/10.1029/2000JA000005.

Forbes, T.G., Isenberg, P.A., 1991. A Catastrophe Mechanism for Coronal Mass Ejections. Astrophys J 373, 294. https://doi.org/10.1086/170051.

Forbes, T.G., Linker, J.A., Chen, J., Cid, C., Kóta, J., Lee, M.A., Mann, G., Mikić, Z., Potgieter, M.S., Schmidt, J.M., Siscoe, G.L., Vainio, R., Antiochos, S.K., Riley, P., 2006. CME Theory and Models. Space Sci. Rev. 123 (1–3), 251–302. https://doi.org/10.1007/s11214-006-9019-8.

Galano, D., Bemporad, A., Buckley, S., Cernica, I., Dániel, V., Denis, F., de Vos, L., Fineschi, S., Galy, C., Graczyk, R., Horodyska, P., Jacob, J., Jansen, R., Kranitis, N., Kurowski, M., Ladno, M., Ledent, P., Loreggia, D., Melich, R., Mollet, D., Mosdorf, M., Paschalis, A., Peresty, R., Purica, M., Radzik, B., Rataj, M., Rougeot, R., Salvador, L., Thizy, C., Versluys, J., Walczak, T., Zarzycka, A., Zender, J., & Zhukov, A. (2018). Development of ASPIICS: a coronagraph based on Proba-3 formation flying mission. In M. Lystrup, H.A. MacEwen, G. G. Fazio, N. Batalha, N. Siegler, & E.C. Tong (Eds.), Space Telescopes and Instrumentation 2018: Optical, Infrared, and Millimeter Wave (p. 106982Y). volume 10698 of Society of Photo-Optical Instrumentation Engineers (SPIE) Conference Series. doi:10.1117/12.2312493.

Gallagher, P.T., Moon, Y.-J., Wang, H., 2002. Active-region monitoring and flare forecasting–i. data processing and first results. Sol. Phys. 209 (1), 171–183. https://doi.org/10.1023/A:1020950221179.

Gan, W., Zhu, C., Deng, Y., Zhang, Z., Chen, B., Huang, Y., Deng, L., Wu, H., Zhang, H., Li, H., Su, Y., Su, J., Feng, L., Wu, J., Cui, J., Wang, C., Chang, J., Yin, Z., Xiong, W., Chen, B., Yang, J., Li, F., Lin, J., Hou, J., Bai, X., Chen, D., Zhang, Y., Hu, Y., Liang, Y., Wang, J., Song, K., Guo, Q., He, L., Zhang, G., Wang, P., Bao, H., Cao, C., Bai, Y., Chen, B., He, T., Li, X., Zhang, Y., Liao, X., Jiang, H., Li, Y., Su, Y., Lei, S., Chen, W., Li, Y., Zhao, J., Li, J., Ge, Y., Zou, Z., Hu, T., Su, M., Ji, H., Gu, M., Zheng, Y., Xu, D., Wang, X., 2023. The advanced space-based solar observatory (ASO-s). Sol. Phys. 298 (5). https://doi.org/10.1007/s11207-023-02166-x.

Gan, W.Q., Feng, L., Su, Y., 2022. A Chinese solar observatory in space. Nature Astronomy 6. https://doi.org/10.1038/s41550-021-01593-9, 165–165.

Gan, W.-Q., Zhu, C., Deng, Y.-Y., Li, H., Su, Y., Zhang, H.-Y., Chen, B., Zhang, Z., Wu, J., Deng, L., Huang, Y., Yang, J.-F., Cui, J.-J., Chang, J., Wang, C., Wu, J., Yin, Z.-S., Chen, W., Fang, C., Yan, Y.-H., Lin, J., Xiong, W.-M., Chen, B., Bao, H.-C., Cao, C.-X., Bai, Y.-P., Wang, T., Chen, B.-L., Li, X.-Y., Zhang, Y., Feng, L., Su, J.-T., Li, Y., Chen, W., Li, Y.-P., Su, Y.-N., Wu, H.-Y., Gu, M., Huang, L., Tang, X.-J., 2019. Advanced Space-based Solar Observatory (ASO-S): an overview. Research in Astronomy and Astrophysics 19 (11), 156. https://doi.org/10.1088/1674-4527/19/11/156.

Gary, G.A., Hagyard, M.J., 1990. Transformation of vector magnetograms and the problems associated with the effects of perspective and the azimuthal ambiguity. Sol. Phys. 126, 21–36. https://doi.org/10.1007/BF00158295.

Georgoulis, M.K., 2012. Are Solar Active Regions with Major Flares More Fractal, Multifractal, or Turbulent Than Others? Solar Phys. 276 (1–2), 161–181. https://doi.org/10.1007/s11207-010-9705-2, arXiv:1101.0547.

Georgoulis, M.K. (2012b). On Our Ability to Predict Major Solar Flares. In The Sun: New Challenges (p. 93). volume 30 of Astrophysics and Space Science Proceedings. doi:10.1007/978-3-642-29417-4_9.

Georgoulis, M.K., Bloomfield, D.S., Piana, M., Massone, A.M., Soldati, M., Gallagher, P.T., Pariat, E., Vilmer, N., Buchlin, E., Baudin, F., Csillaghy, A., Sathiapal, H., Jackson, D.R., Alingery, P., Benvenuto, F., Campi, C., Florios, K., Gontikakis, C., Guennou, C., Guerra, J.A., Kontogiannis, I., Latorre, V., Murray, S.A., Park, S.-H., von Stachelski, S., Torbica, A., Vischi, D., & Worsfold, M. (2021). The flare likelihood and region eruption forecasting (FLARECAST) project: flare forecasting in the big data & amp machine learning era. J. Space Weather Space Clim., 11, 39. URL: doi: 10.1051/swsc/2021023. doi:10.1051/swsc/2021023.

Georgoulis, M.K., Nindos, A., Zhang, H., 2019. The source and engine of coronal mass ejections. Philosophical Transactions of the Royal Society of London Series A 377 (2148), 20180094. https://doi.org/10.1098/rsta.2018.0094.

Georgoulis, M.K., Rust, D.M., 2007. Quantitative Forecasting of Major Solar Flares. Astrophys. J. Lett. 661 (1), L109–L112. https://doi.org/10.1086/518718.

Georgoulis, M.K., Titov, V.S., Mikić, Z., 2012. Non-neutralized Electric Current Patterns in Solar Active Regions: Origin of the Shear-generating Lorentz Force. Astrophys J 761 (1), 61. https://doi.org/10.1088/0004-637X/761/1/61, arXiv:1210.2919.

Georgoulis, M.K., Tziotziou, K., Themelis, K., Magiati, M., & Angelopoulou, G. (2016). Solar Flare Prediction Science-to-Operations: the ESA/SSA SWE A-EFFort Service. In 41st COSPAR Scientific Assembly (pp. PSW.1–10–16). volume 41.

Ghosh, A., Chatterjee, S., Khan, A.R., Tripathi, D., Ramaprakash, A.N., Banerjee, D., Chordia, P., Gandorfer, A.M., Krivova, N., Nandy, D., Rajarshi, C., Solanki, S.K., & Sriram, S. (2016). The Solar Ultraviolet Imaging Telescope onboard Aditya-L1. In J.-W.A. den Herder, T. Takahashi, & M. Bautz (Eds.), Space Telescopes and Instrumentation 2016: Ultraviolet to Gamma Ray (p. 990503). International Society for Optics and Photonics SPIE volume 9905. URL: https://doi.org/10.1117/12.2232266. doi:10.1117/12.2232266.

Gibb, G.P.S., Mackay, D.H., Green, L.M., Meyer, K.A., 2014. Simulating the Formation of a Sigmoidal Flux Rope in AR10977 from SOHO/MDI Magnetograms. Astrophys J 782 (2), 71. https://doi.org/10.1088/0004-637X/782/2/71.

Gibson, S.E., Foster, D., Burkepile, J., de Toma, G., Stanger, A., 2006. The Calm before the Storm: The Link between Quiescent Cavities and Coronal Mass Ejections. Astrophys J 641 (1), 590–605. https://doi.org/10.1086/500446.

Gibson, S.E., Vourlidas, A., Hassler, D.M., Rachmeler, L.A., Thompson, M.J., Newmark, J., Velli, M., Title, A., McIntosh, S.W., 2018. Solar Physics from Unconventional Viewpoints. Frontiers in Astronomy and Space Sciences 5, 32. https://doi.org/10.3389/fspas.2018.00032, arXiv:1805.09452.

Gontikakis, C., Kontogiannis, I., Georgoulis, M.K., Guennou, C., Syntelis, P., Park, S.H., & Buchlin, E. (2020). Differential Emission Measure Evolution as a Precursor of Solar Flares. arXiv e-prints, (p. arXiv:2011.06433). arXiv:2011.06433.

Goodfellow, I., Bengio, Y., Courville, A., 2016. Deep learning. MIT press, Cambridge, Ma, URL: http://www.deeplearningbook.org.

Gopalswamy, N. (2022). The Sun and Space Weather. Atmosphere, 13 (11), 1781. doi:10.3390/atmos13111781. arXiv:2211.06775.

Gopalswamy, N., Yashiro, S., Michalek, G., Stenborg, G., Vourlidas, A., Freeland, S., Howard, R., 2009. The SOHO/LASCO CME catalog. Earth, Moon, and Planets 104 (1–4), 295–313. https://doi.org/10.1007/s11038-008-9282-7.

Goyal, S., Kumar, P., Janardhan, P., Vadawale, S., Sarkar, A., Shanmugam, M., Subramanian, K., Bapat, B., Chakrabarty, D., Adhyaru, P., Patel, A., Banerjee, S., Shah, M.S., Tiwari, N.K., Adalja, H., Ladiya, T., Dadhania, M., Sarda, A., Hait, A., Chauhan, M., & Bhavsar, R. (2018). Aditya solarwind particle experiment (aspex) onboard the aditya-l1 mission. Planetary and Space Science, 163, 42–55. URL: https://www.sciencedirect.com/science/article/pii/S0032063317304786. doi: 10.1016/j.pss.2018.04.008.

Green, L.M., Kliem, B., 2009. Flux Rope Formation Preceding Coronal Mass Ejection Onset. Astrophys J 700 (2), L83–L87. https://doi.org/10.1088/0004-637X/700/2/L83, arXiv:0906.4794.

Green, L.M., Kliem, B., Wallace, A.J., 2011. Photospheric flux cancellation and associated flux rope formation and eruption. Astron. Astrophys. 526, A2. https://doi.org/10.1051/0004-6361/201015146, arXiv:1011.1227.

Green, L.M., Thalmann, J.K., Valori, G., Pariat, E., Linan, L., Moraitis, K., 2022. Magnetic Helicity Evolution and Eruptive Activity in NOAA Active Region 11158. Astrophys J 937 (2), 59. https://doi.org/10.3847/1538-4357/ac88cb.

Green, L.M., Török, T., Vršnak, B., Manchester, W., Veronig, A., 2018. The Origin, Early Evolution and Predictability of Solar Eruptions. Space Sci. Rev. 214 (1), 46. https://doi.org/10.1007/s11214-017-0462-5, arXiv:1801.04608.

Gressl, C., Veronig, A., Temmer, M., Odstrčil, D., Linker, J., Mikić, Z., Riley, P., 2014. Comparative study of mhd modeling of the background solar wind. Sol. Phys. 289, 1783–1801. https://doi.org/10.1007/s11207-013-0421-6.

Griffiths, B., Fawcett, L., Green, A.C., 2022. Bayesian inference for solar flare extremes. Space Weather 20 (3). https://doi.org/10.1029/2021sw002886.

Guastavino, S., Marchetti, F., Benvenuto, F., Campi, C., Piana, M., 2022. Implementation paradigm for supervised flare forecasting studies: A deep learning application with video data. Astron. Astrophys. 662, A105. https://doi.org/10.1051/0004-6361/202243617.

Guastavino, S., Marchetti, F., Benvenuto, F., Campi, C., Piana, M., 2022. Operational solar flare forecasting via video-based deep learning. Front. Astron. Space Sci. Sec. Stellar and Solar Physics 9. https://doi.org/10.3389/fspas.2022.1039805.

Guastavino, S., Piana, M., Benvenuto, F., 2022. Bad and good errors: Value-weighted skill scores in deep ensemble learning. In: IEEE Transactions on Neural Networks and Learning Systems, pp. 1–10. https://doi.org/10.1109/TNNLS.2022.3186068.

Guennou, C., Pariat, E., Leake, J.E., Vilmer, N., 2017. Testing predictors of eruptivity using parametric flux emergence simulations. Journal of Space Weather and Space Climate 7, A17. https://doi.org/10.1051/swsc/2017015, arXiv:1706.04915.

Guerra, J.A., Murray, S.A., Bloomfield, D.S., Gallagher, P.T., 2020. Ensemble forecasting of major solar flares: methods for combining models. J. Space Weather Space Clim. 10, 38. https://doi.org/10.1051/swsc/2020042.

Guerra, J.A., Murray, S.A., Doornbos, E., 2020. The Use of Ensembles in Space Weather Forecasting. Space Weather 18 (2), e02443. https://doi.org/10.1029/2020SW002443.

Guerra, J.A., Park, S.H., Gallagher, P.T., Kontogiannis, I., Georgoulis, M.K., Bloomfield, D.S., 2018. Active Region Photospheric Magnetic Properties Derived from Line-of-Sight and Radial Fields. Sol. Phys. 293 (1), 9. https://doi.org/10.1007/s11207-017-1231-z, arXiv:1712.06902.

Guerra, J.A., Pulkkinen, A., Uritsky, V.M., 2015. Ensemble forecasting of major solar flares: First results. Space Weather 13 (10), 626–642. https://doi.org/10.1002/2015sw001195.

Gupta, M., Thalmann, J.K., Veronig, A.M., 2021. Magnetic helicity and energy budget around large confined and eruptive solar flares. Astron. Astrophys. 653, A69. https://doi.org/10.1051/0004-6361/202140591, arXiv:2106.08781.

Hagyard, M.J., Moore, R.L., Emslie, A.G., 1984a. The role of magnetic field shear in solar flares. Adv. Space Res. 4 (7), 71–80. https://doi.org/10.1016/0273-1177(84)90162-5.

Hagyard, M.J., Smith, J., J.B., Teuber, D., & West, E.A. (1984b). A Quantitative Study Relating Observed Shear in Photospheric Magnetic Fields to Repeated Flaring. Solar Physics, 91(1), 115–126. doi:10.1007/BF00213618.

Hapgood, M., 2019. The impact of space weather on human missions to mars: The need for good engineering and good forecasts. In: The Human Factor in a Mission to Mars. Springer International Publishing, pp. 69–91. https://doi.org/10.1007/978-3-030-02059-0_4, URL: https://doi.org/10.1007/978-3-030-02059-0_4.

Hapgood, M., Angling, M.J., Attrill, G., Bisi, M., Cannon, P.S., Dyer, C., Eastwood, J.P., EKasapisidge, S., Gibbs, M., Harrison, R.A., Hord, C., Horne, R.B., Jackson, D.R., Jones, B., Machin, S., Mitchell, C.N., Preston, J., Rees, J., Rogers, N.C., Routledge, G., Ryden, K., Tanner, R., Thomson, A.W.P., Wild, J.A., & Willis, M. (2021). Development of space weather reasonable worst-case scenarios for the UK national risk assessment. Space Weather, 19(4). URL: https://doi.org/10.1029/2020sw002593. doi:10.1029/2020sw002593.

Harrison, R.A., 1995. The nature of solar flares associated with coronal mass ejection. Astron. Astrophys. 304, 585, URL: https://ui.adsabs.harvard.edu/abs/1995A&A...304.585H.

Harrison, R.A., Lyons, M., 2000. A spectroscopic study of coronal dimming associated with a coronal mass ejection. Astron. Astrophys. 358, 1097–1108, URL: https://ui.adsabs.harvard.edu/abs/2000A&A...358.1097H.

Harvey, K.L., Zwaan, C., 1993. Properties and Emergence Patterns of Bipolar Active Regions - Part One. Sol. Phys. 148 (1), 85–118. https://doi.org/10.1007/BF00675537.

He, H., Garcia, E.A., 2009. Learning from imbalanced data. IEEE Transactions on knowledge and data engineering 21 (9), 1263–1284. https://doi.org/10.1109/TKDE.2008.239.

Heidke, P., 1926. Berechnung des erfolges und der güte der windstärkevorhersagen im sturmwarnungsdienst. Geogr. Ann. 8, 301. https://doi.org/10.2307/519729.

Higgins, P.A., Gallagher, P.T., McAteer, R.J., Bloomfield, D.S., 2011. Solar magnetic feature detection and tracking for space weather monitoring. Adv. Space Res. 47 (12), 2105–2117. https://doi.org/10.1016/j.asr.2010.06.024.

Hill, F., 2018. The Global Oscillation Network Group Facility—An Example of Research to Operations in Space Weather. Space Weather 16 (10), 1488–1497. https://doi.org/10.1029/2018SW002001.

Hoeksema, J.T., Liu, Y., Hayashi, K., Sun, X., Schou, J., Couvidat, S., Norton, A., Bobra, M., Centeno, R., Leka, K.D., Barnes, G., Turmon, M., 2014. The Helioseismic and Magnetic Imager (HMI) Vector Magnetic Field Pipeline: Overview and Performance. Sol. Phys. 289 (9), 3483–3530. https://doi.org/10.1007/s11207-014-0516-8, arXiv:1404.1881.

Hotta, H., Toriumi, S., 2020. Formation of superstrong horizontal magnetic field in delta-type sunspot in radiation magnetohydrodynamic simulations. Mon. Not. R. Astron. Soc. 498 (2), 2925–2935. https://doi.org/10.1093/mnras/staa2529, arXiv:2008.07741.

Howard, T.A., Harrison, R.A., 2013. Stealth coronal mass ejections: A perspective. Sol. Phys. 285 (1–2), 269–280. https://doi.org/10.1007/s11207-012-0217-0.

Howard, T.A., Tappin, S.J., Odstrcil, D., DeForest, C.E., 2013. The Thomson Surface. III. Tracking Features in 3D. Astrophys J 765 (1), 45. https://doi.org/10.1088/0004-637X/765/1/45.

Hu, J., Li, G., Ao, X., Zank, G.P., Verkhoglyadova, O., 2017. Modeling Particle Acceleration and Transport at a 2-D CME-Driven Shock. Journal of Geophys. Research 122 (11), 10938–10963. https://doi.org/10.1002/2017JA024077.

Huang, X., Wang, H., Xu, L., Liu, J., Li, R., Dai, X., 2018. Deep Learning Based Solar Flare Forecasting Model. I. Results for Line-of-sight Magnetograms. Astrophys J 856 (1), 7. https://doi.org/10.3847/1538-4357/aaae00.

Huang, X., Wang, H.-N., 2013. Solar flare prediction using highly stressed longitudinal magnetic field parameters. Research in Astronomy and Astrophysics 13 (3), 351–358. https://doi.org/10.1088/1674-4527/13/3/010.

Huang, X., Yu, D., Hu, Q., Wang, H., Cui, Y., 2010. Short-term solar flare prediction using predictor teams. Sol. Phys. 263 (1), 175–184. https://doi.org/10.1007/s11207-010-9542-3.

Hudson, H.S., Acton, L.W., Freeland, S.L., 1996. A Long-Duration Solar Flare with Mass Ejection and Global Consequences. Astrophys J 470, 629. https://doi.org/10.1086/177894.

Hurlburt, N., Cheung, M., Schrijver, C., Chang, L., Freeland, S., Green, S., Heck, C., Jaffey, A., Kobashi, A., Schiff, D., Serafin, J., Seguin, R., Slater, G., Somani, A., Timmons, R., 2012. Heliophysics Event Knowledgebase for the Solar Dynamics Observatory (SDO) and Beyond. Sol. Phys. 275 (1–2), 67–78. https://doi.org/10.1007/s11207-010-9624-2, arXiv:1008.1291.

Huwyler, C., Melchior, M., 2022. Using multiple instance learning for explainable solar flare prediction. Astronomy and Computing 41, 100668. https://doi.org/10.1016/j.ascom.2022.100668.

Inceoglu, F., Jeppesen, J.H., Kongstad, P., Marcano, N.J.H., Jacobsen, R. H., Karoff, C., 2018. Using machine learning methods to forecast if solar flares will be associated with CMEs and SEPs. Astrophys J 861 (2), 128. https://doi.org/10.3847/1538-4357/aac81e.

Ivezić, Ž., Connolly, A., Vanderplas, J., Gray, A., 2014. Statistics, Data Mining and Machine Learning in Astronomy. Princeton University Press, Princeton, NJ.

Jackson, B.V., Buffington, A., Hick, P.P., Wang, X., Webb, D., 2006. Preliminary three-dimensional analysis of the heliospheric response to the 28 october 2003 CME using SMEI white-light observations. J. Geophys. Res. 111 (A4). https://doi.org/10.1029/2004ja010942.

Jacobs, C., Poedts, S., van der Holst, B., 2006. The effect of the solar wind on CME triggering by magnetic foot point shearing. Astron. Astrophys. 450 (2), 793–803. https://doi.org/10.1051/0004-6361:20054670.

Jaeggli, S.A., Norton, A.A., 2016. The Magnetic Classification of Solar Active Regions 1992–2015. Astrophys. J. Lett. 820 (1), L11. https://doi.org/10.3847/2041-8205/820/1/L11, arXiv:1603.02552.

James, A.W., Valori, G., Green, L.M., Liu, Y., Cheung, M.C.M., Guo, Y., van Driel-Gesztelyi, L., 2018. An Observationally Constrained Model of a Flux Rope that Formed in the Solar Corona. Astrophys. J. Lett. 855 (2), L16. https://doi.org/10.3847/2041-8213/aab15d, arXiv:1802.07965.

James, A.W., Williams, D.R., O'Kane, J., 2022. Evolution of the critical torus instability height and coronal mass ejection likelihood in solar active regions. Astron. Astrophys. 665, A37. https://doi.org/10.1051/0004-6361/202142910, arXiv:2206.10639.

Japkowicz, N. (2000). The class imbalance problem: Significance and strategies. In Proc. of the Int'l Conf. on Artificial Intelligence. Citeseer volume 56.

Jarolim, R., Veronig, A., Podladchikova, T., Thalmann, J., Narnhofer, D., Hofinger, M., & Pock, T. (2022). Interpretable solar flare prediction with deep learning.

Jarolim, R., Thalmann, J.K., Veronig, A.M., Podladchikova, T., 2023. Probing the solar coronal magnetic field with physics-informed neural networks. Nat. Astronomy 7 (10), 1171–1179. https://doi.org/10.1038/s41550-023-02030-9.

Ji, A., Arya, A., Kempton, D., Angryk, R., Georgoulis, M.K., Aydin, B., 2021. A modular approach to building solar energetic particle event forecasting systems. In: In 2021 IEEE Third International Conference on Cognitive Machine Intelligence (CogMI), pp. 106–115. https://doi.org/10.1109/CogMI52975.2021.00022.

Ji, A., Aydin, B., Georgoulis, M.K., Angryk, R., 2020. All-clear flare prediction using interval-based time series classifiers. In: In 2020 IEEE International Conference on Big Data (Big Data). IEEE. https://doi.org/10.1109/bigdata50022.2020.9377906.

Jiang, H., Li, Q., Liu, N., Hu, Z., Abduallah, Y., Jing, J., Xu, Y., Wang, J. T.L., Wang, H., 2023. Generating Photospheric Vector Magnetograms of Solar Active Regions for SOHO/MDI Using SDO/HMI and BBSO Data with Deep Learning. Sol. Phys. 298 (7), 87. https://doi.org/10.1007/s11207-023-02180-z, arXiv:2211.02278.

Jiao, Z., Sun, H., Wang, X., Manchester, W., Gombosi, T., Hero, A., Chen, Y., 2020. Solar flare intensity prediction with machine learning models. Space Weather 18 (7). https://doi.org/10.1029/2020SW002440, e2020SW002440.

Jolliffe, I.T., & Stephenson, D.B. (Eds.) (2011). Forecast Verification. Wiley, Hoboken, NJ, USA. URL: https://doi.org/10.1002/9781119960003. doi:10.1002/9781119960003.

Jordan, M.I., Mitchell, T.M., 2015. Machine learning: Trends, perspectives, and prospects. Science 349 (6245), 255–260. https://doi.org/10.1126/science.aaa8415.

Kahler, S.W., Ling, A., 2015. Dynamic SEP event probability forecasts. Space. Weather 13 (10), 665–675. https://doi.org/10.1002/2015sw001222.

Kahler, S.W., Ling, A., White, S.M., 2015. Forecasting sep events with same active region prior flares. Space Weather 13 (2), 116–123. https://doi.org/10.1002/2014SW001099.

Kahler, S.W., Ling, A.G., 2018. Forecasting solar energetic particle (SEP) events with flare x-ray peak ratios. J. Space Weather Space Clim. 8, A47. https://doi.org/10.1051/swsc/2018033.

Kahler, S.W., Sheeley, J., N.R., Howard, R.A., Michels, D.J., Koomen, M.J., McGuire, R.E., von Rosenvinge, T.T., & Reames, D.V. (1984). Associations beteen coronal mass ejections and solar energetic proton events. Journal of Geophysical Research, 89(A11), 9683–9694. doi:10.1029/JA089iA11p09683.

Kahler, S.W., White, S.M., Ling, A.G., 2017. Forecasting E > 50-MeV proton events with the proton prediction system (PPS). J. Space Weather Space Clim. 7, A27. https://doi.org/10.1051/swsc/2017025.

Kaiser, M.L., Kucera, T.A., Davila, J.M., Cyr, O.C.S., Guhathakurta, M., Christian, E., 2007. The STEREO mission: An introduction. Space Sci. Rev. 136 (1–4), 5–16. https://doi.org/10.1007/s11214-007-9277-0.

Kaneko, T., Hotta, H., Toriumi, S., Kusano, K., 2022. Impact of subsurface convective flows on the formation of sunspot magnetic field and energy build-up. Mon. Not. R. Astron. Soc. 517 (2), 2775–2786. https://doi.org/10.1093/mnras/stac2635, arXiv:2209.06311.

Karniadakis, G.E., Kevrekidis, I.G., Lu, L., Perdikaris, P., Wang, S., Yang, L., 2021. Physics-informed machine learning. Nature Reviews Physics 3 (6), 422–440. https://doi.org/10.1038/s42254-021-00314-5.

Karpen, J.T., Antiochos, S.K., DeVore, C.R., 2012. The Mechanisms for the Onset and Explosive Eruption of Coronal Mass Ejections and Eruptive Flares. Astrophys J 760 (1), 81. https://doi.org/10.1088/0004-637X/760/1/81.

Kasapis, S., Zhao, L., Chen, Y., Wang, X., Bobra, M., Gombosi, T., 2022. Interpretable machine learning to forecast SEP events for solar cycle 23. Space Weather 20 (2). https://doi.org/10.1029/2021sw002842.

Kazachenko, M.D., Fisher, G.H., Welsch, B.T., 2014. A Comprehensive Method of Estimating Electric Fields from Vector Magnetic Field and Doppler Measurements. Astrophys. J. 795 (1), 17. https://doi.org/10.1088/0004-637X/795/1/17, arXiv:1404.4027.

Klein, K.-L., 2021. Radio astronomical tools for the study of solar energetic particles I. Correlations and diagnostics of impulsive acceleration and particle propagation. Frontiers in Astronomy and Space Sciences 7, 105. https://doi.org/10.3389/fspas.2020.580436.

Klein, K.-L., 2021. Radio astronomical tools for the study of solar energetic particles II.Time-extended acceleration at subrelativistic and relativistic energies. Frontiers in Astronomy and Space Sciences 7, 93. https://doi.org/10.3389/fspas.2020.580445.

Klein, K.-L., Matamoros, C.S., Zucca, P., 2018. Solar radio bursts as a tool for space weather forecasting. Comptes Rendus Physique (Physical Reports) 19 (1–2), 36–42. https://doi.org/10.1016/j.crhy.2018.01.005.

Kliem, B., Lee, J., Liu, R., White, S.M., Liu, C., Masuda, S., 2021. Nonequilibrium Flux Rope Formation by Confined Flares Preceding a Solar Coronal Mass Ejection. Astrophys J 909 (1), 91. https://doi.org/10.3847/1538-4357/abda37, arXiv:2101.02181.

Kliem, B., Lin, J., Forbes, T.G., Priest, E.R., Török, T., 2014. Catastrophe versus Instability for the Eruption of a Toroidal Solar Magnetic Flux Rope. Astrophys J 789 (1), 46. https://doi.org/10.1088/0004-637X/789/1/46, arXiv:1404.5922.

Kliem, B., Török, T., 2006. Torus Instability. Phys. Rev. Lett. 96 (25), 255002. https://doi.org/10.1103/PhysRevLett.96.255002, arXiv:-physics/0605217.

Knipp, D.J., 2016. Advances in Space Weather Ensemble Forecasting. Space Weather 14 (2), 52–53. https://doi.org/10.1002/2016SW001366.

Knizhnik, K.J., Linton, M.G., DeVore, C.R., 2018. The Role of Twist in Kinked Flux Rope Emergence and Delta-spot Formation. Astrophys J 864 (1), 89. https://doi.org/10.3847/1538-4357/aad68c, arXiv:1808.05562.

Komm, R., Ferguson, R., Hill, F., Barnes, G., Leka, K.D., 2011. Subsurface Vorticity of Flaring versus Flare-Quiet Active Regions. Sol. Phys. 268 (2), 389–406. https://doi.org/10.1007/s11207-010-9552-1.

Kontogiannis, I., 2023. The characteristics of flare- and CME-productive solar active regions. Adv. Space Res. 71 (4), 2017–2037. https://doi.org/10.1016/j.asr.2022.10.008, arXiv:2210.05453.

Kontogiannis, I., Georgoulis, M.K., Guerra, J.A., Park, S.-H., Bloomfield, D.S., 2019. Which Photospheric Characteristics Are Most Relevant to Active-Region Coronal Mass Ejections? Sol. Phys. 294 (9), 130. https://doi.org/10.1007/s11207-019-1523-6, arXiv:1909.06088.

Kontogiannis, I., Georgoulis, M.K., Park, S.-H., Guerra, J.A., 2017. Non-neutralized Electric Currents in Solar Active Regions and Flare Productivity. Sol. Phys. 292 (11), 159. https://doi.org/10.1007/s11207-017-1185-1, arXiv:1708.07087.

Kontogiannis, I., Georgoulis, M.K., Park, S.-H., Guerra, J.A., 2018. Testing and improving a set of morphological predictors of flaring activity. Sol. Phys. 293 (6). https://doi.org/10.1007/s11207-018-1317-2.

Korsós, M., Erdélyi, R., Liu, J., Morgan, H., 2021. Testing and validating two morphological flare predictors by logistic regression machine learning. Frontiers in Astronomy and Space Sciences 7, 571186. https://doi.org/10.3389/fspas.2020.571186.

Korsós, M.B., Georgoulis, M.K., Gyenge, N., Bisoi, S.K., Yu, S., Poedts, S., Nelson, C.J., Liu, J., Yan, Y., Erdélyi, R., 2020. Solar Flare Prediction Using Magnetic Field Diagnostics above the Photosphere. Astrophys J 896 (2), 119. https://doi.org/10.3847/1538-4357/ab8fa2, arXiv:2005.12180.

Korsós, M.B., Ludmány, A., Erdélyi, R., Baranyi, T., 2015. On Flare Predictability Based on Sunspot Group Evolution. Astrophys. J. Lett. 802 (2), L21. https://doi.org/10.1088/2041-8205/802/2/L21, arXiv:1503.04634.

Korsós, M.B., Yang, S., Erdélyi, R., 2019. Investigation of pre-flare dynamics using the weighted horizontal magnetic gradient method: From small to major flare classes. J. Space Weather Space Clim. 9, A6. https://doi.org/10.1051/swsc/2019002, arXiv:1901.05984.

Krall, K.R., Smith Jr., J.B., Hagyard, M.J., West, E.A., Cummings, N.P., 1982. Vector Magnetic Field Evolution, Energy Storage, and Associated Photospheric Velocity Shear within a Flare-Productive Active Region. Sol. Phys. 79, 59–75. https://doi.org/10.1007/BF00146973.

Krawczyk, B., 2016. Learning from imbalanced data: open challenges and future directions. Progress in Artificial Intelligence 5 (4), 221–232. https://doi.org/10.1007/s13748-016-0094-0.

Kubat, M., & Matwin, S. (1997). Addressing the curse of imbalanced training sets: One-sided selection. In Proceedings of the 14th International Conference on Machine Learning (pp. 179–186). volume 97.

Kubo, Y., Den, M., Ishii, M., 2017. Verification of operational solar flare forecast: Case of regional warning center japan. J. Space Weather Space Clim. 7, A20. https://doi.org/10.1051/swsc/2017018.

Künzel, H., 1960. Die Flare-Häufigkeit in Fleckengruppen unterschiedlicher Klasse und magnetischer Struktur (The Flare Frequency in Sunspot Groups of Different Class and Magnetic Structure). Astronomische Nachrichten (Astronomical News) 285 (5), 271. https://doi.org/10.1002/asna.19592850516.

Kusano, K., Iju, T., Bamba, Y., Inoue, S., 2020. A physics-based method that can predict imminent large solar flares. Science 369 (6503), 587–591. https://doi.org/10.1126/science.aaz2511.

LaBonte, B.J., Georgoulis, M.K., Rust, D.M., 2007. Survey of Magnetic Helicity Injection in Regions Producing X-Class Flares. Astrophys J 671 (1), 955–963. https://doi.org/10.1086/522682.

LaBonte, B.J., Georgoulis, M.K., Rust, D.M., 2007. Survey of Magnetic Helicity Injection in Regions Producing X-Class Flares. Astrophys J 671 (1), 955–963. https://doi.org/10.1086/522682.

Lamy, P., Damé, L., Vivès, S., Zhukov, A., 2010. Space Telescopes and Instrumentation 2010: Optical, Infrared, and Millimeter Wave. In: Oschmann, J., Jacobus, M., Clampin, M.C., MacEwen, H.A. (Eds.), volume 7731 of Society of Photo-Optical Instrumentation Engineers (SPIE) Conference Series, p. 773118. https://doi.org/10.1117/12.858247.

Landi, E., Li, W., Brage, T., Hutton, R., 2021. Hinode/EIS Coronal Magnetic Field Measurements at the Onset of a C2 Flare. Astrophys J 913 (1), 1. https://doi.org/10.3847/1538-4357/abf6d1, arXiv:2102.06072.

Laurenza, M., Cliver, E.W., Hewitt, J., Storini, M., Ling, A.G., Balch, C. C., Kaiser, M.L., 2009. A technique for short-term warning of solar energetic particle events based on flare location, flare size, and evidence of particle escape. Space Weather 7 (4), S04008. https://doi.org/10.1029/2007SW000379.

Lavasa, E., Giannopoulos, G., Papaioannou, A., Anastasiadis, A., Daglis, I.A., Aran, A., Pacheco, D., Sanahuja, B., 2021. Assessing the Predictability of Solar Energetic Particles with the Use of Machine Learning Techniques. Sol. Phys. 296 (7), 107. https://doi.org/10.1007/s11207-021-01837-x.

LeCun, Y., Bengio, Y., Hinton, G., 2015. Deep learning. Nature 521 (7553), 436–444. https://doi.org/10.1038/nature14539.

Lee, K., Moon, Y.J., Lee, J.-Y., Lee, K.-S., Na, H., 2012. Solar Flare Occurrence Rate and Probability in Terms of the Sunspot Classification Supplemented with Sunspot Area and Its Changes. Sol. Phys. 281 (2), 639–650. https://doi.org/10.1007/s11207-012-0091-9.

Lee, S., Oh, S., Lee, J., Hong, S., 2013. The study on the new approach to the prediction of the solar flares: The statistical relation from the SOHO archive. In: In AGU Fall Meeting Abstracts, p. SH53A-2155, volume 2013.

Leka, K., & Barnes, G. (2018). Chapter 3 - solar flare forecasting: Present methods and challenges. In N. Buzulukova (Ed.), Extreme Events in Geospace (pp. 65–98). Elsevier. URL: https://www.sciencedirect.com/science/article/pii/B9780128127001000030. doi:10.1016/B978-0-12-812700-1.00003-0.

Leka, K., Dissauer, K., Barnes, G., Wagner, E.L., 2023. Properties of Flare-Imminent versus Flare-Quiet Active Regions from the Chromosphere through the Corona II: NonParametric Discriminant Analysis Results from the NWRA Classification Infrastructure (NCI). Astrophys J 942, 84. https://doi.org/10.3847/1538-4357/ac9c04, arXiv:2212.11255.

Leka, K.D., Barnes, G., 2003a. Photospheric Magnetic Field Properties of Flaring versus Flare-quiet Active Regions. I. Data, General Approach, and Sample Results. Astrophys J 595 (2), 1277–1295. https://doi.org/10.1086/377511.

Leka, K.D., Barnes, G., 2003b. Photospheric Magnetic Field Properties of Flaring versus Flare-quiet Active Regions. II. Discriminant Analysis. The Astrophysical Journal 595 (2), 1296–1306. https://doi.org/10.1086/377512.

Leka, K.D., Barnes, G., 2007. Photospheric magnetic field properties of flaring versus flare-quiet active regions. IV. A statistically significant sample. Astrophys J 656 (2), 1173. https://doi.org/10.1086/510282.

Leka, K.D., Barnes, G., Wagner, E., 2018. The NWRA Classification Infrastructure: description and extension to the Discriminant Analysis Flare Forecasting System (DAFFS). J. Space Weather Space Clim. 8, A25. https://doi.org/10.1051/swsc/2018004, arXiv:1802.06864.

Leka, K.D., Barnes, G., Wagner, E.L., 2017. Evaluating (and Improving) Estimates of the Solar Radial Magnetic Field Component from Line-of-Sight Magnetograms. Sol. Phys. 292, 36. https://doi.org/10.1007/s11207-017-1057-8, arXiv:1701.04836.

Leka, K.D., Canfield, R.C., McClymont, A.N., van Driel-Gesztelyi, L., 1996. Evidence for Current-carrying Emerging Flux. Astrophys J 462, 547. https://doi.org/10.1086/177171.

Leka, K.D., Park, S.-H., Kusano, K., Andries, J., Barnes, G., Bingham, S., Bloomfield, D.S., McCloskey, A.E., Delouille, V., Falconer, D., Gallagher, P.T., Georgoulis, M.K., Kubo, Y., Lee, K., Lee, S., Lobzin, V., Mun, J., Murray, S.A., Hamad Nageem, T.A.M., Qahwaji, R., Sharpe, M., Steenburgh, R.A., Steward, G., Terkildsen, M., 2019a. A Comparison of Flare Forecasting Methods. II. Benchmarks, Metrics, and Performance Results for Operational Solar Flare Forecasting

Systems. Astrophys. J. Suppl. Series 243 (2), 36. https://doi.org/10.3847/1538-4365/ab2e12, arXiv:1907.02905.

Leka, K.D., Park, S.-H., Kusano, K., Andries, J., Barnes, G., Bingham, S., Bloomfield, D.S., McCloskey, A.E., Delouille, V., Falconer, D., Gallagher, P.T., Georgoulis, M.K., Kubo, Y., Lee, K., Lee, S., Lobzin, V., Mun, J., Murray, S.A., Nageem, T.A.M.H., Qahwaji, R., Sharpe, M., Steenburgh, R.A., Steward, G., Terkildsen, M., 2019b. A comparison of flare forecasting methods. III. systematic behaviors of operational solar flare forecasting systems. Astrophys J 881 (2), 101. https://doi.org/10.3847/1538-4357/ab2e11.

Lemen, J.R., Title, A.M., Akin, D.J., Boerner, P.F., Chou, C., Drake, J. F., Duncan, D.W., Edwards, C.G., Friedlaender, F.M., Heyman, G. F., Hurlburt, N.E., Katz, N.L., Kushner, G.D., Levay, M., Lindgren, R.W., Mathur, D.P., McFeaters, E.L., Mitchell, S., Rehse, R.A., Schrijver, C.J., Springer, L.A., Stern, R.A., Tarbell, T.D., Wuelser, J.-P., Wolfson, C.J., Yanari, C., Bookbinder, J.A., Cheimets, P.N., Caldwell, D., Deluca, E.E., Gates, R., Golub, L., Park, S., Podgorski, W.A., Bush, R.I., Scherrer, P.H., Gummin, M.A., Smith, P., Auker, G., Jerram, P., Pool, P., Soufli, R., Windt, D.L., Beardsley, S., Clapp, M., Lang, J., Waltham, N., 2012. The Atmospheric Imaging Assembly (AIA) on the Solar Dynamics Observatory (SDO). Sol. Phys. 275 (1–2), 17–40. https://doi.org/10.1007/s11207-011-9776-8.

Li, M., Cui, Y., Luo, B., Ao, X., Liu, S., Wang, J., Li, S., Du, C., Sun, X., Wang, X., 2022. Knowledge-informed deep neural networks for solar flare forecasting. Space Weather 20 (8). https://doi.org/10.1029/2021SW002985, e2021SW002985.

Li, R., Wang, H., Cui, Y., Huang, X., 2011. Solar flare forecasting using learning vector quantity and unsupervised clustering techniques. Science China Physics, Mechanics and Astronomy 54 (8), 1546–1552. https://doi.org/10.1007/s11433-011-4391-0.

Li, R., Wang, H.-N., He, H., Cui, Y.-M., Du, Z.-L., 2007. Support vector machine combined with k-nearest neighbors for solar flare forecasting. Chin. J. Astron. Astrophys. 7 (3), 441. https://doi.org/10.1088/1009-9271/7/3/15.

Lin, P.H., Kusano, K., Leka, K.D., 2021. Eruptivity in solar flares: The challenges of magnetic flux ropes. Astrophys J 913, 124. https://doi.org/10.3847/1538-4357/abf3c1.

Lin, P.H., Kusano, K., Shiota, D., Inoue, S., Leka, K.D., Mizuno, Y., 2020. A new parameter of the photospheric magnetic field to distinguish eruptive-flare producing solar active regions. Astrophys J 894, 20. https://doi.org/10.3847/1538-4357/ab822c.

Linton, M.G., Antiochos, S.K., Barnes, G., Fan, Y., Liu, Y., Lynch, B.J., Afanasyev, A.N., Arge, C.N., Burkepile, J., Cheung, M.C., Dahlin, J. T., DeRosa, M.L., de Toma, G., DeVore, C.R., Fisher, G.H., Henney, C.J., Jones, S.I., Karpen, J.T., Kazachenko, M.D., Leake, J.E., Török, T., Welsch, B.T., 2023. Recent progress on understanding coronal mass ejection/flare onset by a NASA living with a star focused science team. Adv. Space Res. https://doi.org/10.1016/j.asr.2023.06.045, URL: https://doi.org/10.1016/j.asr.2023.06.045.

Linton, M.G., Longcope, D.W., Fisher, G.H., 1996. The Helical Kink Instability of Isolated, Twisted Magnetic Flux Tubes. Astrophys. J. 469, 954. https://doi.org/10.1086/177842.

Liokati, E., Nindos, A., Liu, Y., 2022. Magnetic helicity and energy of emerging solar active regions and their erruptivity. Astron. Astrophys. 662, A6. https://doi.org/10.1051/0004-6361/202142868, arXiv:2202.04353.

Liu, C., Deng, N., Wang, J.T.L., Wang, H., 2017. Predicting solar flares using sdo/hmi vector magnetic data products and the random forest algorithm. Astrophys J 843 (2), 104. https://doi.org/10.3847/1538-4357/aa789b.

Liu, H., Liu, C., Wang, J.T.L., Wang, H., 2019. Predicting solar flares using a long short-term memory network. Astrophys J 877 (2), 121. https://doi.org/10.3847/1538-4357/ab1b3c.

Liu, H., Liu, C., Wang, J.T.L., Wang, H., 2020. Predicting coronal mass ejections using sdo/hmi vector magnetic data products and recurrent neural networks. Astrophys J 890 (1), 12. https://doi.org/10.3847/1538-4357/ab6850.

Liu, S., Xu, L., Zhao, Z., Erdélyi, R., Korsós, M.B., Huang, X., 2022. Deep learning based solar flare forecasting model. ii. influence of image resolution. Astrophys J 941 (1), 20. https://doi.org/10.3847/1538-4357/ac99dc.

Liu, Y., 2008. Magnetic field overlying solar eruption regions and kink and torus instabilities. Astrophys J 679, L151–L154. https://doi.org/10.1086/589282.

Liu, Y., Welsch, B.T., Valori, G., Georgoulis, M.K., Guo, Y., Pariat, E., Park, S.-H., Thalmann, J.K., 2023. Changes of Magnetic Energy and Helicity in Solar Active Regions from Major Flares. Astrophys J 942 (1), 27. https://doi.org/10.3847/1538-4357/aca3a6.

Lockwood, J., 1971. Forbush decreases in the cosmic radiation. Space Sci. Rev. 12 (5). https://doi.org/10.1007/bf00173346.

López Fuentes, M.C., Demoulin, P., Mandrini, C.H., van Driel-Gesztelyi, L., 2000. The Counterkink Rotation of a Non-Hale Active Region. Astrophys J 544 (1), 540–549. https://doi.org/10.1086/317180, arXiv:1412.1456.

Low, B.C., 1994. Magnetohydrodynamic processes in the solar corona: Flares, coronal mass ejections, and magnetic helicity. Phys. Plasmas 1 (5), 1684–1690. https://doi.org/10.1063/1.870671.

Lu, E.T., Hamilton, R.J., 1991. Avalanches and the distribution of solar flares. Astrophys J 380, L89–L92. https://doi.org/10.1086/186180.

Lu, L., Li, H., Huang, Y., Feng, L., Zhu, B., Wang, P., Song, D.-C., Gan, W.-Q., 2020. The Trigger and Termination Scheme for the Event Mode of the Lyman-alpha Solar Telescope (LST) onboard the ASO-S Mission. Chin. Astron. Astrophy 44 (4), 490–506. https://doi.org/10.1016/j.chinastron.2020.11.005.

Lugaz, N., Liu, H., Hapgood, M., Morley, S., 2021. Machine-learning research in the space weather journal: Prospects, scope, and limitations. Space. Weather 19 (12). https://doi.org/10.1029/2021sw003000.

Lundberg, S.M., & Lee, S.-I. (2017). A unified approach to interpreting model predictions. In I. Guyon, U.V. Luxburg, S. Bengio, H. Wallach, R. Fergus, S. Vishwanathan, & R. Garnett (Eds.), Advances in Neural Information Processing Systems. Curran Associates, Inc. volume 30. URL: https://proceedings.neurips.cc/paper_files/paper/2017/file/8a20a8621978632d76c43dfd28b67767-Paper.pdf.

Lv, M.J., Liu, T., 2022. Solar flare forecasting with data-driven interpretable model. In: In NeurIPS 2022 AI for Science: Progress and Promises, URL: https://openreview.net/forum?id=dWfv4vqbE8f.

Lynch, B.J., Antiochos, S.K., DeVore, C.R., Luhmann, J.G., Zurbuchen, T.H., 2008. Topological Evolution of a Fast Magnetic Breakout CME in Three Dimensions. Astrophys J 683 (2), 1192–1206. https://doi.org/10.1086/589738.

MacAlester, M.H., Murtagh, W., 2014. Extreme space weather impact: An emergency management perspective. Space. Weather 12 (8), 530–537. https://doi.org/10.1002/2014sw001095.

Machol, J., Viereck, R., Peck, C., & III, J.M. (2022). Goes x-ray sensor (xrs) operational data. https://ngdc.noaa.gov/stp/satellite/goes/doc/GOES_XRS_readme.pdf.

Mackay, D.H., Green, L.M., van Ballegooijen, A., 2011. Modeling the Dispersal of an Active Region: Quantifying Energy Input into the Corona. Astrophys J 729 (2), 97. https://doi.org/10.1088/0004-637X/729/2/97, arXiv:1102.5296.

Mackay, D.H., van Ballegooijen, A.A., 2006a. Models of the Large-Scale Corona. I. Formation, Evolution, and Liftoff of Magnetic Flux Ropes. Astrophys J 641 (1), 577–589. https://doi.org/10.1086/500425.

Mackay, D.H., van Ballegooijen, A.A., 2006b. Models of the Large-Scale Corona. II. Magnetic Connectivity and Open Flux Variation. Astrophys J 642 (2), 1193–1204. https://doi.org/10.1086/501043.

MacTaggart, D., Hood, A.W., 2009. On the emergence of toroidal flux tubes: general dynamics and comparisons with the cylinder model. Astron. Astrophys. 507 (2), 995–1004. https://doi.org/10.1051/0004-6361/200912930, arXiv:0909.3987.

Malandraki, O.E., & Crosby, N.B. (Eds.) (2018). Solar Particle Radiation Storms Forecasting and Analysis: The HESPERIA HORIZON 2020 Project and Beyond. Springer International Publishing. URL:

https://doi.org/10.1007/978-3-319-60051-2. doi:10.1007/978-3-319-60051-2.

Manchester, I., W., Gombosi, T., DeZeeuw, D., & Fan, Y. (2004). Eruption of a Buoyantly Emerging Magnetic Flux Rope. The Astrophysical Journal, 610(1), 588–596. doi:10.1086/421516.

Marchetti, F., Guastavino, S., Piana, M., Campi, C., 2022. Score-oriented loss (sol) functions. Pattern Recogn. 132, 108913. https://doi.org/10.1016/j.patcog.2022.108913.

Marsh, M.S., Dalla, S., Dierckxsens, M., Laitinen, T., Crosby, N.B., 2015. SPARX: A modeling system for Solar Energetic Particle Radiation Space Weather forecasting. Space Weather 13 (6), 386–394. https://doi.org/10.1002/2014SW001120, arXiv:1409.6368.

Martens, P.C.H., Attrill, G.D.R., Davey, A.R., Engell, A., Farid, S., Grigis, P.C., Kasper, J., Korreck, K., Saar, S.H., Savcheva, A., Su, Y., Testa, P., Wills-Davey, M., Bernasconi, P.N., Raouafi, N.E., Delouille, V.A., Hochedez, J.F., Cirtain, J.W., DeForest, C.E., Angryk, R.A., De Moortel, I., Wiegelmann, T., Georgoulis, M.K., McAteer, R.T.J., Timmons, R.P., 2012. Computer Vision for the Solar Dynamics Observatory (SDO). Sol. Phys. 275 (1–2), 79–113. https://doi.org/10.1007/s11207-010-9697-y.

Martínez-Sykora, J., Hansteen, V.H., De Pontieu, B., Landi, E., 2022. A Novel Inversion Method to Determine the Coronal Magnetic Field Including the Impact of Bound-Free Absorption. Astrophys J 938 (1), 60. https://doi.org/10.3847/1538-4357/ac8d5b. arXiv:2208.13984.

Martres, M., Bruzek, A., 1977. Active regions. In: Illustrated Glossary for Solar and Solar-Terrestrial Physics. Springer, Dordrecht, pp. 53–70.

Mason, J.P., Hoeksema, J.T., 2010. Testing Automated Solar Flare Forecasting with 13 Years of Michelson Doppler Imager Magnetograms. Astrophys J 723 (1), 634–640. https://doi.org/10.1088/0004-637X/723/1/634.

Mason, J.P., Woods, T.N., Webb, D.F., Thompson, B.J., Colaninno, R. C., Vourlidas, A., 2016. Relationship of EUV Irradiance Coronal Dimming Slope and Depth to Coronal Mass Ejection Speed and Mass. Astrophys J 830, 20. https://doi.org/10.3847/0004-637X/830/1/20, arXiv:1607.05284.

Massa, P., Emslie, A.G., 2022. Efficient identification of pre-flare features in SDO/AIA images through use of spatial fourier transforms. In: Frontiers in Astronomy and Space Sciences, p. 9. https://doi.org/10.3389/fspas.2022.1040099, URL: https://www.frontiersin.org/articles/10.3389/fspas.2022.1040099.

Massone, A.M., Piana, M., & the FLARECAST Consortium (2018). Machine learning for flare forecasting. In Machine Learning Techniques for Space Weather (pp. 355–364). Elsevier. URL: doi: 10.1016/b978-0-12-811788-0.00014-7. doi:10.1016/b978-0-12-811788-0.00014-7.

Mays, M.L., Taktakishvili, A., Pulkkinen, A., MacNeice, P.J., Rastätter, L., Odstrcil, D., Jian, L.K., Richardson, I.G., LaSota, J.A., Zheng, Y., Kuznetsova, M.M., 2015. Ensemble Modeling of CMEs Using the WSA-ENLIL+Cone Model. Sol. Phys. 290 (6), 1775–1814. https://doi.org/10.1007/s11207-015-0692-1, arXiv:1504.04402.

McAteer, R.T.J., Gallagher, P.T., Conlon, P.A., 2010. Turbulence, complexity, and solar flares. Adv. Space Res. 45 (9), 1067–1074. https://doi.org/10.1016/j.asr.2009.08.026, arXiv:0909.5636.

McAteer, R.T.J., Gallagher, P.T., Ireland, J., 2005. Statistics of Active Region Complexity: A Large-Scale Fractal Dimension Survey. Astrophys J 631 (1), 628–635. https://doi.org/10.1086/432412.

McCloskey, A.E., Gallagher, P.T., Bloomfield, D.S., 2018. Flare forecasting using the evolution of mcintosh sunspot classifications. J. Space Weather Space Clim. 8, A34. https://doi.org/10.1051/swsc/2018022.

McIntosh, P.S., 1990. The Classification of Sunspot Groups. Sol. Phys. 125 (2), 251–267. https://doi.org/10.1007/BF00158405.

Merceret, F.J., O'Brien, T.P., Roeder, W.P., Huddleston, L.L., Bauman, W.H., Jedlovec, G.J., 2013. Transitioning research to operations: Transforming the "valley of death" into a "valley of opportunity". Space Weather 11 (11), 637–640. https://doi.org/10.1002/swe.20099.

Mertens, C.J., Slaba, T.C., 2019. Characterization of solar energetic particle radiation dose to astronaut crew on deep-space exploration missions. Space. Weather 17 (12), 1650–1658. https://doi.org/10.1029/2019sw002363.

Meyers, R.A., 2010. Extreme environmental events: complexity in forecasting and early warning, volume 1. Springer Science & Business Media, New York.

Mikić, Z., Lee, M.A., 2006. An Introduction to Theory and Models of CMEs, Shocks, and Solar Energetic Particles. Space Sci. Rev. 123 (1–3), 57–80. https://doi.org/10.1007/s11214-006-9012-2.

Mikic, Z., Linker, J.A., 1994. Disruption of Coronal Magnetic Field Arcades. Astrophys J 430, 898. https://doi.org/10.1086/174460.

Mitchell, T.M., 1997. Machine learning, volume 1. McGraw-Hill New York.

Mitchell, T.M., 2006. The discipline of machine learning, volume 9. Carnegie Mellon University, School of Computer Science, Pittsburgh, PA.

Moore, R.L., & Roumeliotis, G. (1992). Triggering of Eruptive Flares - Destabilization of the Preflare Magnetic Field Configuration. In Z. Svestka, B.V. Jackson, & M.E. Machado (Eds.), IAU Colloq. 133: Eruptive Solar Flares (p. 69). volume 399. doi:10.1007/3-540-55246-4_79.

Moore, R.L., Sterling, A.C., Hudson, H.S., Lemen, J.R., 2001. Onset of the Magnetic Explosion in Solar Flares and Coronal Mass Ejections. Astrophys J 552 (2), 833–848. https://doi.org/10.1086/320559.

Moraitis, K., Sun, X., Pariat, É., Linan, L., 2019. Magnetic helicity and eruptivity in active region 12673. Astron. Astrophys. 628, A50. https://doi.org/10.1051/0004-6361/201935870, arXiv:1907.06365.

Morales, L.F., Santos, N.A., 2020. Predicting extreme solar flare events using lu and hamilton avalanche model. Sol. Phys. 295 (11), 1–12. https://doi.org/10.1007/s11207-020-01713-0.

Möstl, C., Amla, K., Hall, J.R., Liewer, P.C., De Jong, E.M., Colaninno, R.C., Veronig, A.M., Rollett, T., Temmer, M., Peinhart, V., et al., 2014. Connecting speeds, directions and arrival times of 22 coronal mass ejections from the sun to 1 au. Astrophys J 787 (2), 119. https://doi.org/10.1088/0004-637X/787/2/119.

Munro, R.H., Gosling, J.T., Hildner, E., MacQueen, R.M., Poland, A.I., Ross, C.L., 1979. The association of coronal mass ejection transients with other forms of solar activity. Sol. Phys. 61 (1), 201–215. https://doi.org/10.1007/bf00155456.

Muranushi, T., Shibayama, T., Muranushi, Y.H., Isobe, H., Nemoto, S., Komazaki, K., Shibata, K., 2015. Ufcorin: A fully automated predictor of solar flares in goes x-ray flux. Space. Weather 13 (11), 778–796. https://doi.org/10.1002/2015sw001257.

Murphy, A.H., & Epstein, E.S. (1989). Skill scores and correlation coefficients in model verification. Monthly Weather Review, 117(3), 572–582. URL: doi: 10.1175/1520-0493(1989)117<0572:ssacci>2.0.co;2. doi:10.1175/1520-0493(1989)117<0572:ssacci>2.0.co;2.

Murray, M.J., Hood, A.W., 2007. Simple emergence structures from complex magnetic fields. Astron. Astrophys. 470 (2), 709–719. https://doi.org/10.1051/0004-6361:20077251.

Murray, S.A., 2018. The Importance of Ensemble Techniques for Operational Space Weather Forecasting. Space. Weather 16 (7), 777–783. https://doi.org/10.1029/2018SW001861, arXiv:1806.09861.

Murray, S.A., Bingham, S., Sharpe, M., Jackson, D.R., 2017. Flare forecasting at the met office space weather operations centre. Space. Weather 15 (4), 577–588. https://doi.org/10.1002/2016sw001579.

Murray, S.A., Guerra, J.A., Zucca, P., Park, S.-H., Carley, E.P., Gallagher, P.T., Vilmer, N., Bothmer, V., 2018. Connecting Coronal Mass Ejections to Their Solar Active Region Sources: Combining Results from the HELCATS and FLARECAST Projects. Sol. Phys. 293 (4), 60. https://doi.org/10.1007/s11207-018-1287-4, arXiv:1803.06529.

Mylne, K.R., 2002. Decision-making from probability forecasts based on forecast value. Meteorological Applications 9 (3), 307–315. https://doi.org/10.1017/S1350482702003043.

Nandy, D., Sankarasubramanian, K., Srivastava, A.K., Chakrabarty, D., Banerjee, D., Tripathi, D., Srivastava, N., Rajaguru, S., Hasan, M., 2020. Report of the Committee on Aditya L1 Space Weather Monitoring and Predictions Plan. Submitted to Indian Space Research. Organization.

NASA_Data_Processing_Levels ( ). Eosdis data processing levels. https://ghrc.nsstc.nasa.gov/home/proc_level.

Nindos, A., Aurass, H., Klein, K.L., Trottet, G., 2008. Radio Emission of Flares and Coronal Mass Ejections. Invited Review. Solar Physics 253 (1–2), 3. https://doi.org/10.1007/s11207-008-9258-9.

Nindos, A., Patsourakos, S., Vourlidas, A., Cheng, X., Zhang, J., 2020. When do solar erupting hot magnetic flux ropes form? Astron. Astrophys. 642, A109. https://doi.org/10.1051/0004-6361/202038832, arXiv:2008.04380.

Nindos, A., Patsourakos, S., Vourlidas, A., Tagikas, C., 2015. How Common Are Hot Magnetic Flux Ropes in the Low Solar Corona? A Statistical Study of EUV Observations. Astrophys J 808 (2), 117. https://doi.org/10.1088/0004-637X/808/2/117, arXiv:1507.03766.

Nishizuka, N., Kubo, Y., Sugiura, K., Den, M., Ishii, M., 2020. Reliable probability forecast of solar flares: deep flare net-reliable (DeFN-R). Astrophys J 899 (2), 150. https://doi.org/10.3847/1538-4357/aba2f2.

Nishizuka, N., Kubo, Y., Sugiura, K., Den, M., Ishii, M., 2021. Operational solar flare prediction model using deep flare net. Earth, Planets and Space 73 (1), 1–12. https://doi.org/10.1186/s40623-021-01381-9.

Nishizuka, N., Sugiura, K., Kubo, Y., Den, M., Ishii, M., 2018. Deep flare net (DeFN) model for solar flare prediction. Astrophys J 858 (2), 113. https://doi.org/10.3847/1538-4357/aab9a7.

Nishizuka, N., Sugiura, K., Kubo, Y., Den, M., Watari, S., Ishii, M., 2017. Solar flare prediction model with three machine-learning algorithms using ultraviolet brightening and vector magnetograms. Astrophys J 835 (2), 156. https://doi.org/10.3847/1538-4357/835/2/156.

Nishizuka, N., Sugiura, K., Kubo, Y., Den, M., Watari, S., Ishii, M., 2017. Solar flare prediction model with three machine-learning algorithms using ultraviolet brightening and vector magnetograms. Astrophys J 835 (2), 156. https://doi.org/10.3847/1538-4357/835/2/156.

Nita, G., Ahmadzadeh, A., Criscuoli, S., Davey, A., Gary, D., Georgoulis, M., Hurlburt, N., Kitiashvili, I., Kempton, D., Kosovichev, A., Martens, P., McGranaghan, R., Oria, V., Reardon, K., Sadykov, V., Timmons, R., Wang, H., & Wang, J.T.L. (2022). Revisiting the Solar Research Cyberinfrastructure Needs: A White Paper of Findings and Recommendations. arXiv e-prints, (p. arXiv:2203.09544). doi:10.48550/arXiv.2203.09544. arXiv:2203.09544.

Nita, G., Georgoulis, M., Kitiashvili, I., Sadykov, V., Camporeale, E., Kosovichev, A., Wang, H., Oria, V., Wang, J., Angryk, R., Aydin, B., Ahmadzadeh, A., Bai, X., Bastian, T., Boubrahimi, S.F., Chen, B., Davey, A., Fereira, S., Fleishman, G., Gary, D., Gerrard, A., Hellbourg, G., Herbert, K., Ireland, J., Illarionov, E., Kuroda, N., Li, Q., Liu, C., Liu, Y., Kim, H., Kempton, D., Ma, R., Martens, P., McGranaghan, R., Semones, E., Stefan, J., Stejko, A., Collado-Vega, Y., Wang, M., Xu, Y., & Yu, S. (2020). Machine learning in heliophysics and space weather forecasting: A white paper of findings and recommendations. URL: https://arxiv.org/abs/2006.12224. doi:10.48550/ARXIV.2006.12224.

Nitta, N.V., Mulligan, T., Kilpua, E.K.J., Lynch, B.J., Mierla, M., O'Kane, J., Pagano, P., Palmerio, E., Pomoell, J., Richardson, I.G., Rodriguez, L., Rouillard, A.P., Sinha, S., Srivastava, N., Talpeanu, D.-C., Yardley, S.L., Zhukov, A.N., 2021. Understanding the origins of problem geomagnetic storms associated with "stealth" coronal mass ejections. Space Sci. Rev. 217 (8). https://doi.org/10.1007/s11214-021-00857-0.

Norton, A.A., Levens, P.J., Knizhnik, K.J., Linton, M.G., Liu, Y., 2022. Characterizing the Umbral Magnetic Knots of δ-Sunspots. Astrophys J 938 (2), 117. https://doi.org/10.3847/1538-4357/ac8eb2, arXiv:2209.09381.

NRC (2008). Severe Space Weather Events–Understanding Societal and Economic Impacts. National Academies Press. URL: https://doi.org/10.17226/12507. doi:10.17226/12507.

Núñez, M. (2022). Evaluation of the UMASEP-10 Version 2 Tool for Predicting All > 10 MeV SEP Events of Solar Cycles 22, 23 and 24. Universe, 8(1), 35. doi:10.3390/universe8010035.

O'Kane, J., Green, L., Long, D.M., Reid, H., 2019. Stealth coronal mass ejections from active regions. Astrophys J 882 (2), 85. https://doi.org/10.3847/1538-4357/ab371b.

Opgenoorth, H.J., Wimmer-Schweingruber, R.F., Belehaki, A., Berghmans, D., Hapgood, M., Hesse, M., Kauristie, K., Lester, M., Lilensten, J., Messerotti, M., Temmer, M., 2019. Assessment and recommendations for a consolidated european approach to space weather – as part of a global space weather effort. J. Space Weather Space Clim. 9, A37. https://doi.org/10.1051/swsc/2019033.

Oughton, E.J., Hapgood, M., Richardson, G.S., Beggan, C.D., Thomson, A.W.P., Gibbs, M., Burnett, C., Gaunt, C.T., Trichas, M., Dada, R., Horne, R.B., 2018. A risk assessment framework for the socioeconomic impacts of electricity transmission infrastructure failure due to space weather: An application to the united kingdom. Risk Anal. 39 (5), 1022–1043. https://doi.org/10.1111/risa.13229.

Paassilta, M., Vainio, R., Papaioannou, A., Raukunen, O., Barcewicz, S., Anastasiadis, A., 2023. Magnetic connectivity and solar energetic proton event intensity profiles at deka-MeV energy. Adv. Space Res. 71 (3), 1840–1854. https://doi.org/10.1016/j.asr.2022.11.051.

Pagano, P., Mackay, D.H., Yardley, S.L., 2019. A New Space Weather Tool for Identifying Eruptive Active Regions. Astrophys J 886 (2), 81. https://doi.org/10.3847/1538-4357/ab4cf110.48550/arXiv.1910.04226, arXiv:1910.04226.

Pagano, P., Mackay, D.H., Yardley, S.L., 2019. A Prospective New Diagnostic Technique for Distinguishing Eruptive and Noneruptive Active Regions. Astrophys J 883 (2), 112. https://doi.org/10.3847/1538-4357/ab3e4210.48550/arXiv.1908.09223, arXiv:1908.09223.

Palomba, M., & Luntama, J.-P. (2022). Vigil: ESA Space Weather Mission in L5. In 44th COSPAR Scientific Assembly. Held 16–24 July (p. 3544). volume 44.

Pandey, C., Angryk, R.A., Aydin, B., 2021. Solar flare forecasting with deep neural networks using compressed full-disk hmi magnetograms. In: In 2021 IEEE International Conference on Big Data (Big Data). IEEE, pp. 1725–1730. https://doi.org/10.1109/BigData52589.2021.9671322.

Pandey, C., Ji, A., Angryk, R.A., Georgoulis, M.K., Aydin, B., 2022. Towards coupling full-disk and active region-based flare prediction for operational space weather forecasting. Frontiers in Astronomy and Space Sciences 9. https://doi.org/10.3389/fspas.2022.897301.

Panos, B., Kleint, L., 2020. Real-time flare prediction based on distinctions between flaring and non-flaring active region spectra. Astrophys J 891 (1), 17. https://doi.org/10.3847/1538-4357/ab700b.

Papaioannou, A., Anastasiadis, A., Kouloumvakos, A., Paassilta, M., Vainio, R., Valtonen, E., Belov, A., Eroshenko, E., Abunina, M., Abunin, A., 2018. Nowcasting Solar Energetic Particle Events Using Principal Component Analysis. Sol. Phys. 293 (7), 100. https://doi.org/10.1007/s11207-018-1320-7.

Papaioannou, A., Sandberg, I., Anastasiadis, A., Kouloumvakos, A., Georgoulis, M.K., Tziotziou, K., Tsiropoula, G., Jiggens, P., Hilgers, A., 2016. Solar flares, coronal mass ejections and solar energetic particle event characteristics. J. Space Weather Space Clim. 6, A42. https://doi.org/10.1051/swsc/2016035.

Papaioannou, A., Vainio, R., Raukunen, O., Jiggens, P., Aran, A., Dierckxsens, M., Mallios, S.A., Paassilta, M., Anastasiadis, A., 2022. The probabilistic solar particle event forecasting (PROSPER) model. J. Space Weather Space Clim. 12, 24. https://doi.org/10.1051/swsc/2022019.

Pariat, E., Leake, J.E., Valori, G., Linton, M.G., Zuccarello, F.P., Dalmasse, K., 2017. Relative magnetic helicity as a diagnostic of solar eruptivity. Astron. Astrophys. 601, A125. https://doi.org/10.1051/0004-6361/201630043, arXiv:1703.10562.

Park, S.-H., Chae, J., Wang, H., 2010. Productivity of Solar Flares and Magnetic Helicity Injection in Active Regions. Astrophys J 718 (1), 43–51. https://doi.org/10.1088/0004-637X/718/1/43, arXiv:1005.3416.

Park, S.-H., Guerra, J.A., Gallagher, P.T., Georgoulis, M.K., & Bloomfield, D.S. (2018). Photospheric Shear Flows in Solar Active Regions and Their Relation to Flare Occurrence. Solar Physics, 293(8), 114. doi:10.1007/s11207-018-1336-z. arXiv:1807.07714.

Park, S.-H., Leka, K.D., Kusano, K., Andries, J., Barnes, G., Bingham, S., Bloomfield, D.S., McCloskey, A.E., Delouille, V., Falconer, D., Gallagher, P.T., Georgoulis, M.K., Kubo, Y., Lee, K., Lee, S., Lobzin, V., Mun, J., Murray, S.A., Hamad Nageem, T.A.M., Qahwaji, R., Sharpe, M., Steenburgh, R.A., Steward, G., Terkildsen, M., 2020. A Comparison of Flare Forecasting Methods. IV. Evaluating Consecutive-day Forecasting Patterns. Astrophys J 890 (2), 124. https://doi.org/10.3847/1538-4357/ab65f0, arXiv:2001.02808.

Patsourakos, S., Vourlidas, A., Stenborg, G., 2013. Direct Evidence for a Fast Coronal Mass Ejection Driven by the Prior Formation and Subsequent Destabilization of a Magnetic Flux Rope. Astrophys J 764 (2), 125. https://doi.org/10.1088/0004-637X/764/2/125, arXiv:1211.7211.

Patsourakos, S., Vourlidas, A., Török, T., Kliem, B., Antiochos, S.K., Archontis, V., Aulanier, G., Cheng, X., Chintzoglou, G., Georgoulis, M.K., Green, L.M., Leake, J.E., Moore, R., Nindos, A., Syntelis, P., Yardley, S.L., Yurchyshyn, V., Zhang, J., 2020. Decoding the Pre-Eruptive Magnetic Field Configurations of Coronal Mass Ejections. Space Sci. Rev. 216 (8), 131. https://doi.org/10.1007/s11214-020-00757-9, arXiv:2010.10186.

Patty, S.R., Hagyard, M.J., 1986. Delta-Configurations - Flare Activity and Magnetic-Field Structure. Sol. Phys. 103, 111–128. https://doi.org/10.1007/BF00154862.

Pesnell, W.D., Thompson, B.J., Chamberlin, P.C., 2012. The Solar Dynamics Observatory (SDO). Sol. Phys. 275 (1–2), 3–15. https://doi.org/10.1007/s11207-011-9841-3.

Pestourie, R., Mroueh, Y., Rackauckas, C., Das, P., Johnson, S.G., 2023. Physics-enhanced deep surrogates for partial differential equations. Nature. Machine Intelligence 5 (12), 1458–1465. https://doi.org/10.1038/s42256-023-00761-y.

Phillips, K.J.H., Feldman, U., Landi, E., 2008. Ultraviolet and X-ray Spectroscopy of the Solar Atmosphere. Cambridge University Press, Cambridge.

Plainaki, C., Lilensten, J., Radioti, A., Andriopoulou, M., Milillo, A., Nordheim, T.A., Dandouras, I., Coustenis, A., Grassi, D., Mangano, V., Massetti, S., Orsini, S., Lucchetti, A., 2016. Planetary space weather: scientific aspects and future perspectives. J. Space Weather Space Clim. 6, A31. https://doi.org/10.1051/swsc/2016024.

Pohjolainen, S., Vilmer, N., Khan, J.I., & Hillaris, A.E. (2005). Early signatures of large-scale field line opening. Multi-wavelength analysis of features connected with a "halo" CME event. Astronomy and Astrophysics, 434(1), 329–341. doi:10.1051/0004-6361:20041378.

Pomoell, J., Lumme, E., Kilpua, E., 2019. Time-dependent Data-driven Modeling of Active Region Evolution Using Energy-optimized Photospheric Electric Fields. Sol. Phys. 294 (4), 41. https://doi.org/10.1007/s11207-019-1430-x.

Posner, A., 2007. Up to 1-hour forecasting of radiation hazards from solar energetic ion events with relativistic electrons. Space. Weather 5 (5), S05001. https://doi.org/10.1029/2006SW000268, URL: https://agupubs.onlinelibrary.wiley.com/doi/abs/10.1029/2006SW000268.

Posner, A., Arge, C.N., Staub, J., StCyr, O.C., Folta, D., Solanki, S.K., Strauss, R.D.T., Effenberger, F., Gandorfer, A., Heber, B., Henney, C. J., Hirzberger, J., Jones, S.I., Kühl, P., Malandraki, O., Sterken, V.J., 2021. A multi-purpose heliophysics l4 mission. Space Weather 19 (9). https://doi.org/10.1029/2021sw002777.

Price, D.J., Pomoell, J., Kilpua, E.K.J., 2020. Exploring the coronal evolution of AR 12473 using time-dependent, data-driven magnetofrictional modelling. Astron. Astrophys. 644, A28. https://doi.org/10.1051/0004-6361/202038925.

Priest, E., 2014. Magnetohydrodynamics of the Sun. Cambridge University Press, New York.

Qahwaji, R., Colak, T., 2007. Automatic short-term solar flare prediction using machine learning and sunspot associations. Sol. Phys. 241 (1), 195–211. https://doi.org/10.1007/s11207-006-0272-5.

Raboonik, A., Safari, H., Alipour, N., Wheatland, M.S., 2016. Prediction of solar flares using unique signatures of magnetic field images. Astrophys J 834 (1), 11. https://doi.org/10.3847/1538-4357/834/1/11.

Raghavendra Prasad, B., Banerjee, D., Singh, J., Nagabhushana, S., Kumar, A., Kamath, P.U., Kathiravan, S., Venkata, S., Rajkumar, N., Natarajan, V., Juneja, M., Somu, P., Pant, V., Shaji, N., Sankarsubramanian, K., Patra, A., Venkateswaran, R., Adoni, A.A., Narendra, S., Haridas, T.R., Mathew, S.K., Mohan Krishna, R., Amareswari, K., Jaiswal, B., 2017. Visible Emission Line Coronagraph on Aditya-L1. Curr. Sci. 113 (4), 613. https://doi.org/10.18520/cs/v113/i04/613-615.

Raissi, M., Perdikaris, P., Karniadakis, G., 2019. Physics-informed neural networks: A deep learning framework for solving forward and inverse problems involving nonlinear partial differential equations. J. Comput. Phys. 378, 686–707. https://doi.org/10.1016/j.jcp.2018.10.045.

Raouafi, N.E., Gibson, S., Upton, L., Hoeksema, J.T., Newmark, J., Berger, T., Vourlidas, A., Hassler, D.M., Kinnison, J., Ho, G., Mason, G., Vievering, J., Viall, N., Szabo, A., Casti, M., Case, A., Lepri, S., Velli, M., Georgoulis, M., Bourouaine, S., Jagarlamudi, V., Laming, J., & J.P.Mason (2022). Firefly: Exploring the heliosphere from the solar interior to the solar wind. http://surveygizmoresponseuploads.s3.amazonaws.com/fileuploads/623127/6920789/68-16030f9cb9d69d20ef782b4de10a8012_2024-2033_SSPH_Decadal_-White_Paper_Firefly-HMCS_Mission_Concept.pdf.

Reames, D.V., 2015. What are the sources of solar energetic particles? element abundances and source plasma temperatures. Space Sci. Rev. 194 (1–4), 303–327. https://doi.org/10.1007/s11214-015-0210-7.

Reinard, A.A., Henthorn, J., Komm, R., Hill, F., 2010. Evidence That Temporal Changes in Solar Subsurface Helicity Precede Active Region Flaring. Astrophys. J. Lett. 710 (2), L121–L125. https://doi.org/10.1088/2041-8205/710/2/L121.

Ribeiro, M.T., Singh, S., & Guestrin, C. (2016). why should i trust you? explaining the predictions of any classifier. In Proceedings of the 22nd ACM SIGKDD international conference on knowledge discovery and data mining (pp. 1135–1144). doi:10.1145/2939672.2939778.

Richardson, I., Mays, M., Thompson, B., 2018. Prediction of solar energetic particle event peak proton intensity using a simple algorithm based on cme speed and direction and observations of associated solar phenomena. Space Weather 16 (11), 1862–1881. https://doi.org/10.1029/2018SW002032.

Richardson, I.G., von Rosenvinge, T.T., Cane, H.V., Christian, E.R., Cohen, C.M.S., Labrador, A.W., Leske, R.A., Mewaldt, R.A., Wiedenbeck, M.E., Stone, E.C., 2014. $>$ 25 MeV Proton Events Observed by the High Energy Telescopes on the STEREO A and B Spacecraft and/or at Earth During the First $\sim$Seven Years of the STEREO Mission. Sol. Phys. 289 (8), 3059–3107. https://doi.org/10.1007/s11207-014-0524-8.

Robbrecht, E., Berghmans, D., Van der Linden, R., 2009. Automated LASCO CME catalog for solar cycle 23: are CMEs scale invariant? Astrophys J 691 (2), 1222. https://doi.org/10.1088/0004-637X/691/2/1222.

Robbrecht, E., Patsourakos, S., Vourlidas, A., 2009. No Trace Left Behind: STEREO Observation of a Coronal Mass Ejection Without Low Coronal Signatures. Astrophys J 701 (1), 283–291. https://doi.org/10.1088/0004-637X/701/1/283, arXiv:0905.2583.

Robinson, R.M., 2012. Research to operations: Space weather's valley of opportunity. Space. Weather 10 (10), S01000. https://doi.org/10.1029/2012sw000854.

Rodriguez, L., Barnes, D., Hosteaux, S., Davies, J.A., Willems, S., Pant, V., Harrison, R.A., Berghmans, D., Bothmer, V., Eastwood, J.P., Gallagher, P.T., Kilpua, E.K.J., Magdalenic, J., Mierla, M., Möstl, C., Rouillard, A.P., Odstrčil, D., Poedts, S., 2022. Comparing the heliospheric cataloging, analysis, and techniques service (HELCATS) manual and automatic catalogues of coronal mass ejections using solar terrestrial relations observatory/heliospheric imager (STEREO/HI) data. Sol. Phys. 297 (2). https://doi.org/10.1007/s11207-022-01959-w.

Roiger, R.J., 2017. Data mining: a tutorial-based primer. Chapman and Hall/CRC, Beaverton.

Rosner, R., Vaiana, G.S., 1978. Cosmic flare transients: constraints upon models for energy storage and release derived from the event frequency distribution. Astrophys J 222, 1104–1108. https://doi.org/10.1086/156227.

Rotti, S., Aydin, B., Georgoulis, M.K., Martens, P.C., 2022. Integrated Geostationary Solar Energetic Particle Events Catalog: GSEP. Astrophys. J. Suppl. Ser. 262 (1), 29. https://doi.org/10.3847/1538-4365/ac87ac, arXiv:2204.12021.

Rotti, S.A., Martens, P.C.H., Aydin, B., 2020. A catalog of solar flare events observed by the SOHO/EIT. Astrophys. J. Suppl. Ser. 249 (2), 20. https://doi.org/10.3847/1538-4365/ab9a42.

Rust, D.M., Kumar, A., 1996. Evidence for Helically Kinked Magnetic Flux Ropes in Solar Eruptions. Astrophys. J. 464 (2), L199–L202. https://doi.org/10.1086/310118.

Sadykov, V., Kosovichev, A., Kitiashvili, I., Oria, V., Nita, G.M., Illarionov, E., O'Keefe, P., Jiang, Y., Fereira, S., Ali, A., 2021. Prediction of Solar Proton Events with Machine Learning: Comparison with Operational Forecasts and "All-Clear" Perspectives. arXiv e-prints (p. arXiv:2107.03911). arXiv:2107.03911.

Sakurai, T., 1976. Magnetohydrodynamic interpretation of the motion of prominences. Proc. Astron. Soc. Japan 28 (2), 177–198, URL: https://ui.adsabs.harvard.edu/abs/1976PASJ...28.177S.

Sammis, I., Tang, F., Zirin, H., 2000. The Dependence of Large Flare Occurrence on the Magnetic Structure of Sunspots. Astrophys J 540 (1), 583–587. https://doi.org/10.1086/309303.

Sankarasubramanian, K., Ramadevi, M.C., Bug, M., Umapathy, C.N., Seetha, S., Sreekumar, P., & Kumar (2011). SoLEXS - A low energy X-ray spectrometer for solar coronal studies. In Astronomical Society of India Conference Series (pp. 63–69). volume 2. doi:10.48550/arXiv.1111.5820. arXiv:1111.5820.

Sankarasubramanian, K., Sudhakar, M., Nandi, A., Ramadevi, M.C., Adoni, A.A., Kushwaha, A., Agarwal, A., Dey, A., Joshi, B., Singh, B., Girish, V., Tomar, I., Majhi, K.K., Olekar, M., Bug, M., Pala, M., Thakur, M.K., Badagandi, R.R., Ravishankar, B.T., Garg, S., Sitaramamurthy, N., Sridhara, N., Umapathy, C.N., Gupta, V.K., Agrawal, V.K., Yougandar, B., 2017. X-ray spectrometers on-board Aditya-L1 for solar flare studies. Curr. Sci. 113 (4), 625. https://doi.org/10.18520/cs/v113/i04/625-627.

Sawyer, C., Warwick, J.W., Dennett, J.T., 1986. Solar Flare Prediction. Colorado Associated University Press, Boulder CO, Boulder, CO.

Scherrer, P.H., Bogart, R.S., Bush, R.I., Hoeksema, J.T., Kosovichev, A. G., Schou, J., Rosenberg, W., Springer, L., Tarbell, T.D., Title, A., Wolfson, C.J., Zayer, I., & MDI Engineering Team (1995). The Solar Oscillations Investigation - Michelson Doppler Imager. Solar Physics, 162(1-2), 129–188. doi:10.1007/BF00733429.

Scherrer, P.H., Schou, J., Bush, R.I., Kosovichev, A.G., Bogart, R.S., Hoeksema, J.T., Liu, Y., Duvall, T.L., Zhao, J., Title, A.M., Schrijver, C.J., Tarbell, T.D., Tomczyk, S., 2012. The Helioseismic and Magnetic Imager (HMI) Investigation for the Solar Dynamics Observatory (SDO). Sol. Phys. 275 (1–2), 207–227. https://doi.org/10.1007/s11207-011-9834-2.

Schmieder, B., Aulanier, G., Vršnak, B., 2015. Flare-CME Models: An Observational Perspective (Invited Review). Sol. Phys. 290 (12), 3457–3486. https://doi.org/10.1007/s11207-015-0712-1.

Schou, J., Scherrer, P.H., Bush, R.I., Wachter, R., Couvidat, S., Rabello-Soares, M.C., Bogart, R.S., Hoeksema, J.T., Liu, Y., Duvall, T.L., Akin, D.J., Allard, B.A., Miles, J.W., Rairden, R., Shine, R.A., Tarbell, T.D., Title, A.M., Wolfson, C.J., Elmore, D.F., Norton, A.A., Tomczyk, S., 2012. Design and Ground Calibration of the Helioseismic and Magnetic Imager (HMI) Instrument on the Solar Dynamics Observatory (SDO). Sol. Phys. 275 (1–2), 229–259. https://doi.org/10.1007/s11207-011-9842-2.

Schrijver, C.J., Kauristie, K., Aylward, A.D., Denardini, C.M., Gibson, S. E., Glover, A., Gopalswamy, N., Grande, M., Hapgood, M., Heynderickx, D., Jakowski, N., Kalegaev, V.V., Lapenta, G., Linker, J.A., Liu, S., Mandrini, C.H., Mann, I.R., Nagatsuma, T., Nandy, D., Obara, T., Paul O'Brien, T., Onsager, T., Opgenoorth, H.J., Terkildsen, M., Valladares, C.E., Vilmer, N., 2015. Understanding space weather to shield society: A global road map for 2015–2025 commissioned by COSPAR and ILWS. Adv. Space Res. 55 (12), 2745–2807. https://doi.org/10.1016/j.asr.2015.03.023, arXiv:1503.06135.

Schunker, H., Braun, D.C., Birch, A.C., Burston, R.B., Gizon, L., 2016. SDO/HMI survey of emerging active regions for helioseismology. Astron. Astrophys. 595, A107. https://doi.org/10.1051/0004-6361/201628388, arXiv:1608.08005.

Schwenn, R., 2006. Space Weather: The Solar Perspective. Living Rev. Sol. Phys. 3 (1), 2. https://doi.org/10.12942/lrsp-2006-2.

Seetha, S., Megala, S., 2017. Aditya-L1 mission. Curr. Sci. 113 (4), 610. https://doi.org/10.18520/cs/v113/i04/610-612.

Severny, A.B., 1964. Solar Flares. Ann. Rev. Astron. Astrophys. 2, 363. https://doi.org/10.1146/annurev.aa.02.090164.002051.

Sharma, A.S., Bunde, A., Dimri, V.P., Baker, D.N., 2012. Extreme Events and Natural Hazards: The Complexity. Perspective. volume 196. https://doi.org/10.1029/GM196.

Sharpe, M.A., Murray, S.A., 2017. Verification of space weather forecasts issued by the met office space weather operations centre. Space Weather 15 (10), 1383–1395. https://doi.org/10.1002/2017sw001683.

Sheeley, N.R., Walters, J.H., Wang, Y.M., Howard, R.A., 1999. Continuous tracking of coronal outflows: Two kinds of coronal mass ejections. J. Geophys. Res. 104 (A11), 24739–24768. https://doi.org/10.1029/1999JA900308.

Shestov, S.V., Zhukov, A.N., Inhester, B., Dolla, L., Mierla, M., 2021. Expected performances of the PROBA-3/ASPIICS solar coronagraph: Simulated data. Astron. Astrophys. 652, A4. https://doi.org/10.1051/0004-6361/202140467.

Shimizu, T., Imada, S., Kawate, T., Suematsu, Y., Hara, H., Tsuzuki, T., Katsukawa, Y., Kubo, M., Ishikawa, R., Watanabe, T., Toriumi, S., Ichimoto, K., Nagata, S., Hasegawa, T., Yokoyama, T., Watanabe, K., Tsuno, K., Korendyke, C.M., Warren, H., De Pontieu, B., Boerner, P., Solanki, S.K., Teriaca, L., Schuehle, U., Matthews, S., Long, D., Thomas, W., Hancock, B., Reid, H., Fludra, A., Auchère, F., Andretta, V., Naletto, G., Poletto, L., & Harra, L. (2020). The Solar-C (EUVST) mission: the latest status. In Society of Photo-Optical Instrumentation Engineers (SPIE) Conference Series (p. 114440N). volume 11444 of Society of Photo-Optical Instrumentation Engineers (SPIE) Conference Series. doi:10.1117/12.2560887.

Shrikumar, A., Greenside, P., & Kundaje, A. (2017). Learning important features through propagating activation differences. In D. Precup, & Y.W. Teh (Eds.), Proceedings of the 34th International Conference on Machine Learning (pp. 3145–3153). PMLR volume 70 of Proceedings of Machine Learning Research. URL: https://proceedings.mlr.press/v70/shrikumar17a.html.

Sinha, S., Gupta, O., Singh, V., Lekshmi, B., Nandy, D., Mitra, D., Chatterjee, S., Bhattacharya, S., Chatterjee, S., Srivastava, N., Brandenburg, A., Pal, S., 2022. A comparative analysis of machine-learning models for solar flare forecasting: Identifying high-performing active region flare indicators. Astrophys J 935 (1), 45. https://doi.org/10.3847/1538-4357/ac7955.

Sinha, S., Srivastava, N., Nandy, D., 2019. Solar filament eruptions as precursors to flare–CME events: Establishing the temporal connection. Astrophys J 880 (2), 84. https://doi.org/10.3847/1538-4357/ab2239.

Song, H., Tan, C., Jing, J., Wang, H., Yurchyshyn, V., Abramenko, V., 2009. Statistical assessment of photospheric magnetic features in imminent solar flare predictions. Sol. Phys. 254 (1), 101–125.

Song, H.Q., Zhang, J., Chen, Y., Cheng, X., 2014. Direct Observations of Magnetic Flux Rope Formation during a Solar Coronal Mass Ejection. Astrophys. J. Lett. 792 (2), L40. https://doi.org/10.1088/2041-8205/792/2/L40, arXiv:1408.2000.

Sornette, D. (2009). Dragon-Kings, Black Swans and the Prediction of Crises. arXiv e-prints, (p. arXiv:0907.4290). arXiv:0907.4290.

Springenberg, J.T., Dosovitskiy, A., Brox, T., & Riedmiller, M. (2014). Striving for simplicity: The all convolutional net. arXiv preprint arXiv:1412.6806.

Steenburgh, R.A., Biesecker, D.A., Millward, G.H., 2013. From predicting solar activity to forecasting space weather: Practical examples of research-to-operations and operations-to-research. Sol. Phys. 289 (2), 675–690. https://doi.org/10.1007/s11207-013-0308-6.

Sterling, A.C., Moore, R.L., 2004. Evidence for Gradual External Reconnection before Explosive Eruption of a Solar Filament. Astrophys J 602 (2), 1024–1036. https://doi.org/10.1086/379763.

Steward, G., Lobzin, V., Cairns, I.H., Li, B., Neudegg, D., 2017. Automatic recognition of complex magnetic regions on the Sun in SDO magnetogram images and prediction of flares: Techniques and results for the revised flare prediction program Flarecast. Space Weather 15 (9), 1151–1164. https://doi.org/10.1002/2017SW001595.

Steward, G.A., Lobzin, V.V., Wilkinson, P.J., Cairns, I.H., Robinson, P. A., 2011. Automatic recognition of complex magnetic regions on the Sun in GONG magnetogram images and prediction of flares: Techniques for the flare warning program Flarecast. Space Weather 9 (11), S11004. https://doi.org/10.1029/2011SW000703.

Strugarek, A., Charbonneau, P., 2014. Predictive capabilities of avalanche models for solar flares. Sol. Phys. 289 (11), 4137–4150. https://doi.org/10.1007/s11207-014-0570-2.

Stumpo, M., Benella, S., Laurenza, M., Alberti, T., Consolini, G., Marcucci, M.F., 2021. Open Issues in Statistical Forecasting of Solar Proton Events: A Machine Learning Perspective. Space. Weather 19 (10). https://doi.org/10.1029/2021SW002794, e2021SW002794.

Sun, H., Manchester IV, W., Chen, Y., 2021. Improved and interpretable solar flare predictions with spatial and topological features of the polarity inversion line masked magnetograms. Space Weather 19 (12). https://doi.org/10.1029/2021SW002837, e2021SW002837. E2021SW002837 2021SW002837.

Sun, X., Hoeksema, J.T., Liu, Y., Wiegelmann, T., Hayashi, K., Chen, Q., Thalmann, J., 2012. Evolution of Magnetic Field and Energy in a Major Eruptive Active Region Based on SDO/HMI Observation. Astrophys J 748 (2), 77. https://doi.org/10.1088/0004-637X/748/2/77, arXiv:1201.3404.

Sun, Z., Bobra, M.G., Wang, X., Wang, Y., Sun, H., Gombosi, T., Chen, Y., Hero, A., 2022. Predicting solar flares using cnn and lstm on two solar cycles of active region data. Astrophys J 931 (2), 163. https://doi.org/10.3847/1538-4357/ac64a6.

Syntelis, P., Gontikakis, C., Patsourakos, S., Tsinganos, K., 2016. The spectroscopic imprint of the pre-eruptive configuration resulting into two major coronal mass ejections. Astron. Astrophys. 588, A16. https://doi.org/10.1051/0004-6361/201526829, arXiv:1602.03680.

Syntelis, P., Lee, E.J., Fairbairn, C.W., Archontis, V., Hood, A.W., 2019. Eruptions and flaring activity in emerging quadrupolar regions. Astron. Astrophys. 630, A134. https://doi.org/10.1051/0004-6361/201936246, arXiv:1909.01446.

Takasao, S., Fan, Y., Cheung, M.C.M., Shibata, K., 2015. Numerical Study on the Emergence of Kinked Flux Tube for Understanding of Possible Origin of <texmath type="inline">delta </texmath>-spot Regions. Astrophys J 813 (2), 112. https://doi.org/10.1088/0004-637X/813/2/112, arXiv:1511.02863.

Taleb, N.N., 2007. The Black Swan: The Impact of the Highly Improbable. Random House Group, New York.

Tanaka, K., 1991. Studies on a very flare-active δgroup: Peculiar δspot evolution and inferred subsurface magnetic rope structure. Sol. Phys. 136 (1), 133–149. https://doi.org/10.1007/BF00151700.

Tang, R., Liao, W., Chen, Z., Zeng, X., Wang, J.-S., Luo, B., Chen, Y., Cui, Y., Zhou, M., Deng, X., et al., 2021. Solar flare prediction based on the fusion of multiple deep-learning models. Astrophys. J. Suppl. Ser. 257 (2), 50. https://doi.org/10.3847/1538-4365/ac249e.

Temmer, M., 2021. Space weather: the solar perspective. Living Rev. Sol. Phys. 18 (1). https://doi.org/10.1007/s41116-021-00030-3.

Temmer, M., Scolini, C., Richardson, I.G., Heinemann, S.G., Paouris, E., Vourlidas, A., Bisi, M.M., Al-Haddad, N., Amerstorfer, T., Barnard, L., Burešová, D., Hofmeister, S., Iwai, K., Jackson, B., Jarolim, R., Jian, L., Linker, J., Lugaz, N., Manoharan, P., Mays, M., Mishra, W., Owens, M., Palmerio, E., Perri, B., Pomoell, J., Pinto, R., Samara, E., Singh, T., Sur, D., Verbeke, C., Veronig, A., Zhuang, B., 2023. CME propagation through the heliosphere: Status and future of observations and model development. Advances in Space Research, URL:. https://doi.org/10.1016/j.asr.2023.07.003, URL: https://doi.org/10.1016/j.asr.2023.07.003.

Thacker, B., Doebling, S., Hemez, F., Anderson, M., Pepin, J., Rodriguez, E., 2004. Concepts of model verification and validation, no. la-14167. Los Alamos National Lab, Los Alamos, NM (US).

Thalmann, J.K., Moraitis, K., Linan, L., Pariat, E., Valori, G., Dalmasse, K., 2019. Magnetic Helicity Budget of Solar Active Regions Prolific of Eruptive and Confined Flares. Astrophys J 887 (1), 64. https://doi.org/10.3847/1538-4357/ab4e15, arXiv:1910.06563.

Thampi, R., Alok, A., Bhardwaj, A., & Yadav, V. (2014). Plasma analyser package for aditya (PAPA) - a novel plasma analyser to study the composition and dynamics of the solarwind. In NLST-Aditya Meeting.

Thibeault, C., Strugarek, A., Charbonneau, P., Tremblay, B., 2022. Forecasting solar flares by data assimilation in sandpile models. Sol. Phys. 297 (9), 1–23. https://doi.org/10.1007/s11207-022-02055-9.

Thompson, B.J., Cliver, E.W., Nitta, N., Delannée, C., Delaboudinière, J.-P., 2000. Coronal dimmings and energetic CMEs in April-May 1998. Geophys. Res. Lett. 27, 1431–1434. https://doi.org/10.1029/1999GL003668.

Thompson, B.J., Plunkett, S.P., Gurman, J.B., Newmark, J.S., St. Cyr, O. C., & Michels, D.J. (1998). SOHO/EIT observations of an Earth-directed coronal mass ejection on May 12, 1997. Geophysical Research Letters, 25, 2465–2468. doi:10.1029/98GL50429.

Thompson, W.T., 2006. Coordinate systems for solar image data. Astron. Astrophys. 449 (2), 791–803. https://doi.org/10.1051/0004-6361:20054262, URL: https://doi.org/10.1051/0004-6361:20054262.

Tian, H., McIntosh, S.W., Xia, L., He, J., Wang, X., 2012. What can We Learn about Solar Coronal Mass Ejections, Coronal Dimmings, and Extreme-ultraviolet Jets through Spectroscopic Observations? Astrophys J 748, 106. https://doi.org/10.1088/0004-637X/748/2/106, arXiv:1201.2204.

Titov, V.S., Török, T., Mikic, Z., Linker, J.A., 2014. A Method for Embedding Circular Force-free Flux Ropes in Potential Magnetic Fields. Astrophys J 790 (2), 163. https://doi.org/10.1088/0004-637X/790/2/163.

Toriumi, S., Hotta, H., 2019. Spontaneous Generation of δ-sunspots in Convective Magnetohydrodynamic Simulation of Magnetic Flux Emergence. Astrophys. J. Lett. 886 (1), L21. https://doi.org/10.3847/2041-8213/ab55e7, arXiv:1911.03909.

Toriumi, S., Hotta, H., Kusano, K., 2023. Turbulent convection as a significant hidden provider of magnetic helicity in solar eruptions. Scientific Reports 13 (1). https://doi.org/10.1038/s41598-023-36188-z.

Toriumi, S., Iida, Y., Kusano, K., Bamba, Y., Imada, S., 2014. Formation of a Flare-Productive Active Region: Observation and Numerical Simulation of NOAA AR 11158. Sol. Phys. 289 (9), 3351–3369. https://doi.org/10.1007/s11207-014-0502-1, arXiv:1403.4029.

Toriumi, S., Schrijver, C.J., Harra, L.K., Hudson, H., Nagashima, K., 2017. Magnetic Properties of Solar Active Regions That Govern Large Solar Flares and Eruptions. Astrophys J 834 (1), 56. https://doi.org/10.3847/1538-4357/834/1/56, arXiv:1611.05047.

Toriumi, S., Takasao, S., 2017. Numerical Simulations of Flare-productive Active Regions: <texmath type="inline">delta </texmath>-sunspots, Sheared Polarity Inversion Lines, Energy Storage, and Predictions. Astrophys J 850 (1), 39. https://doi.org/10.3847/1538-4357/aa95c210.48550/arXiv.1710.08926, arXiv:1710.08926.

Toriumi, S., Wang, H., 2019. Flare-productive active regions. Living Rev. Sol. Phys. 16 (1), 3. https://doi.org/10.1007/s41116-019-0019-7, arXiv:1904.12027.

Török, T., Downs, C., Linker, J.A., Lionello, R., Titov, V.S., Mikić, Z., Riley, P., Caplan, R.M., & Wijaya, J. (2018). Sun-to-Earth MHD Simulation of the 2000 July 14 "Bastille Day" Eruption. The Astrophysical Journal, 856(1), 75. doi:10.3847/1538-4357/aab36d. arXiv:1801.05903.

Török, T., Kliem, B., 2005. Confined and Ejective Eruptions of Kink-unstable Flux Ropes. Astrophys. J. Lett. 630 (1), L97–L100. https://doi.org/10.1086/462412, arXiv:astro-ph/0507662.

Török, T., Kliem, B., 2007. Numerical simulations of fast and slow coronal mass ejections. Astronomische Nachrichten (Astronomical News) 328 (8), 743. https://doi.org/10.1002/asna.200710795, arXiv:0705.2100.

Török, T., Kliem, B., Titov, V.S., 2004. Ideal kink instability of a magnetic loop equilibrium. Astron. Astrophys. 413, L27–L30. https://doi.org/10.1051/0004-6361:20031691, arXiv:astro-ph/0311198.

Török, T., Leake, J.E., Titov, V.S., Archontis, V., Mikić, Z., Linton, M. G., Dalmasse, K., Aulanier, G., Kliem, B., 2014. Distribution of Electric Currents in Solar Active Regions. Astrophys. J. Lett. 782 (1), L10. https://doi.org/10.1088/2041-8205/782/1/L10, arXiv:1401.2931.

Torres, J., Zhao, L., Chan, P.K., Zhang, M., 2022. A machine learning approach to predicting SEP events using properties of coronal mass ejections. Space. Weather 20 (7). https://doi.org/10.1029/2021sw002797.

Tripathi, D., Ramaprakash, A.N., Khan, A., Ghosh, A., Chatterjee, S., Banerjee, D., Chordia, P., Gandorfer, A., Krivova, N., Nandy, D., Rajarshi, C., Solanki, S.K., 2017. The Solar Ultraviolet Imaging Telescope on-board Aditya-L1. Curr. Sci. 113 (4), 616. https://doi.org/10.18520/cs/v113/i04/616-619, arXiv:2204.07732.

Tsagouri, I., Borries, C., Perry, C., Dierckxsens, M., de Patoul, J., Cid, C., Moretto-Jorgenson, T., & Bloomfield, D.S. (2020). Guidelines for common validation in the SSA SWE Network. https://bit.ly/3kz89hP.

Tziotziou, K., Georgoulis, M.K., Liu, Y., 2013. Interpreting Eruptive Behavior in NOAA AR 11158 via the Region's Magnetic Energy and Relative-helicity Budgets. Astrophys J 772 (2), 115. https://doi.org/10.1088/0004-637X/772/2/115, arXiv:1306.2135.

Tziotziou, K., Georgoulis, M.K., Raouafi, N.-E., 2012. The Magnetic Energy-Helicity Diagram of Solar Active Regions. Astrophys. J. Lett. 759 (1), L4. https://doi.org/10.1088/2041-8205/759/1/L4, arXiv:1209.5612.

Ugarte-Urra, I., Warren, H.P., Winebarger, A.R., 2007. The Magnetic Topology of Coronal Mass Ejection Sources. Astrophys J 662 (2), 1293–1301. https://doi.org/10.1086/514814, arXiv:astro-ph/0703049.

Vainio, R., Valtonen, E., Heber, B., Malandraki, O.E., Papaioannou, A., Klein, K.-L., Afanasiev, A., Agueda, N., Aurass, H., Battarbee, M., et al., 2013. The first sepserver event catalogue 68-mev solar proton events observed at 1 au in 1996–2010. J. Space Weather Space Clim. 3, A12. https://doi.org/10.1051/swsc/2013030.

van Ballegooijen, A.A., Martens, P.C.H., 1989. Formation and Eruption of Solar Prominences. Astrophys J 343, 971. https://doi.org/10.1086/167766.

Van Horn, R.L., 1971. Validation of simulation results. Manage. Sci. 17 (5), 247–258. https://doi.org/10.1287/mnsc.17.5.247.

Vlahos, L., Georgoulis, M., Kluiving, R., Paschos, P., 1995. The statistical flare. Astron. Astrophys. 299, 897, URL: https://ui.adsabs.harvard.edu/abs/1995A&A...299.897V.

Vlahos, L., Georgoulis, M.K., 2004. On the self-similarity of unstable magnetic discontinuities in solar active regions. Astrophys J 603 (1), L61. https://doi.org/10.1086/383032.

Vourlidas, A., 2015. Mission to the sun-earth lsub5/sublagrangian point: An optimal platform for space weather research. Space. Weather 13 (4), 197–201. https://doi.org/10.1002/2015sw001173.

Vourlidas, A., 2021. Improving the medium-term forecasting of space weather: A big picture review from a solar observer's perspective. Frontiers in Astronomy and Space Sciences 8. https://doi.org/10.3389/fspas.2021.651527.

Vourlidas, A., Carley, E.P., Vilmer, N., 2020. Radio Observations of Coronal Mass Ejections: Space Weather Aspects. Frontiers in Astronomy and Space Sciences 7, 43. https://doi.org/10.3389/fspas.2020.00043.

Vourlidas, A., Liewer, P.C., Velli, M., & Webb, D. (2018). Solar Polar Diamond Explorer (SPDEx): Understanding the Origins of Solar Activity Using a New Perspective. arXiv e-prints, (p. arXiv:1805.04172). arXiv:1805.04172.

Vourlidas, A., Lynch, B.J., Howard, R.A., Li, Y., 2013. How Many CMEs Have Flux Ropes? Deciphering the Signatures of Shocks, Flux Ropes, and Prominences in Coronagraph Observations of CMEs. Sol. Phys. 284 (1), 179–201. https://doi.org/10.1007/s11207-012-0084-8, arXiv:1207.1599.

Vourlidas, A., Turner, D., Biesecker, D., Coster, A., Engell, A., Ho, G., Immel, T., Keys, C., Lanzerotti, L., Lu, G., Lugaz, N., Luhmann, J., Mays, L., O'Brien, P., Semones, E., Spence, H., Upton, L., & White, S. (2021). Space weather science and observation gap analysis for the national aeronautics and space administration. https://science.nasa.gov/science-pink/s3fs-public/atoms/files/GapAnalysisReport_full_final.pdf.

Wang, D., Liu, R., Wang, Y., Liu, K., Chen, J., Liu, J., Zhou, Z., Zhang, M., 2017. Critical height of the torus instability in two-ribbon solar flares. Astrophys. J. Lett. 843, L9. https://doi.org/10.3847/2041-8213/aa79f0.

Wang, H., Ewell, J., M.W., Zirin, H., & Ai, G. (1994). Vector Magnetic Field Changes Associated with X-Class Flares. The Astrophysical Journal, 424, 436. doi:10.1086/173901.

Wang, H.-M., Song, H., Jing, J., Yurchyshyn, V., Deng, Y.-Y., Zhang, H.-Q., Falconer, D., Li, J., 2006. The relationship between magnetic gradient and magnetic shear in five super active regions producing great flares. Chin. J. Astron. Astrophys. 6 (4), 477–488. https://doi.org/10.1088/1009-9271/6/4/11.

Wang, J., Ao, X., Wang, Y., Wang, C., Cai, Y., Luo, B., Liu, S., Shen, C., Zhuang, B., Xue, X., et al., 2018. An operational solar wind prediction system transitioning fundamental science to operations. J. Space Weather Space Clim. 8, A39. https://doi.org/10.1051/swsc/2018025.

Wang, W., Zhu, C., Qiu, J., Liu, R., Yang, K.E., Hu, Q., 2019. Evolution of a Magnetic Flux Rope toward Eruption. Astrophys J 871 (1), 25. https://doi.org/10.3847/1538-4357/aaf3ba, arXiv:1812.03437.

Wang, X., Chen, Y., Toth, G., Manchester, W.B., Gombosi, T.I., Hero, A.O., Jiao, Z., Sun, H., Jin, M., Liu, Y., 2020. Predicting solar flares with machine learning: Investigating solar cycle dependence. Astrophys J 895 (1), 3. https://doi.org/10.3847/1538-4357/ab89ac.

Wang, Y., Bai, X., Chen, C., Chen, L., Cheng, X., Deng, L., Deng, L., Deng, Y., Feng, L., Gou, T., Guo, J., Guo, Y., Hao, X., He, J., Hou, J., Huang, J., Huang, Z., Ji, H., Jiang, C., Jiang, J., Jin, C., Li, X., Li, Y., Liu, J., Liu, K., Liu, L., Liu, R., Liu, R., Qiu, C., Shen, C., Shen, F., Shen, Y., Shi, X., Su, J., Su, Y., Su, Y., Sun, M., Tan, B., Tian, H., Wang, Y., Xia, L., Xie, J., Xiong, M., Xu, M., Yan, X., Yan, Y., Yang, S., Yang, S., Zhang, S., Zhang, Q., Zhang, Y., Zhao, J., Zhou, G., Zou, H., 2023. Solar ring mission: Building a panorama of the Sun and inner-heliosphere. Adv. Space Res. 71 (1), 1146–1164. https://doi.org/10.1016/j.asr.2022.10.04510.48550/arXiv.2210.10402.

Webb, D., Howard, T., Fry, C., Kuchar, T., Odstrcil, D., Jackson, B., Bisi, M., Harrison, R., Morrill, J., Howard, R., et al., 2009. Study of cme propagation in the inner heliosphere: Soho lasco, smei and stereo hi observations of the january 2007 events. Sol. Phys. 256, 239–267. https://doi.org/10.1007/s11207-009-9351-8.

Welsch, B.T., Li, Y., Schuck, P.W., Fisher, G.H., 2009. What is the Relationship Between Photospheric Flow Fields and Solar Flares? Astrophys J 705 (1), 821–843. https://doi.org/10.1088/0004-637X/705/1/821, arXiv:0905.0529.

Wheatland, M., 2004. A bayesian approach to solar flare prediction. Astrophys J 609 (2), 1134. https://doi.org/10.1086/421261.

Wheatland, M., 2005. A statistical solar flare forecast method. Space. Weather 3 (7). https://doi.org/10.1029/2004SW000131.

Whitman, K., Egeland, R., Richardson, I.G., Allison, C., Quinn, P., et al., 2022. Review of solar energetic particle models. Adv. Space Res. https://doi.org/10.1016/j.asr.2022.08.006, URL: https://www.sciencedirect.com/science/article/pii/S0273117722007244.

Wilkinson, M.D., Dumontier, M., Aalbersberg, I.J., Appleton, G., Axton, M., Baak, A., Blomberg, N., Boiten, J.-W., da Silva Santos, L.B., Bourne, P.E., Bouwman, J., Brookes, A.J., Clark, T., Crosas, M., Dillo, I., Dumon, O., Edmunds, S., Evelo, C.T., Finkers, R., Gonzalez-Beltran, A., Gray, A.J.G., Groth, P., Goble, C., Grethe, J. S., Heringa, J., 'T Hoen, P.A.C., Hooft, R., Kuhn, T., Kok, R., Kok, J., Lusher, S.J., Martone, M.E., Mons, A., Packer, A.L., Persson, B., Rocca-Serra, P., Roos, M., van Schaik, R., Sansone, S.-A., Schultes, E., Sengstag, T., Slater, T., Strawn, G., Swertz, M.A., Thompson, M., van der Lei, J., van Mulligen, E., Velterop, J., Waagmeester, A., Wittenburg, P., Wolstencroft, K., Zhao, J., & Mons, B. (2016). The FAIR Guiding Principles for scientific data management and stewardship. Scientific Data, 3, 160018. doi:10.1038/sdata.2016.18.

Winter, E. (2002). Chapter 53 the shapley value. (pp. 2025–2054). Elsevier volume 3 of Handbook of Game Theory with Economic Applications. URL: https://www.sciencedirect.com/science/article/pii/S1574000502030163. doi: 10.1016/S1574-0005(02)03016-3.

Woodcock, F., 1976. The evaluation of yes/no forecasts for scientific and administrative purposes. Mon. Weather Rev. 104 (10), 1209–1214. https://doi.org/10.1175/1520-0493(1976)104<1209:TEOYFF>2.0.CO;2.

Woods, M.M., Inoue, S., Harra, L.K., Matthews, S.A., Kusano, K., 2020. Serial Flaring in an Active Region: Exploring Why Only One Flare Is Eruptive. Astrophys J 890 (1), 84. https://doi.org/10.3847/1538-4357/ab6bc8.

Wyper, P.F., Antiochos, S.K., DeVore, C.R., 2017. A universal model for solar eruptions. Nature 544 (7651), 452–455. https://doi.org/10.1038/nature22050.

Xu, L., Yan, Y., Huang, X., 2022. Deep Learning in Solar Astronomy. Springer Singapore. https://doi.org/10.1007/978-981-19-2746-1.

Xue, Z., Yan, X., Cheng, X., Yang, L., Su, Y., Kliem, B., Zhang, J., Liu, Z., Bi, Y., Xiang, Y., Yang, K., Zhao, L., 2016. Observing the release of twist by magnetic reconnection in a solar filament eruption. Nat. Commun. 7, 11837. https://doi.org/10.1038/ncomms11837.

Xue, Z., Yan, X., Yang, L., Wang, J., Zhao, L., 2017. Observing Formation of Flux Rope by Tether-cutting Reconnection in the Sun. Astrophys. J. Lett. 840 (2), L23. https://doi.org/10.3847/2041-8213/aa7066.

Yadav, V.K., Srivastava, N., Ghosh, S., Srikar, P., Subhalakshmi, K., 2018. Science objectives of the magnetic field experiment onboard Aditya-L1 spacecraft. Adv. Space Res. 61 (2), 749–758. https://doi.org/10.1016/j.asr.2017.11.008, URL: https://www.sciencedirect.com/science/article/pii/S0273117717308037.

Yan, X., Wang, J., Guo, Q., Xue, Z., Yang, L., Tan, B., 2021. The Formation Process of the First Halo Coronal Mass Ejection in Solar Cycle 25: Magnetic Cancellation, Bidirectional Jet, and Hot Channel. Astrophys J 919 (1), 34. https://doi.org/10.3847/1538-4357/ac116d.

Yan, Y., Deng, Y., Karlický, M., Fu, Q., Wang, S., Liu, Y., 2001. The Magnetic Rope Structure and Associated Energetic Processes in the 2000 July 14 Solar Flare. Astrophys. J. Lett. 551 (1), L115–L119. https://doi.org/10.1086/319829.

Yang, M., Wang, J., Wang, C., Zong, Q., Zhang, X., Dai, S., Deng, Y., Feng, X., Wang, Y., Zhu, C., Zhang, Y., Zhang, Q., Shen, F., Tian, B., Zhou, W., Li, L., Yan, Y., Zhou, G., Yang, S., Xiong, M., Zhang, A., He, J., Tian, H., Li, J., Gan, W., Xia, L., Peng, J., Huang1, C., Jiang, J., & Quan, L. (2023). Envisioning the solar stereo exploration mission. Chinese Science Bulletin, 68.

Yang, S., Zhang, J., Zhu, X., Song, Q., 2017. Block-induced complex structures building the flare-productive solar active region 12673. Astrophys J 849 (2), L21. https://doi.org/10.3847/2041-8213/aa9476.

Yang, W., Sturrock, P., Antiochos, S., 1986. Force-free magnetic fields-the magneto-frictional method. Astrophys J 309, 383–391. https://doi.org/10.1086/164610.

Yardley, S.L., Green, L.M., James, A.W., Stansby, D., Mihailescu, T., 2022. The magnetic field environment of active region 12673 that produced the energetic particle events of september 2017. Astrophys J 937 (2), 57. https://doi.org/10.3847/1538-4357/ac8d69.

Yardley, S.L., Green, L.M., van Driel-Gesztelyi, L., Williams, D.R., Mackay, D.H., 2018a. The Role of Flux Cancellation in Eruptions from Bipolar ARs. Astrophys J 866 (1), 8. https://doi.org/10.3847/1538-4357/aade4a, arXiv:1808.10635.

Yardley, S.L., Mackay, D.H., & Green, L.M. (2018b). Simulating the Coronal Evolution of AR 11437 Using SDO/HMI Magnetograms. The Astrophysical Journal, 852(2), 82. doi:10.3847/1538-4357/aa9f20. arXiv:1712.00396.

Yardley, S.L., Mackay, D.H., & Green, L.M. (2021a). Simulating the Coronal Evolution of Bipolar Active Regions to Investigate the Formation of Flux Ropes. Solar Physics, 296(1), 10. doi:10.1007/s11207-020-01749-2. arXiv:2012.07708.

Yardley, S.L., Pagano, P., Mackay, D.H., Upton, L.A., 2021b. Determining the source and eruption dynamics of a stealth CME using NLFFF modelling and MHD simulations. Astron. Astrophys. 652, A160. https://doi.org/10.1051/0004-6361/202141142, arXiv:2106.14800.

Yashiro, S., 2005. Visibility of coronal mass ejections as a function of flare location and intensity. J. Geophys. Res. 110 (A12). https://doi.org/10.1029/2005ja011151.

Yi, K., Moon, Y.-J., Lim, D., Park, E., Lee, H., 2021. Visual explanation of a deep learning solar flare forecast model and its relationship to physical parameters. Astrophys J 910 (1), 8. https://doi.org/10.3847/1538-4357/abdebe.

Yi, K., Moon, Y.-J., Shin, G., Lim, D., 2020. Forecast of major solar x-ray flare flux profiles using novel deep learning models. Astrophys. J. Lett. 890 (1), L5. https://doi.org/10.3847/2041-8213/ab701b.

Yu, D., Huang, X., Wang, H., Cui, Y., 2009. Short-term solar flare prediction using a sequential supervised learning method. Sol. Phys. 255 (1), 91–105. https://doi.org/10.1007/s11207-009-9318-9.

Yuan, Y., Shih, F.Y., Jing, J., Wang, H.-M., 2010. Automated flare forecasting using a statistical learning technique. Research in Astronomy and Astrophysics 10 (8), 785. https://doi.org/10.1088/1674-4527/10/8/008.

Zaman, F.A., Townsend, L.W., de Wet, W.C., Looper, M.D., Brittingham, J.M., Burahmah, N.T., Spence, H.E., Schwadron, N.A., Smith, S.S., 2022. Modeling the lunar radiation environment: A comparison among FLUKA, geant4, HETC-HEDS, MCNP6, and PHITS. Space. Weather 20 (8). https://doi.org/10.1029/2021sw002895.

Zhang, H., Li, Q., Yang, Y., Jing, J., Wang, J.T.L., Wang, H., Shang, Z., 2022. Solar flare index prediction using SDO/HMI vector magnetic data products with statistical and machine-learning methods. Astrophys. J. Suppl. Ser. 263 (2), 28. https://doi.org/10.3847/1538-4365/ac9b17, arXiv:2209.13779.

Zhang, J., Cheng, X., Ding, M.-D., 2012. Observation of an evolving magnetic flux rope before and during a solar eruption. Nat. Commun. 3, 747. https://doi.org/10.1038/ncomms1753, arXiv:1203.4859.

Zhang, J., Dere, K.P., 2006. A statistical study of main and residual accelerations of coronal mass ejections. Astrophys J 649 (2), 1100–1109. https://doi.org/10.1086/506903.

Zhang, J., Dere, K.P., Howard, R.A., Kundu, M.R., White, S.M., 2001. On the temporal relationship between coronal mass ejections and flares. Astrophys J 559 (1), 452–462. https://doi.org/10.1086/322405.

Zhang, J., Temmer, M., Gopalswamy, N., Malandraki, O., Nitta, N.V., Patsourakos, S., Shen, F., Vršnak, B., Wang, Y., Webb, D., Desai, M. I., Dissauer, K., Dresing, N., Dumbović, M., Feng, X., Heinemann, S. G., Laurenza, M., Lugaz, N., Zhuang, B., 2021. Earth-affecting solar transients: a review of progresses in solar cycle 24. Progress in Earth and Planetary. Science 8 (1), 56. https://doi.org/10.1186/s40645-021-00426-7, arXiv:2012.06116.

Zheng, Y., Li, X., Wang, X., 2019. Solar flare prediction with the hybrid deep convolutional neural network. Astrophys J 885 (1), 73. https://doi.org/10.3847/1538-4357/ab46bd.

Zhou, Y.-H., Xia, C., Keppens, R., Fang, C., Chen, P.F., 2018. Three-dimensional MHD Simulations of Solar Prominence Oscillations in a Magnetic Flux Rope. Astrophys J 856 (2), 179. https://doi.org/10.3847/1538-4357/aab614, arXiv:1803.03385.

Zhukov, A.N., Auchère, F., 2004. On the nature of EIT waves, EUV dimmings and their link to CMEs. Astron. Astrophys. 427, 705–716. https://doi.org/10.1051/0004-6361:20040351.

Zirin, H., Liggett, M.A., 1987. Delta spots and great flares. Sol. Phys. 113 (1), 267–283. https://doi.org/10.1007/BF00147707.